Dissertation zur Erlangung des Doktorgrades
der Fakultät für Chemie und Pharmazie
der Ludwig-Maximilians-Universität München

Development of a click chemistry-based proximity ligation assay and Synthesis and incorporation of 5-carboxycytidine phosphoramidite in synthetic RNA

Bastien Viverge
aus
Digne-les-Bains, France

2021

Erklärung

Diese Dissertation wurde im Sinne von § 7 der Promotionsordnung vom 28. November 2011 von Herrn *Prof. Dr; Thomas Carell* betreut.

Eidesstattliche Versicherung

Diese Dissertation wurde eigenständig und ohne unerlaubte Hilfe erarbeitet.

Lenzburg, May 18th 2021

Bastien Viverge

Dissertation eingereicht am 29.04.2021

1. Gutachter: Prof. Dr. Thomas Carell
2. Gutachterin: Dr. Sabine Schneider

Mündliche Prüfung am 14.07.2021

To Maria and my parents

“It was one of those events which at a crucial stage in one's development arrive to challenge and stretch one to the limit of one's ability and beyond, so that thereafter one has a new standard by which to judge oneself.”

Kazuo Ishiguro, The Remains of the Day

Part of this work was published or presented at conferences:

Publications

· N. Raddaoui, S. Croce, F. Geiger, A. Borodavka, L. Möckl, S. Stazzoni, B. Viverge, C. Bräuchle, T. Frischmuth, H. Engelke, T. Carell. *ChemBioChem*. **2020**, Accepted Article. *Super-sensitive multi-fluorophore RNA-FISH for early virus detection and flow-FISH using click chemistry.*

· I. N. Michaelides, N. Tago, B. Viverge, T. Carell. *Chem. Eur. J*. **2017**, 23, 15894-15898. *Synthesis of RNA Containing 5-Hydroxymethyl-, 5-Formyl-, and 5-Carboxycytidine*.

· N. Raddaoui, S. Stazzoni, L. Möckl, B. Viverge, F. Geiger, H. Engelke, C. Bräuchle, T. Carell. *ChemBioChem*. **2017**, 18, 1716-1720.
Dendrimer-Based Signal Amplification of Click-Labelled DNA in Situ.

· M. Ehrlich, M. Gattner, B. Viverge, J. Bretzler, D. Eisen, M. Stadlmeier, M. Vrabel, T. Carell. *Chem. Eur. J*. **2015**, 21, 7701–7704.
Orchestrating the biosynthesis of an unnatural pyrrolysine amino acid for its direct incorporation into proteins inside living cells.

Conference presentation

· Lecture presentation:

„*Synthesis of click-chemistry based probes for the detection of specific gene sequences"*

COST Action 1201 (April 2016, Grenoble, France).

Acknowledgments

Herewith, I would like to express my sincere gratitude to all of those who have made this work possible through their help and support.

First and foremost, I am grateful to Prof. Dr. Thomas Carell who offered me the opportunity to join his group and carry the research projects presented in the following pages within the best possible conditions. I greatly appreciated the support and guidance received while benefiting from a high level of trust and independence.

I want to thank Frau Slava Gärtner for her kindness, helpfulness and availability when it came to administrative matters.

I would like to warmly thank Frau Sabine Voß, Kerstin Kurz and Kristof Hufnagel for the fantastic technical support.

I am grateful to Dr. Markus Müller for his scientific inputs and general supports dealing with the everyday challenges of the lab.

I would like to thank Dr. Iacovos Michaelides and Dr. Nobuhiro Tago for their excellent collaboration on the project aiming at the synthesis of a new RNA phosphoramidite.

Special acknowledgments to my former lab mates Kristof Hufnagel, Dr. Charlotte Ebert, Dr. Michael Stadlmeier, Dr. Hidenori Okamura and Dr. Gengo Kashiwasaki. I will always remember the pleasure to work in such a friendly environment and how valuable our collaborations and support to each other have been.

For their careful proofreading and critical comments of my thesis, I am grateful to Dr. Samuele Stazzoni, Dr. Michael Staddlmeier, Dr. Nobuhiro Tago and Leander Runtsch.

I would like to thank the rest of the Carell Group for the wonderful time and the excellent working atmosphere.

Eventually, I would like to express my gratitude to my parents for their constant support in all my decisions and through all the challenges, I have encountered. Likewise, I feel enormously grateful towards my partner and wife-to-be Maria for her love and encouragements.

TABLE OF CONTENTS

TABLE OF CONTENTS I

SUMMARY IV

1. INTRODUCTION 1

1.1 DNA functionalisation by click chemistry 1

1.1.1 DNA 1

1.1.2 Cu(I)-catalysed azide-alkyne cycloaddition 3

1.1.3 CuAAC reaction on nucleic acids 7

1.2 Bioassays based on nucleic acid amplification 9

1.2.1 Real-time Polymerase Chain Reaction 9

1.2.2 Proximity Ligation Assay 14

2. DEVELOPMENT OF A CLICK CHEMISTRY-BASED PROXIMITY LIGATION ASSAY 16

2.1 Objectives 16

2.2 Synthesis of azide functionalized ODN 18

2.2.1 Strategy 18

2.2.2 Synthesis of unsymmetrical picolyl azide/azide linkers 20

2.2.3 Click experiments 24

2.3 Synthesis of alkyne functionalized ODN 28

2.3.1 Strategy 28

2.3.2 Synthesis of picolyl azide/alkyne-TMS linkers 29

2.3.3 Click experiments 30

2.3.4 Synthesis of picolyl azide/alkyne-TES linkers 32

2.3.5 Click experiments and deprotection 35

2.4 ODN design and synthesis 40

2.4.1 Design parameters 40

2.4.2 ODN synthesized 41
2.4.3 Melting temperature (Tm) measurement 44
2.4.4 Click test with dyes 45
2.5 CLICKPLA experiments 46
2.5.1 Double conjugation experiments 46
2.5.2 Concentration experiments 49
2.5.3 Reaction time experiments 50
2.6 Conclusions and Outlook 52
3. SYNTHESIS AND INCORPORATION OF 5-CARBOXYCYTIDINE PHOSPHORAMIDITE IN SYNTHETIC RNA 55
3.1 Objectives 55
3.2 Design and protecting group strategy 57
3.3 Synthesis of a caC RNA phosphoramidite building block 59
3.4 Solid phase synthesis of RNA strands containing caC 61
3.5 Solid phase synthesis of a RNA strand containing all the C modifications 63
3.6 Enzymatic digestion and uHPLC-MS analysis 65
3.7 Conclusions and Outlook 66
4. EXPERIMENTAL 67
4.1 General Methods and Materials for Synthesis 67
4.2 Chemical synthesis 69
4.2.1 Synthesis of the picolyl azide-PEG_{10}-azide linker (17) 69
4.2.2 Synthesis of the picolyl azide/bis-azide linker (19) 73
4.2.3 Synthesis of the picolyl azide-PEG_{11}-TMS protected alkyne linker (34) 80
4.2.4 Synthesis of the picolyl azide-PEG_{11}-TES protected alkyne linker (37) 84
4.2.5 Synthesis of the picolyl azide/bis-TES protected alkyne linker (40) 86
4.2.6 Synthesis of C8-alkyne-dU 93
4.2.7 Synthesis of the caC phosphoramidite building block (42) 96

4.3 Oligonucleotide synthesis 105
4.3.1 General information 105
4.3.2 Synthesis and deprotection of oligodeoxynucleotides containing C8-alkyne-dU 105
4.3.3 Synthesis and deprotection of oligonucleotides containing caC 106
4.4 Click protocols 108
4.4.1 Oligodeoxyribonucleotide functionalization, characterisation and purification ... 108
4.4.2 Template-assisted double conjugation 109
4.5 Biochemical experiments 110
4.5.1 Melting Curve Experiments 110
4.5.2 DNA PAGE 110
4.5.3 Enzymatic digestion of ON 111
4.6- UHPLC-MS analysis 112
5. ABBRIEVATIONS 113
6. REFERENCES 117

SUMMARY

Proximity ligation assays are powerful tools for sensitive detections of proteins. These assays are usually performed with two DNA-tagged aptamers or antibodies binding at proximity to each other on the same protein or interacting proteins. Thanks to the proximity between these two probes, the DNA tags can be ligated and the resulting sequence can be amplified by PCR. Many copies of the target sequence are thus generated and the labelling of this sequence will result in a signal high enough to enable sensitive and robust detection of proteins or/and protein complexes.[1, 2]

The aim of the first project described in the present thesis was to investigate whether the so-called click reaction, could contribute to the development of the existing PLA methods. Therefore, we imagined as a proof of concept a model where three click functional oligonucleotide probes are hybridized next to each other on a single longer oligonucleotide. Upon hybridization on the latter one thus designated as the template, the probes could be conjugated by clicking with each other.

The first part of the project was to envision the synthesis of oligonucleotide probes with the desired click functional groups with reliable, effective and easy to perform protocols. As a starting point and based on previous work achieved in the *Carell* group, we used DNA strand with one alkyne-modified nucleoside incorporated by automated solid phase synthesis.[3] In order to subsequently functionalize oligonucleotides with one or two azido-groups from the single alkyne modification, we decided to rely on a chemoselective strategy (Figure 1A). It has been reported that chelating azides such as picolyl azide are significantly more reactive than non-chelating azides towards CuAAC reactions.[4] This difference in reactivity is such that on small molecules bearing both a picolyl azide and a normal azide, the picolyl azide can be clicked selectively to an alkyne molecule.[5] The non-chelating azide is thus left unreacted and available for a second click reaction. Here, we examined if this strategy could be applied to longer linkers to match our needs. Therefore, we synthesized two unsymmetrical linkers; a first one with one picolyl azide and one non-chelating azide and a second one with one picolyl azide and two non-chelating azide. These linkers were effectively and with very good selectivity clicked to alkyne-modified oligonucleotides thus providing DNA strands functionalized with

one or two azido-groups. Next, we applied a sequential strategy to obtain oligonucleotides with long alkyne functions. The idea here was to synthesize unsymmetrical linkers with one azide at one extremity and one or two protected alkynes on the other extremities. Following the conjugation of these linkers by CuAAC to alkyne modified DNA strands, the protecting group(s) of the alkyne of the linkers was removed leaving it free for further reactions (Figure 1B). This method also proved to be fast, reliable and did not require an extra purification step after the deprotection of the alkyne.

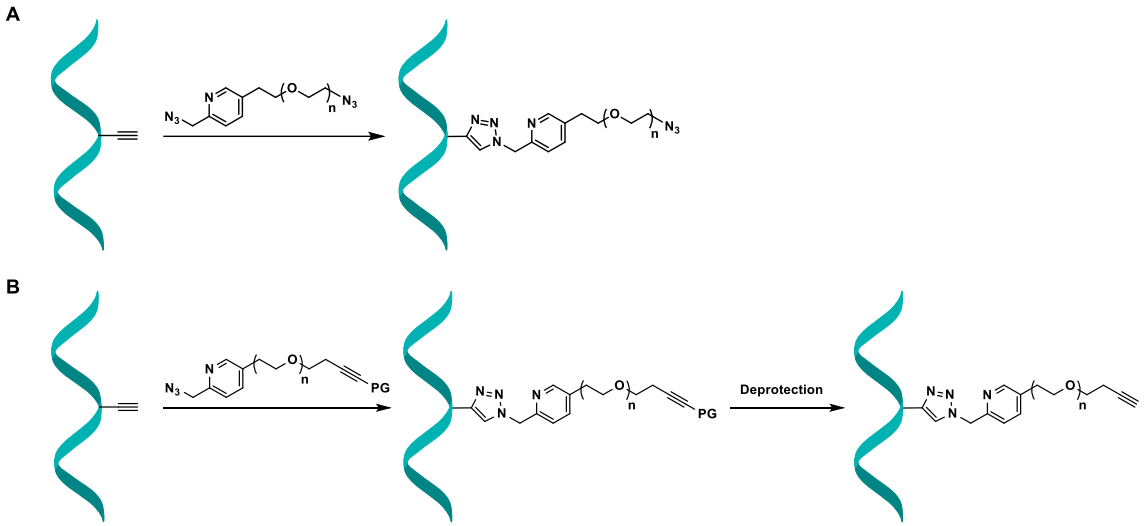

Figure 1: DNA functionalization strategies.

Based on these results, we designed and synthesized two sets of oligonucleotide probes of respectively 11- and 15- mer strands. Each set featured three probes, two single alkyne functionalized side probes and one double azide middle probe as well as a complementary oligonucleotide template. Both sets of probes were hybridized on their respective template and conjugated to each other by CuAAC. The reactions were analysed on denaturing PAGE and showed the successful formation of the double conjugated product between the three probes thanks to the proximity effect provided by the template (Figure 2).

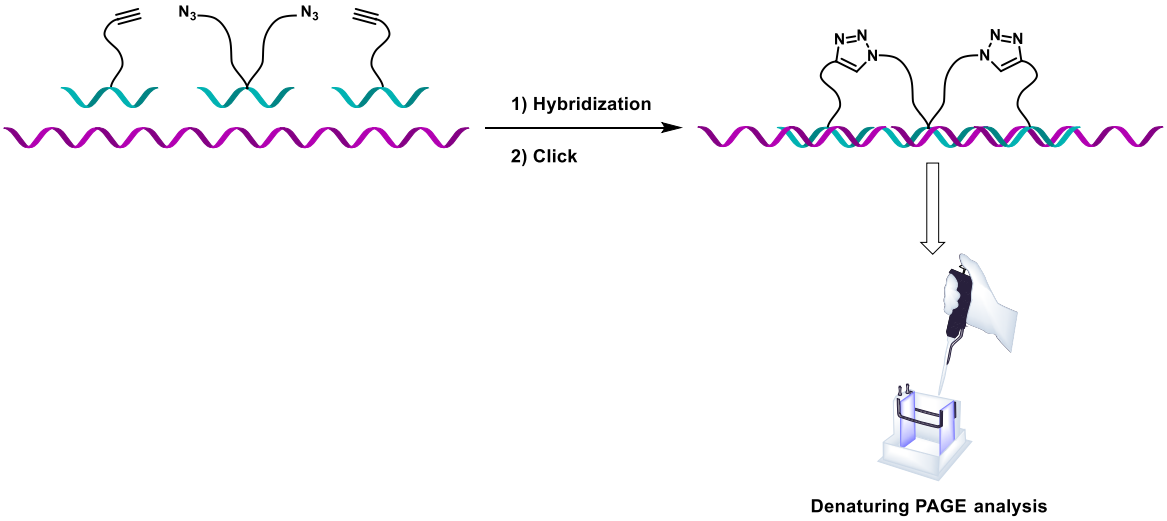

Figure 2: Schematic presentation of the click-chemistry based proximity ligation assay workflow.

Epigenetics could be defined in simple words as the regulations of the gene expression which do not involve changes of the DNA sequence.[6] Different mechanisms co-exist in order to control the gene activities across several layers of regulatory information. At the DNA level, the canonical base cytosine undergoes a chemical reaction in which a methyl group is added on the position C(5). The 5-methylcytosine modification is an epigenetic mark and its presence onto a gene promoter results in the repression of the gene transcription.[7] The discovery during the last years of oxidized derivatives of 5-methylcytosine suggests that the DNA demethylation occurs through a cascade of oxidation reactions at the C(5) position. Thus, 5-methylcytosine is successively transformed into 5-hydroxymethylcytosine (hmC), 5-formylcytosine (fC) and 5-carboxycytosine (caC).[8]

Recently, these modifications have also been discovered in the mRNA of mammalian cells.[9, 10, 11, 12, 13] While hypotheses are being formulated regarding their role within RNA, their exact functions remain elusive and are still to be elucidated. In order to study the structural and functional roles of hmC, fC and caC in the context of RNA, it is essential to access synthetic RNA material containing one or several of these bases at defined positions.

Within the frame of this PhD thesis and as a team-work from the Carell Group, we aimed at developing synthesis towards new RNA phosphoramidite building block the three modified bases. We designed these phosphoramidite building blocks in order to be compatible with

standard automated solid phase synthesis conditions so that they could be routinely used in RNA synthesis.

The present thesis focused on the development of the caC building block. The first step was to design a suitable protecting group strategy. Indeed, the corresponding phosphoramidite needed protecting groups able to resist the solid phase synthesis conditions while being easily removed after the synthesis and without arming the newly generated synthetic RNA strand. As RNA is inherently less stable than DNA, notably towards hydrolysis, it required the use of protecting groups cleavable in mild conditions. Once the design established, we envisioned and performed the synthesis of the caC RNA building block. The new phosphoramidite was successfully incorporated by automated solid phase synthesis and subsequent deprotection steps allowed the synthesis of two RNA strands of different length, respectively 13-mer and 21-mer, containing the caC-modified base at a defined site. In a similar workflow, new RNA phosphoramidite of the modified bases hmC and fC were developed in parallel. In order to prove that the three modified-cytosine RNA phosphoramidites are compatible with regular canonical bases phosphoramidites as well as with each other, we ultimately synthesised a RNA strand containing all the three modified bases.

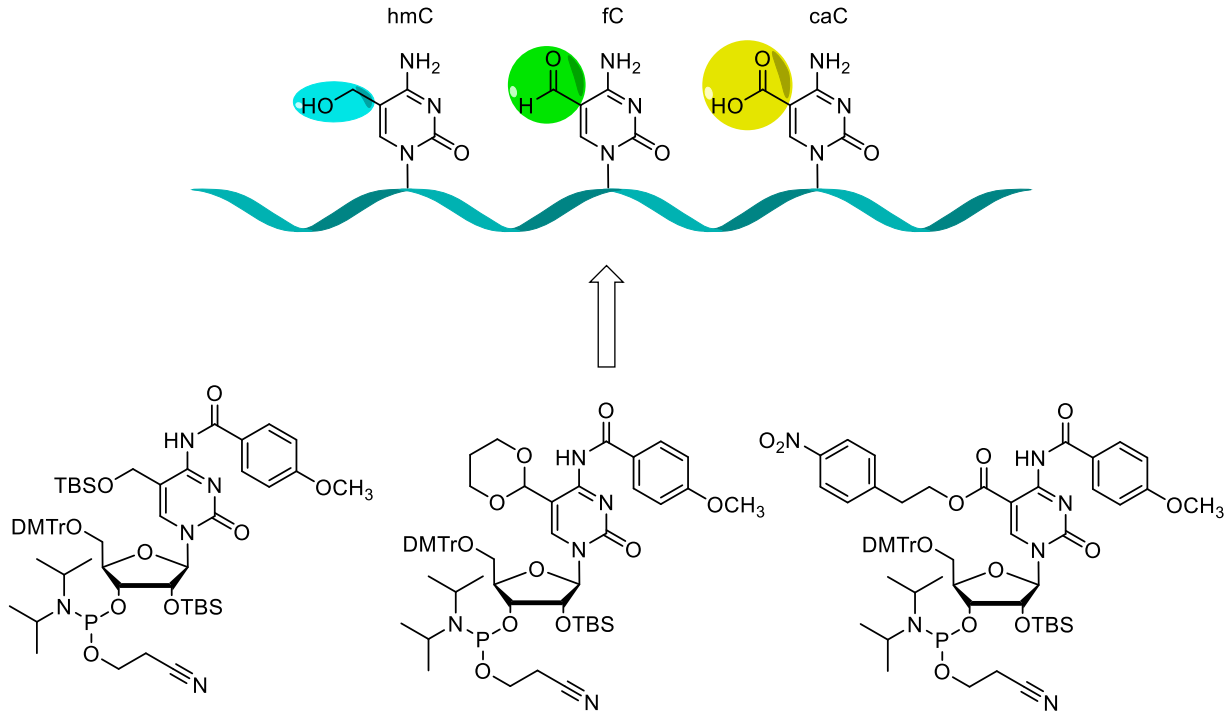

Figure 3: Depiction of the phosphoramidite building blocks developed for the synthesis of RNA containing the modified bases hmC, fC and caC.

1. INTRODUCTION

1.1 DNA functionalisation by click chemistry

1.1.1 DNA

DNA is crucial to every living organism for the storage and the transmission of the genetic information from one generation to the next.[14] Like other biomolecules, DNA is a polymer made of the repetition of similar monomer building blocks. In the case of DNA, there are four monomer units so-called nucleotides. These are composed of a deoxyribose sugar unit, a nitrogenous base (adenine (A), cytosine (C), guanine (G) or thymine (T)) and a phosphate group. In the DNA polymer, the nucleotides are linked to each other via phosphodiester bonds at the 5'- and 3'- hydroxyl group of the deoxyribose. The nucleotide sequence defines the genetic information. DNA is therefore well representative of the biochemical principle stating the close relation between molecular structure and function of the biomolecules.[14]

In 1869, DNA was isolated for the first time from white blood cells by Friedrich Miescher.[15] As he isolated it from the nuclei of the cell, Miescher named the novel substance nuclein. This name remains in today's designation deoxyribonucleic acid. The components of DNA, as well as the nature of the phosphate-sugar bond linking them together, were identified by Phoebus Levene in 1919.[16] It is only in 1944 that the role of carrier of the genetic information was assigned to DNA by Avery *et al*.[17] After isolating and purifying DNA from a strain of pneumococcus, they transferred it to a different strain of bacteria, which was transformed. Thus, they showed that DNA was responsible for the transmission of the genetic information and not proteins as believed until then. James Watson and Francis Crick eventually deduced the structure of DNA in 1953 from X-ray diffraction data obtained by Rosalind Franklin.[18, 19, 20] The structure is an antiparallel double helix composed of two strands. Although several conformations of the double helix exist, genomic DNA is mostly found in the right-handed B-form.[21] In this conformation, the helix makes a full turn every ten bases. The sugar-phosphate backbone of the DNA polymer is facing outside while the nitrogenous bases are in the inside of the double helix. The two strands are held together by hydrogen bonds between the bases of the opposite strands. A forms a specific base pair with opposite in the double helix T by two hydrogen bonds while C and opposite G are specifically paired by three hydrogen bonds. This

specific base pairing is responsible for the conservation of the genetic information.[20] Indeed, the sequence of bases in one strand determines the sequence of the other strand. Therefore, when the double helix is split into two strands, each strand can act as a template for the formation of its complementary strand thus allowing the replication of the parent double helix into two identical copies.[22]

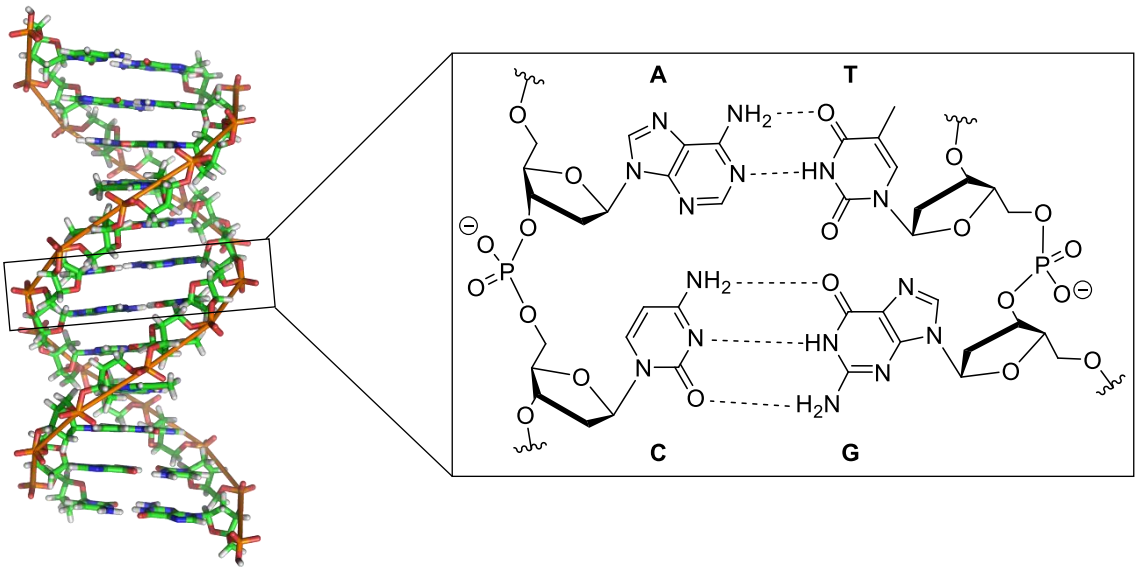

Figure 1.1: Three-dimensional structure of the DNA double helix and representation of the four nucleotide chemical structures, phosphate-sugar bond and selective base pairs between A:T and C:G (hydrogen bonds represented as dotted line).

The genetic information carried by a DNA molecule is encoded by the nucleotide sequence. In order to generate this information, the DNA serves as the template for the formation of a messenger RNA (mRNA) during the so-called transcription process. This mRNA is an intermediate of the protein synthesis and is further translated into a sequence of amino acids. The relationship between the sequence of bases of the mRNA and the sequence of amino acids is defined by the genetic code.[23, 24] It consists of three bases, called a codon, specifying one amino acid and it is universal for all organisms.

1.1.2 Cu(I)-catalysed azide-alkyne cycloaddition

The Cu(I)-catalysed azide-alkyne cycloaddition, abbreviated CuAAC, is a 1,3-dipolar cycloaddition reaction resulting in the formation of a 1,2,3-triazole. The CuAAC reaction is considered to be a catalysed version of the thermally induced reaction originally described at the end of the 19th century by Michael.[25] As its mechanism and synthetic applications were extensively studied by Huigsen in the 1960s, it became known as the Huigsen cycloaddition.[26, 27] In 2001, the use of Cu(I) to catalyse the reaction was reported for the first time by Tornøe and Meldal in the context of solid-phase peptide synthesis.[28] One year later, the reaction gained significant attention when two independent publications by Meldal and Sharpless described the dramatic acceleration on the reaction rate provided by the Cu(I) catalysis.[29, 30] Additionally, the catalysed cycloaddition selectively produced the 1,4-disubstituted triazole as the only regioisomer whereas the original reaction provided a mixture of 1,4- **1** and 1,5-regioisomers **2** (Scheme 1.1) thus limiting its practical scope.

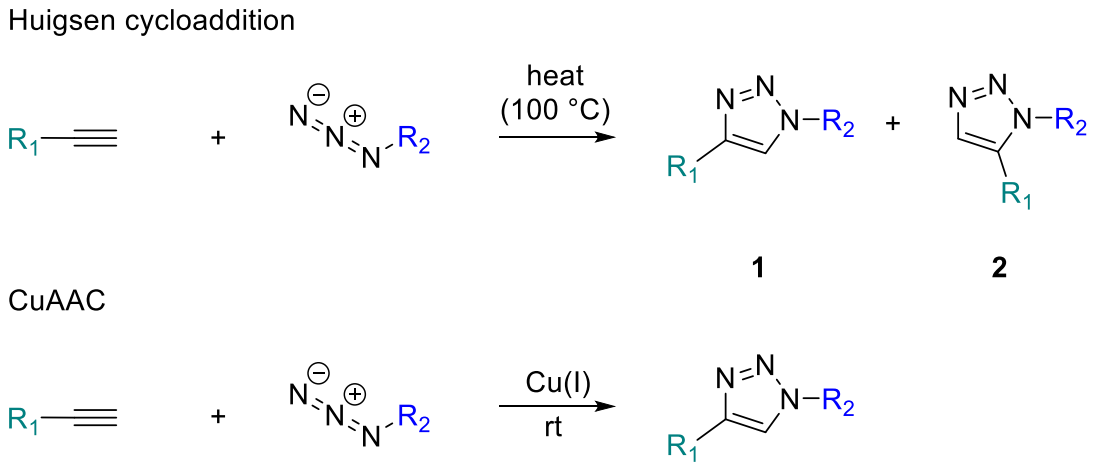

Scheme 1.1: Schematic representation of the Huigsen cycloaddition and the CuAAC.

The reaction in the absence of catalyst has a very high activation barrier (~25 kcal/mol for propyne with methyl azide) and consequently requires high temperatures and long reaction times in order to proceed.[31] The addition of Cu(I) catalyst results in an alternative mechanism during which the reaction proceeds in a stepwise manner via a pathway with notably lower activation barrier. The rate of the reaction is thus increased by a factor superior to 10^7.[31]

The mechanism of the CuAAC reaction has been the subject of much debate and studied since the first mononuclear model proposed by Fokin, Sharpless and co-workers.[30, 31, 32, 33, 34, 35] The commonly accepted current model relies on the formation of dinuclear copper intermediates. Indeed, in 2013 Fokin demonstrated by real-time monitoring of the reaction that dinuclear copper intermediates are involved.[33] Based on these results, Fokin proposed the following mechanism (Scheme 1.2). The first step consists in the formation of a Cu(I)-alkyne π-complex **3**. The addition of a second copper gives a σ, π-di(copper) acetylide intermediate **4** which allows the coordination of the azide **5** via the internal nitrogen to the σ-coordinated copper. The complex **6** thus formed undergoes a stepwise cycloaddition. At first, a metalocyclic intermediate **7** containing an endo- and an exocyclic copper center is formed via C-N bond formation. Elimination of the endocyclic copper forms the triazolide intermediate **8**. The protonation of the latter regenerates the copper catalyst and free the triazole **9**.

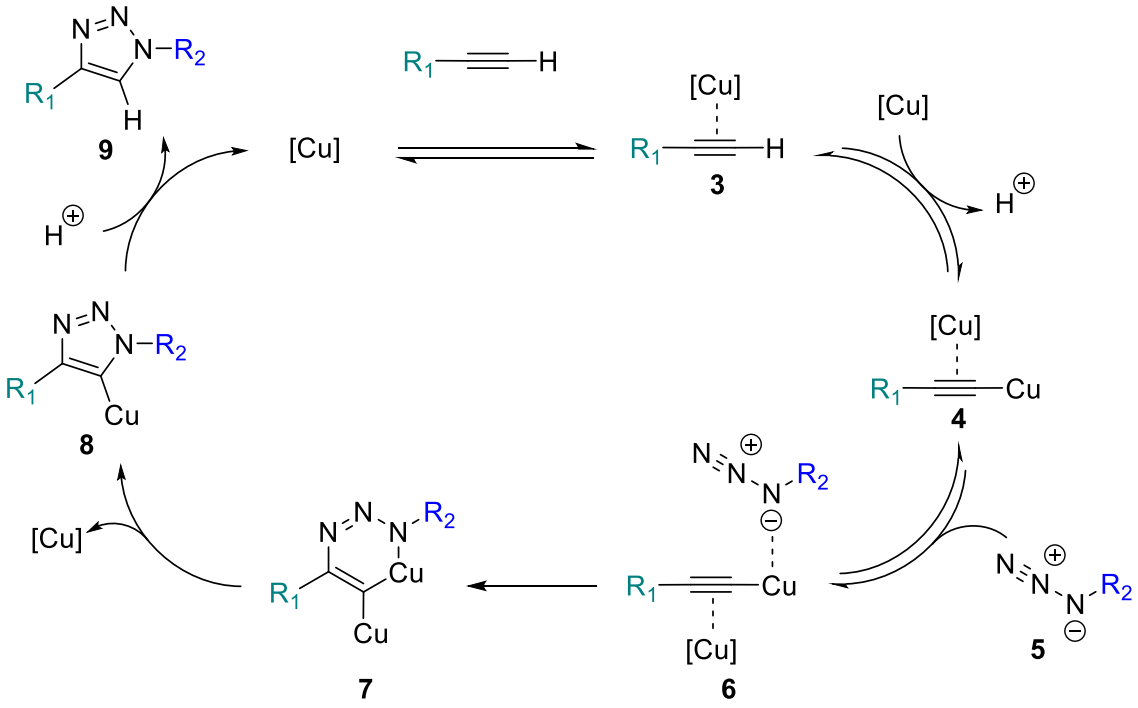

Scheme 1.2: Proposed mechanism of the CuAAC reaction according to Fokin *et al.*[33] R_1 and R_2 = any residue except H.

Since its discovery, the CuAAC reaction is considered the prototypical example of the term "click chemistry". Sharpless formulated this term in 2001 and defined a click chemistry reaction as a reaction with some of the following features:[36] modularity, wide in scope, very high yields, few and inert byproducts, stereospecific and stable in physiological conditions.

Indeed, in addition to its intrinsic impressive reaction rate and regioselectivity, the CuAAC reaction also has the benefits of being very reliable and versatile while the 1, 2, 3-triazole product is a very stable adduct. Thanks to these attributes, the CuAAC reaction has been used in a wide range of applications, from drug discovery[37] to supramolecular chemistry.[38] One speciality area of chemistry where employing the CuAAC reaction was demonstrated to be particularly advantageous is for the conjugation of biomolecules.[39] Indeed, neither alkynes nor azides functionalities naturally exist *in vivo* while both are stable under physiological conditions and inert towards the native chemical functionalities. The CuAAC is, therefore, a bioorthogonal reaction and remains to date one of the most powerful bioconjugation tools.

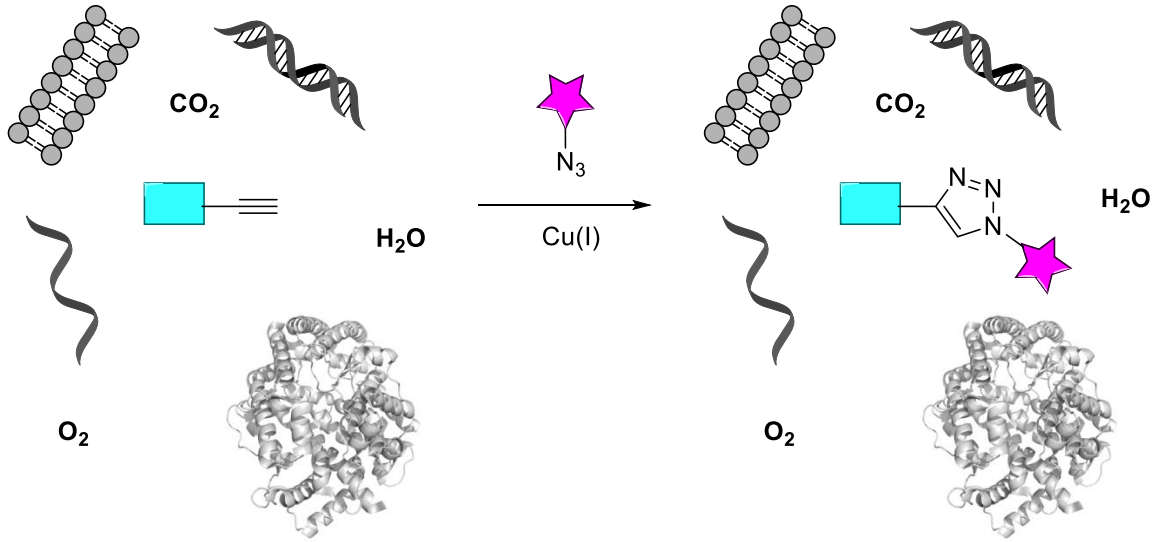

Figure 1.2: Illustration of the bioorthogonality of the CuAAC reaction.

The main limitation of the CuAAC as a bioorthogonal reaction in living systems lies in its reliance on copper catalysis since Cu(I) is potentially toxic in living systems.[40, 41] Cu(I) is unstable under physiological conditions and is oxidized into Cu(II) by O_2 or H_2O_2 via the Fenton reaction (Figure 1.3A). This process promotes, in turn, the production of the ROS superoxide and hydroxyl radicals known to cause oxidative stress to the cells and damage the biomolecules.[42]

Several strategies have been developed in order to decrease the cellular toxicity associated to the Cu(I) catalyst. One of them consists in the incorporation of copper-binding ligands to the reaction.[43, 44] Such ligands will increase the acceleration rate of the reaction by stabilizing the copper catalyst in its active oxidative state while decreasing the risk of causing oxidative stress. To date, even if a variety of ligands have been discovered to be effective, the most commonly

used ones are the ligands from the tris((triazolyl)methyl) amine class: TBTA **10**[43], THPTA **11**[44], BTTAA **12**[45] and TABTA **13**[46] (Figure 1.3B).

A second strategy for decreasing the toxic effect of the Cu(I) is to use copper-chelating azides.[4] Such chelating groups bind the copper directly at the reaction center and are reported to significantly increase the reaction rate while using lower catalyst concentrations without compromising the CuAAC efficiency. For example, in a comparative study with the corresponding non-chelating azide, the picolyl azide group (Figure 1.3C), in combination with BTTAA, provided a 25-fold enhancement in labelling proteins.[47]

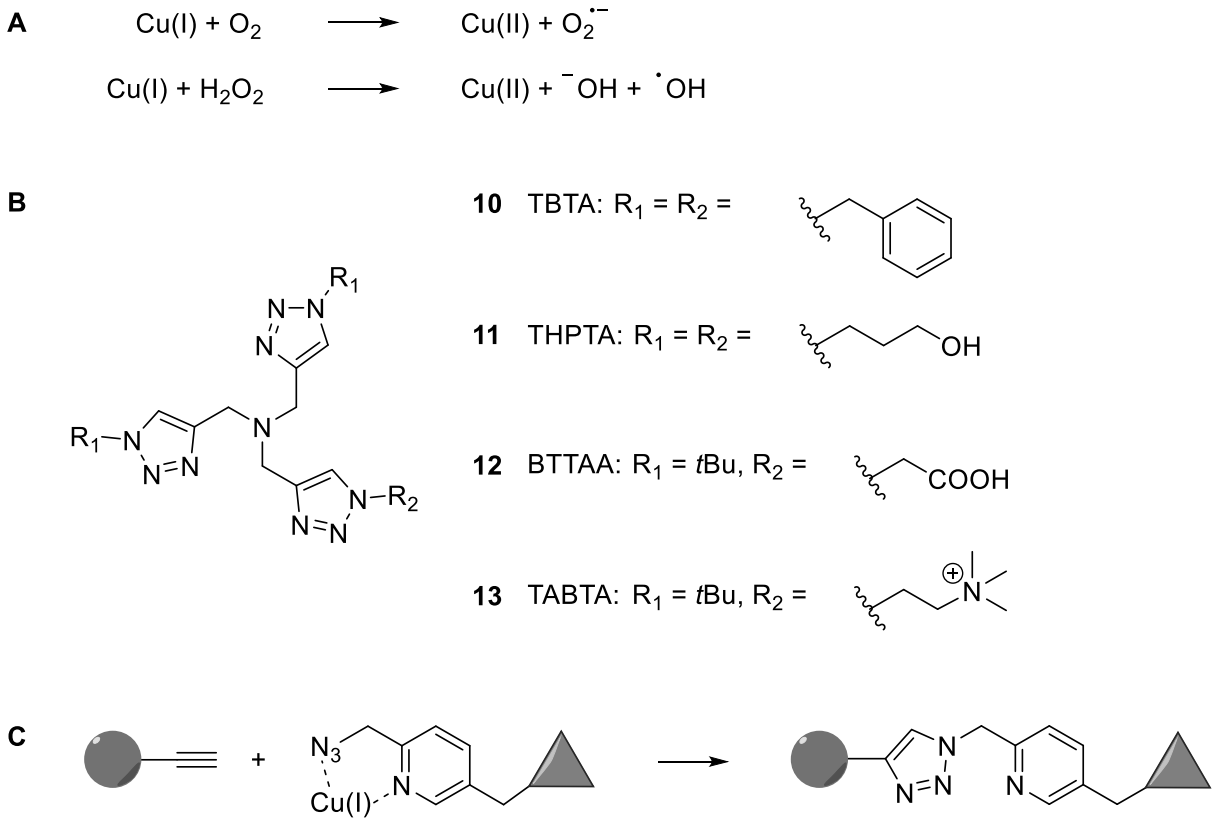

Figure 1.3: A) Cu(I)-promoted generation of ROS; B) Tris((triazolyl)methyl) amine ligands used in the CuAAC reaction; C) CuAAC reaction with a picolyl azide moiety.

1.1.3 CuAAC reaction on nucleic acids

Thanks to its fast reaction kinetics and bioorthogonality, the CuAAC found a significant number of applications in the context of DNA and RNA modifications. Examples of such applications range from the labelling of oligonucleotides with various fluorescent reporters [48, 49, 50], ligation of several DNA strands[51, 52] or surface functionalization in microarrays [53].

The three components of the nucleotide unit, the (deoxy)ribose sugar unit[54], the nucleobase and the phosphate group[55], have been subjected to chemical modifications towards the introduction of click reactive functions. However, the most common type of modifications towards the generation of clickable nucleotide analogues are located on the nitrogenous base moiety[3].

The development of such modified nucleosides as well as the methodologies to efficiently label DNA by click chemistry were initiated by the *Carell* Group. Alkyne nucleosides analogues have been introduced by both automated solid phase synthesis and enzymatic reaction. For the first approach, the synthesis of an alkyne-uridine phosphoramidite enabled the site-specific introduction of alkynes functions inside oligonucleotides[56]. These modifications proved to be compatible with the reaction conditions of solid phase synthesis and the obtained oligonucleotides could be post-synthetically labelled with a high efficiency. In parallel, the corresponding alkyne triphosphates were also synthesized and used in polymerase chain reactions.[57] Not only the modified triphosphates **14** were accepted as substrate for the enzymatic reactions, but also the subsequent click reaction on the PCR product permitted a high-density functionalization while no DNA damages were detected. Indeed, RT-PCR analysis shown that the 887 cytidines of a 2000 base pairs DNA strand had been replaced by their alkyne-modified analogue. Following click reaction with a sugar azide **15**, the DNA products were digested and analysed by HPLC revealing an impressive and almost quantitative efficiency as most alkynes had been converted into the click product.

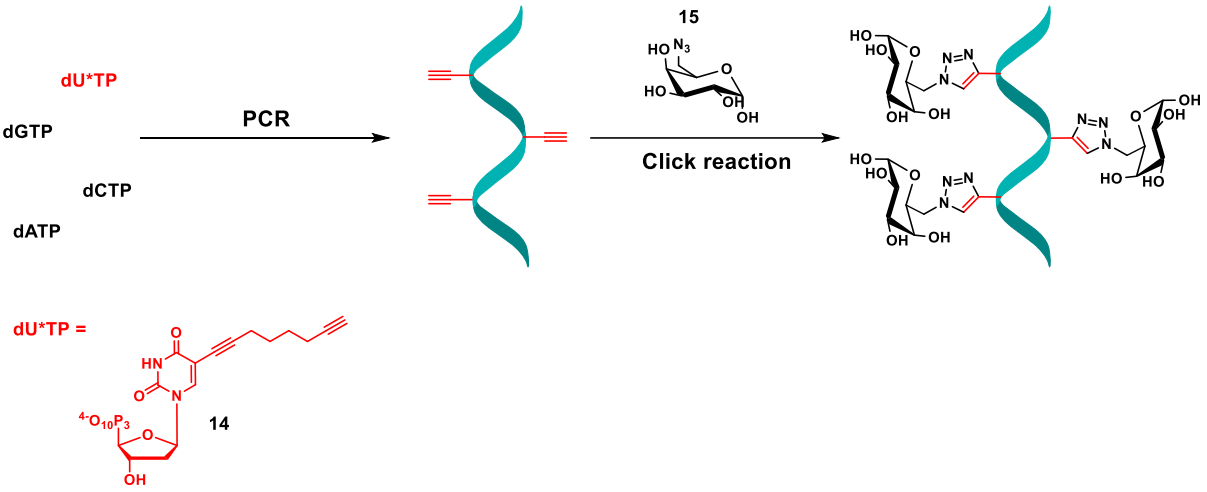

Figure 1.4: PCR in the presence of deoxyadenosine triphosphate (dATP), deoxycytidine triphosphate (dCTP), deoxyguanosine triphosphate (dGTP) and a uridine alkyne triphosphate analogue **14** (d*UTP) and subsequent click reaction of the PCR product with a galactose azide **15**.

1.2 Bioassays based on nucleic acid amplification

DNA and RNA amplification methods represent a great tool for the detection of defined nucleic acid sequences. Indeed, they provide an excellent specificity thanks to the strong affinity between two complementary oligonucleotide strands. Moreover, the intrinsic exponential amplification enables the generation of a large number of identical copies of a target sequence and therefore a potentially very high detection sensitivity. This is particularly important when very small amount of material available to analyse. This can be the case in clinical diagnostics where human samples are being analysed and nucleic acid amplification represents thus a valuable detection method in many areas.

1.2.1 Real-time Polymerase Chain Reaction

Several strategies have been described towards the amplification of DNA or RNA such as polymerase chain reaction (PCR)[58, 59], strand displacement amplification[60] or self-sustaining sequence amplification[61]. PCR was the first of these methods to be developed in the 1980s by Kary Mullis and remains to date the most commonly used one. A PCR assay is performed according to the following steps: first, the reaction solution is heated above the melting point of the complementary DNA strands of the target to be amplified and detected. Once the strands are separated during this so-called denaturing step, the temperature is decreased to allow the primers to bind specifically to the target sequence. This is the annealing step, which is followed by a new increase of temperature enabling the DNA polymerase to extend the primers by adding the nucleoside triphosphates to the developing DNA strand complementary to the target sequence. This completes once cycle of PCR, which is repeated numerous times. At the end of each step, the number of identical copies of the target sequence is doubled and within a few hours, millions of copies are generated.

Table 1.1: Reagents and equipment required for a PCR assay.

Reagents and equipment	Description
Target sequence (or template)	Segment of nucleic acid to be amplified
Deoxynucleoside triphosphates	Building blocks for the construction of the PCR products

Table 1.1: Continued.

Primer	Short DNA strand complementary to a sequence of the target to be amplified
DNA polymerase	Enzyme synthesizing new complementary copies of the target sequence
Thermocycler	Equipment in which the PCR assay is performed. Able to raise and lower the temperature of the samples in precise and pre-programmed steps.[62]

The first PCR application was reported in 1985 and performed for the diagnosis of the genetic disorder sickle cell anemia.[63] The DNA polymerase used was an enzyme isolated from *E. coli*, Klenow fragment DNA polymerase I. However, this enzyme was destroyed at the temperature of the denaturing step and it was necessary to add fresh enzyme for each cycle. An important development for the PCR assays was the introduction of a thermostable DNA polymerase from the bacteria *Thermus aquaticus* (Taq).[64, 65] The latter belongs to a species of bacteria tolerating high temperatures and its enzymes can survive and sustain their activities accordingly. The Taq DNA polymerase can survive the incubation temperature of the denaturing step and it is mostly active at 70 °C. Thus, it circumvented the necessity of adding fresh enzyme at each PCR cycle making the whole assay easier to perform and more rapid and efficient.

A second important advancement for PCR assays was the demonstration of real-time PCR by Higuchi *et al.* at Roche Molecular Systems at the beginning of the 1990s.[66, 67] Indeed, PCR products were formerly detected and visualized by agarose gel electrophoresis. The introduction of real-time PCR permitted the coupling of the tremendous intrinsic sensitivity of PCR to the precision gained from real-time monitoring and detection of amplification products as they are generated. The initial real-time PCR described relied on the double-stranded DNA intercalating fluorescent dye ethidium bromide and the reaction was run under UV light. As the ethidium bromide was intercalated in the increasing amount of DNA produced at each cycle, it induced an increase of fluorescence upon irradiation of the UV light inside the thermocycler. Moreover, by measuring the increase of fluorescence after each cycle, it also allowed the accurate calculation of the initial amount of target DNA. In this regard, the terms real-time and quantitative PCR are often used in combination or as interchangeable. The first commercial instrument was made available on the market in 1996 by Applied Biosystems and it was followed by numerous other companies.[68] The influence of the assay is also reflected

in the number of scientific publications citing real-time quantitative PCR as their number went through an exponential growth over about 10 years following its commercialization.[69]

Since its first iteration by Higuchi *et al.*, many methods for the detection of the PCR product have been described. They can be divided into two categories depending on whether they detect only specific or both specific and non-specific amplification products. For the latter category, double-stranded DNA intercalating agents such as the previously-mentioned ethidium bromide,[66, 67] SYBRGreen,[70] or EvaGreen are used.[71] Specific probes, however, are based on oligonucleotides linked with a fluorescent reporter. Here as well, the specificity of such probes lies in the complementarity between the probe strand and a sequence of the DNA target. These probes can induce the emission of fluorescence upon hybridization by diverse mechanism of actions. The different types of probes thus existing can be distinguished as following: primer-probes acting as a primer with the target sequence; hybridization probes emitting fluorescence upon hybridization on the target sequence; hydrolysis probes emitting fluorescence upon degradation of the probe after hybridization to the target sequence; analogues of nucleic acids with mechanisms of action similar to the previous probes but whose structure is not a conventional oligonucleotide. The table 1.2 provides examples of the different types of specific probes.

Table 1.2: Real-time PCR specific probes.

<table>
<tr><td colspan="2">Primer probe – Scorpions[72]</td></tr>
<tr><td colspan="2"> 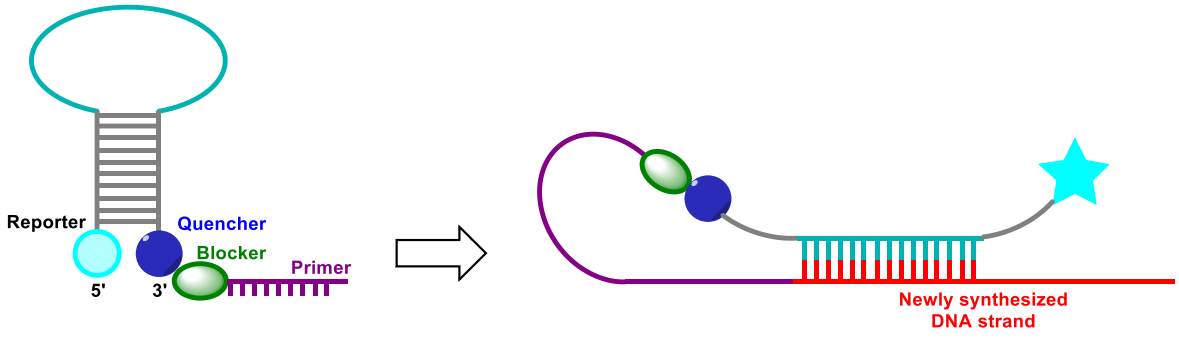
</td></tr>
<tr><td>Structure</td><td>Mechanism of action</td></tr>
<tr><td>Hairpin structure with a reporter at the 5′-end and a quencher at the 3′-end of the hairpin. The latter is attached to the 5′-end of the primer by a short PEG blocker blocking its extension by the polymerase.</td><td>When in solution, the reporter fluorescence is quenched by the proximity with the quencher by FRET-quenching. Once the primer-probe is hybridized on the target DNA, the polymerase amplifies the sequence from the 3′-end of the primer. During the denaturation step, the specific sequence of the probe binds to the complementary region within the same strand of newly amplified DNA. This hybridisation event opens the hairpin loop so that fluorescence is no longer quenched.</td></tr>
</table>

Table 1.2: Continued.

<table>
<tr><td colspan="2">Hybridization probe – Molecular Beacon probe[73]</td></tr>
<tr><td colspan="2"> 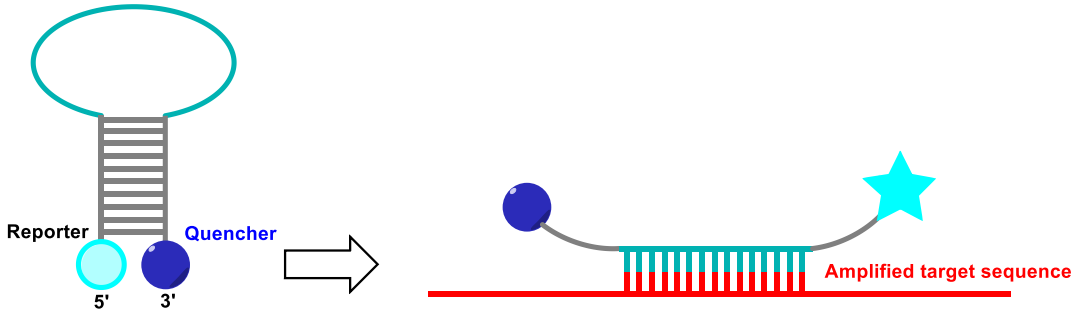
</td></tr>
<tr><td>Structure</td><td>Mechanism of action</td></tr>
<tr><td>Hairpin structure with a reporter at the 5′-end and a quencher at the 3′-end of the hairpin.</td><td>During the annealing phase, this probe unfolds and binds to the target, emitting fluorescence since the reporter is not quenched any longer. If the Molecular Beacon probe and target DNA sequences are not perfectly complementary, there will be no emission of fluorescence as the hairpin structure prevails over the hybridization.</td></tr>
<tr><td colspan="2">Hydrolysis probe – TaqMan[74]</td></tr>
<tr><td colspan="2"> 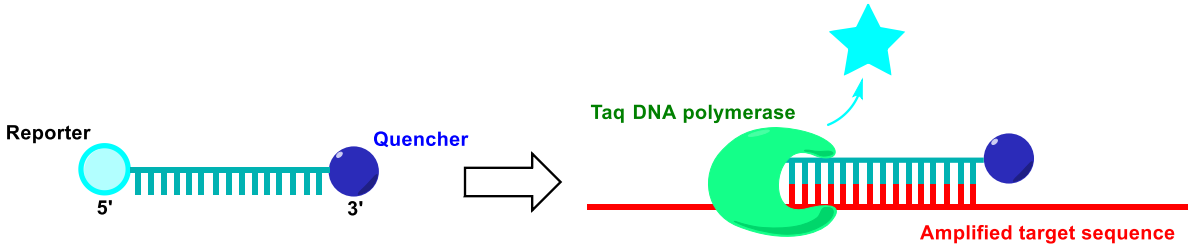
</td></tr>
<tr><td>Structure</td><td>Mechanism of action</td></tr>
<tr><td>Oligonucleotide with a fluorescent reporter at the 5′-end and a quencher at its 3′-end.</td><td>When in solution, the reporter fluorescence is quenched by the proximity with the quencher by FRET-quenching. During the amplification phase, the probe is hydrolysed by the exonuclease activity of the DNA polymerase. This leads to the departure of the reporter, which is no longer in proximity of the quencher and emits a fluorescence signal.</td></tr>
</table>

Table 1.2: Continued.

Analogues of nucleic acids – PNAs[75] and LNAs[76]	
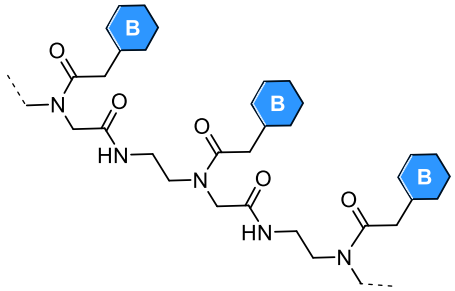 PNA 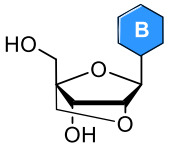 LNA monomere	
Structure	Mechanism of action
PNAs or LNAs probes.	The mechanisms of action of PNAs and LNAs probes are similar to the conventional oligonucleotide ones.

Thanks to its impressive sensitivity and ease of use, real-time quantitative PCR has been widely employed in many different fields of application. It has for example been used in biomedical research for the genotyping of mutations and in particular for single nucleotide polymorphisms by automatically performing a melting curve analysis after completion of the PCR.[77] As a molecular diagnostic tool, it proves its usefulness for the detection of bacterial and viral genetic material.[78] Indeed, it offered the possibility to detect pathogen-specific sequences within complex sample mixture. Another field where the capability to detect low amount of a specific gene sequence represents an important potential is in clinical oncology.[79] Real-time PCR intrinsic sensitivity and precision not only allowed better detection of disease but also provided a convenient tool to measure accurately the efficacy of a given treatment.

1.2.2 Proximity Ligation Assay

One successful method based on nucleic acid amplification and developed for *in vitro* detection and visualisation of proteins is the proximity ligation assay (PLA). PLA was first demonstrated in 2002 by Landegren *et al*.[1] While the method has been developed since its introduction and several variations have been described, the basic principle remains unchanged.[80] The PLA relies on a pair of affinity probes for a protein target. The latter can be either a single protein or a protein complex.[81] In the first demonstration of the assay, the proximity probes used were a pair of DNA aptamers with extended sequences required for the proximity ligation reactions. Alternatively, an assay based on antibodies as affinity probes has also been developed.[82] In this case, the antibodies are attached to DNA strands. Once the two probes are close to each other by binding the same target, an oligonucleotide is hybridized on both probes at the same time. The two probes will then serve as a guide to promote the formation of circular structure from the linear oligonucleotide by joining its two extremities in an enzymatic reaction. Subsequently, one of the DNA strand probes acts as a primer in a rolling circular amplification (RCA) where the previously ligated oligonucleotide is used as a circular template. RCA is an alternative amplification method to PCR, which on the contrary is an isothermal process and does not require a thermocycler. In RCA, the polymerase continuously extends the primer due to the circularity of the template. Therefore, the amplification product is a long DNA single strand remaining attached to the primer and with thousands of successive repetitions of the complementary sequence of the circular template.[83] The amplification product can be detected by fluorescence *in situ* hybridization (FISH) with complementary oligonucleotide probes and its signal can be easily observed with a microscope. Thanks to the extremely low amount of proteins that the assay is able to detect, the PLA became a valuable technology for a large variety of proteomic studies.[84]

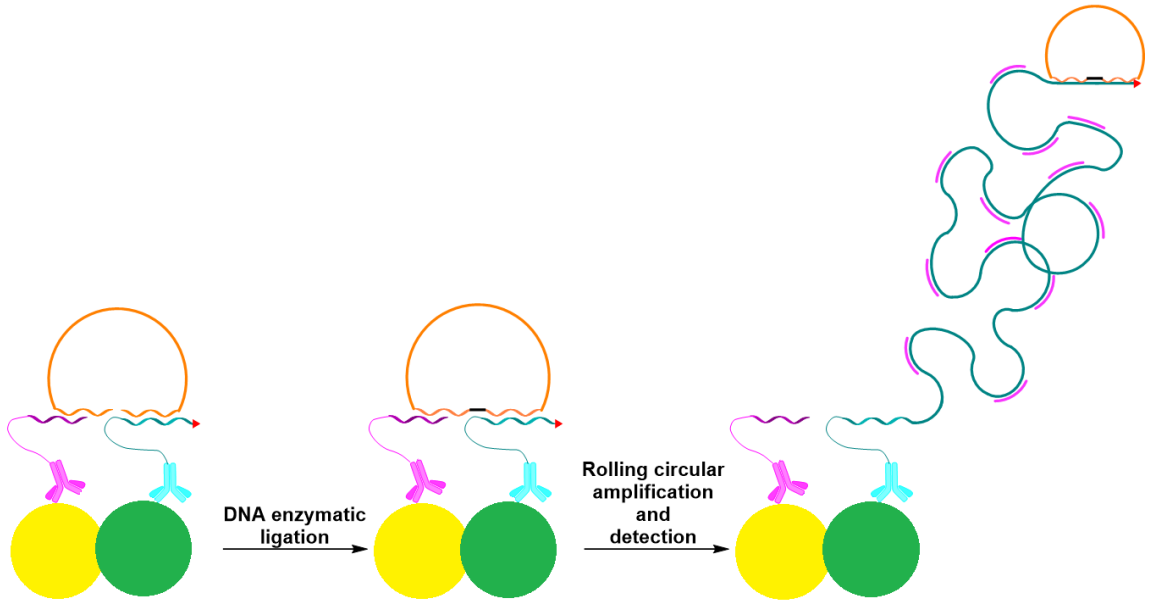

Figure 1.5: Depiction of a Proximity Ligation Assay (PLA). If two proximity probes are close to each other (pink and light blue), by binding a two-protein complex (yellow and green), then subsequently added template (orange) can be hybridized to the proximity probes and transformed into a circular structure by enzymatic DNA ligation. Rolling circular amplification (RCA) is then initiated and the amplification product is detected by FISH probes (pink).

2. DEVELOPMENT OF A CLICK CHEMISTRY-BASED PROXIMITY LIGATION ASSAY

2.1 Objectives

One of the goal of the present thesis was to investigate if the Cu(I)-catalyzed azide-alkyne cycloadditon (CuAAC) could be used in the context of a proximity ligation assay in order to push further the potential of this method. Thanks to its efficiency and its bioorthogonality, we believed that the so-called click reaction can contribute to the development of a more precise and sensitive PLA. Towards this purpose, we developed the following design as a proof of concept: Three oligonucleotide probes, functionalized with alkyne or azide functions, can hybridize with a single non-modified oligonucleotide template. Thanks to the proximity brought by the hybridization on the template, the three probes are then further conjugated to each other by click chemistry providing a single covalently bound product. The template aims therefore in this design at mimicking the proximity of the PLA to react probes when placed close to each other. This design also makes use of three probes instead of two in the PLA, adding thus one degree of precision. We therefore named this assay proof of concept click Proximity Ligation Assay (CLICKPLA). Two versions of this design have been envisioned (Figure 2.1).

One, where the middle probe bears two alkyne functions and the side probes one azide function each. A second one where the middle probe is functionalized with two azide functions and the side ones with one alkyne function each. This project involved therefore the development of the corresponding oligonucleotide functionalization chemistry as well as the synthesis of the linkers required.

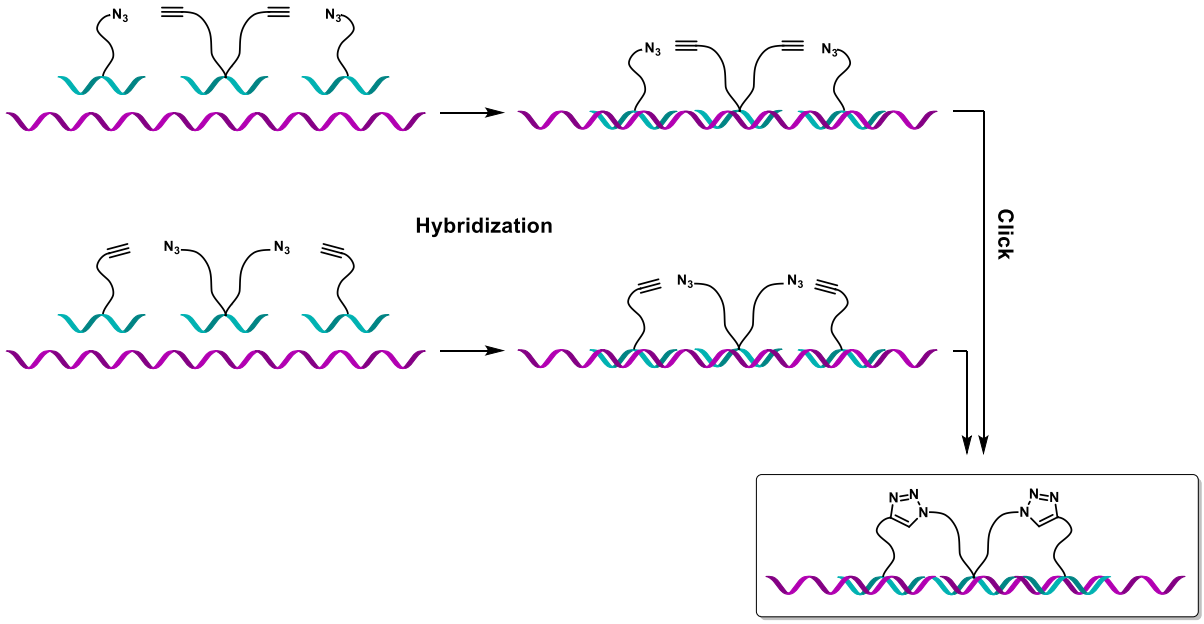

Figure 2.1: Schematic representation of the two CLICKPLA versions. The oligonucleotide probes are represented in green. The oligonucleotide templates are in purple. At first, three probes are hybridized to the complementary template. In a second time, the click reaction can be initiated and the three probes are conjugated to each other.

2.2 Synthesis of azide functionalized ODN

2.2.1 Strategy

The first part of this project was to develop a functional and reliable strategy towards the synthesis of DNA strands modified with one or two azide functions. Even if a few examples of direct incorporation of azide functions during DNA solid phase synthesis have been reported [85, 86], they are usually not compatible with with P(III) as they are prone to Staudinger-type side reactions.[87, 88]. However, for DNA strands, a post oligo synthesis functionalization step is usually performed to introduce azide functionalities and the most common approach consists in reacting an activated ester with an amino modified oligonucleotide.[89] Using this strategy, bifunctional NHS-azide linkers have been reacted with oligonucleotides carrying a modified amine nucleoside or with a 5' or 3' amino modifier.[51, 90] However, this method is not chemoselective and lacks in efficiency as NHS esters can react with other nucleophiles present on DNA. Contrary to azide moieties, alkyne ones are easily introduced during solid phase synthesis of oligonucleotides enabling post-synthetic labelling of the modified strands with various azide reporters by CuAAC.[48, 91] Thus, an alternative method to generate a DNA strand with an azide moiety is to click a symmetrical bis-azide linker on an oligonucleotide with an alkyne modified nucleobase.[92] Here again, the level of selectivity of this method is relative as the second azide group of the linker might react with another strand yet unreacted thus leading to a cross-linked side product.[93, 94] In 2009, Zhu et al. discovered that chelating azides can react in CuAAC reactions with only a small amount of copper (II) acetate (down to 1 mol %) and in the absence of a reducing agent such as sodium ascorbate.[4] This superior reactivity in comparison with non-chelating azide is explained by the chelation of the copper catalyst directly to the catalytic center of the reaction. After testing several auxiliary ligands near the azido group, they reported the pyridyl group as the best capable copper chelating group.[95] The reactivity difference between chelating and non-chelating azide is such that under specific conditions (copper (II) acetate as catalyst, no reducing agent), when both a chelating and a non-chelating azide are present, only the so-called picolyl azide is going to react with an alkyne. Based on these results, they designed unsymmetrical bis-azide (one chelating, one non-chelating) linkers and proved that both azido groups can be reacted in a sequential and chemoselective procedure with two distinct alkynes.[5] Seela et al. successfully applied this method on alkyne nucleosides and oligonucleotides with 2,5-bis(azidomethyl)pyridine as

unsymmetrical bis-azide linker.[96] We decided to adopt a similar approach tailored for the CLICKPLA. In our proof of concept design, the alkyne and azide functionalities to be conjugated with each other needs to be carried at the end of long and flexible linkers. Indeed, these chemical groups will each be incorporated in different strands and thus, short linkers would not allow the click reactions to take place as the CuAAC reactive group could not be nearby each other. Consequently, as a backbone for the linkers to synthesize, we used poly(ethylene-glycol) (PEG) chains. These polymers, contrary to alkyl chains, have the advantages to be non-rigid and water-soluble.[97] Also, they are commercially available in a wide range of lengths allowing us, had it been necessary, to modulate the length of the linkers. As the alkyne component to be incorporated within the oligonucleotides during the solid-phase synthesis, we chose the C8-alkyne-dU nucleoside developed in our group.[91] Eventually, our strategy towards the synthesis of azide functional DNA strands consisted in:

1- Synthesis of oligodeoxyribonucleotides containing one alkyne group;

2- Synthesis of unsymmetrical picolyl azide/azide long and water-soluble linkers;

3- Chemoselective CuAAC conjugation between the alkyne DNA strand and the chelating azido group of the unsymmetrical bis-azide linker leaving the non-chelating azide free and functional for further CuAAC.

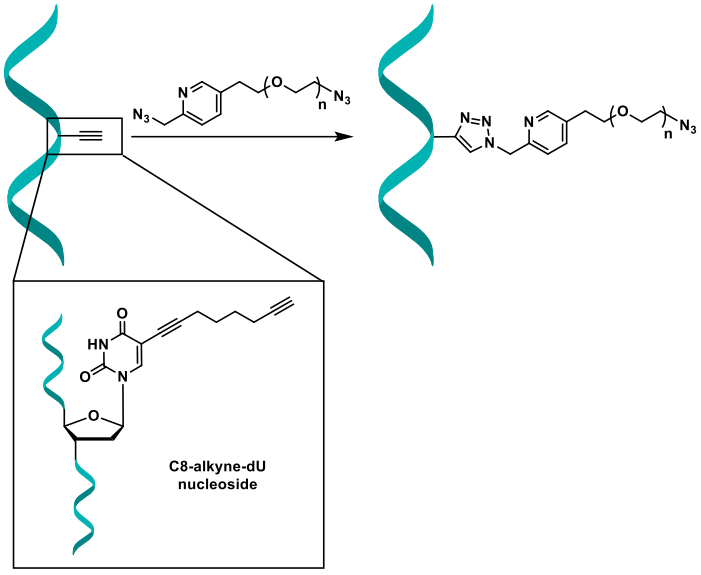

Figure 2.2: Chemoselective strategy towards the synthesis of azido functional DNA strands. The chelating azido group of an unsymmetrical bis-azide linker is conjugated by CuAAC to an oligodeoxynucleotide containing a C8-alkyne-dU artificial nucleoside in a chemoselective procedure.

2.2.2 Synthesis of unsymmetrical picolyl azide/azide linkers

The initial step in order to synthesize unsymmetrical picolyl azide/azide linkers was to obtain a picolyl azide building block able to be further conjugated in a compatible and orthogonal reaction with the azide function. We followed the published procedure from Uttamapinant *et al.* with minor adjustments giving access to a carboxylic acid picolyl azid (6-azidomethylnicotinic acid) **16**.[47] The carboxylic acid, upon activation, was further reacted with the amino group of different molecules via amid coupling. In order to generate an amine reactive ester from the carboxylic acid we used HATU as a reagent along with Hünig's base, this coupling being known to provide high coupling efficiencies and fast rates.[98] The first unsymmetrical picolyl azide-PEG_{10}-azide linker **17** was readily available in one step from coupling the carboxylic acid picolyl azid to a commercial azido-PEG-amine reactant. We chose as starting material an azido-PEG-amine with 10 poly(ethylene oxide) monomer units **18** as we assumed that it would provide a sufficient long linker for the CLICKPLA.

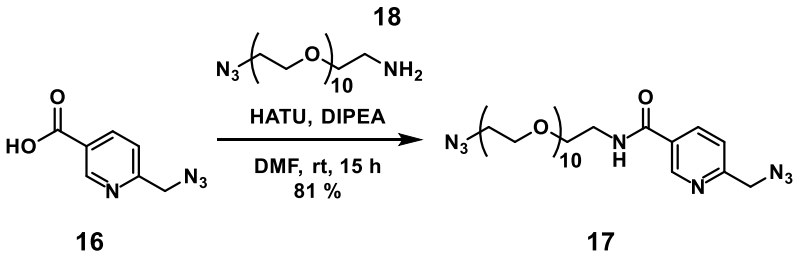

Scheme 2.1: Synthesis of the unsymmetrical picolyl azide-PEG_{10}-azide linker **17**.

In order to prepare a second linker bearing one picolyl azide and two non-chelating azido groups **19**, we imagined a synthesis based on methyl 3,5-dihydroxybenzoate **20** (Scheme 2.2). This starting building block offers the advantage of having two identical chemical groups (two hydroxyl groups) as well as a third protected one (carboxylic acid protected as methyl ester) and thus can be used as a bifunctional core.[99] Therefore, the two hydroxyl groups eventually bear the two azido groups of the final linker whereas the carboxylic acid was coupled to a picolyl azide/amine linker **21**.

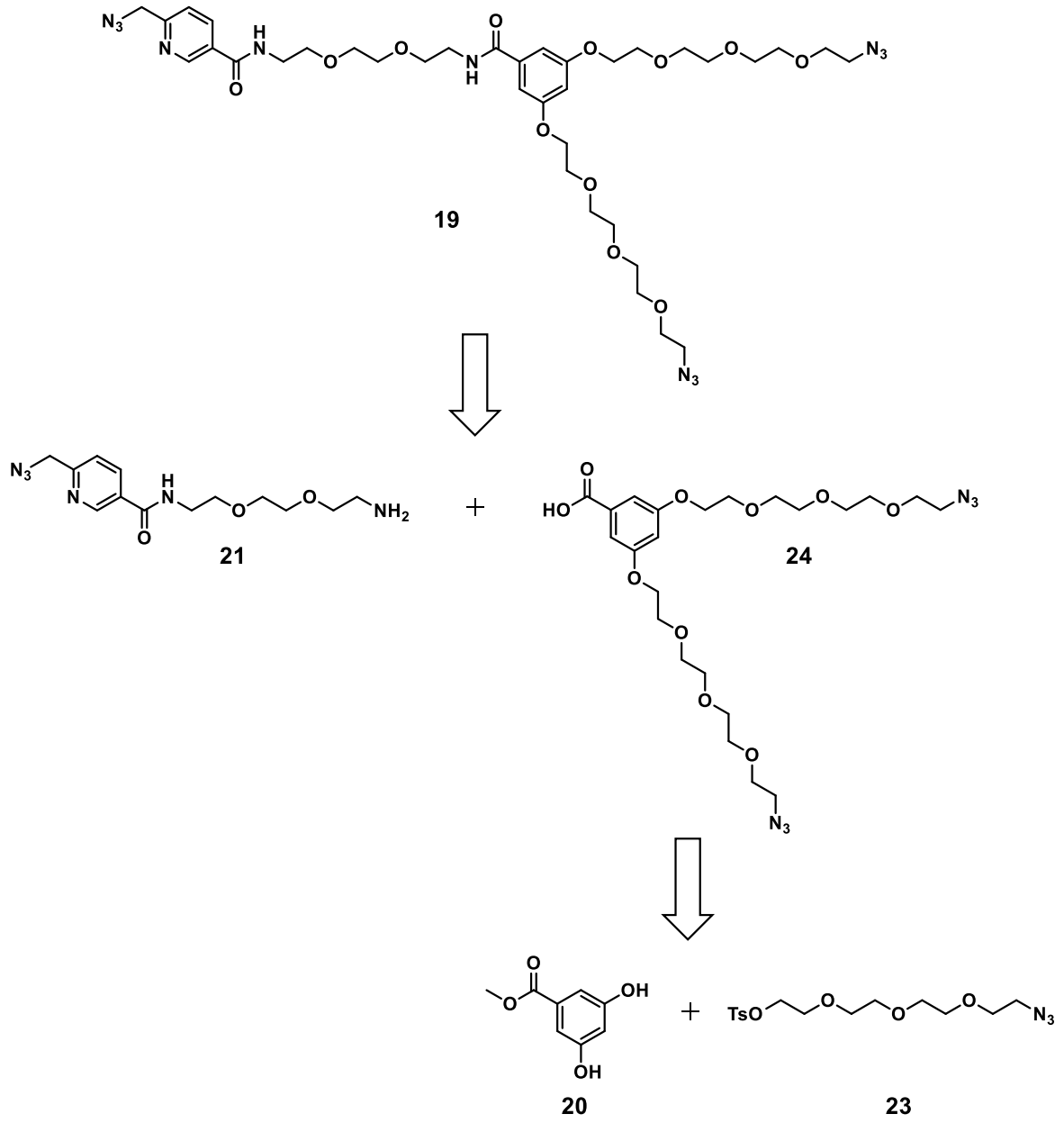

Scheme 2.2: Retrosynthetic analysis of picolyl azide/bis-azide linker **19**.

In order to functionalize the two hydroxyl groups we synthesized a linker based on tetraethylene glycol **22** and bearing on its two respective free alcohol moieties an azido group and a tosylate group **23** (Scheme 2.3). The first hydroxyl group was selectively tosylated by using tosyl chloride. In order to minimize the formation of the double tosylated unwanted product, the tosyl chloride was firstly dissolved in tetrahydrofuran and this solution was subsequently added very carefully (drip in over one hour) to a solution of tetraethylene glycol at 0 °C. The two reactants were finally in stoichiometric rate and the mono tosylated product

was obtained in a satisfying 72 % yield. In the next step the tosylate group was substituted by an azido group by stirring the compound with sodium azide salt. Lastly, the second alcohol of the tretraethylene glycol was tosylated as well.

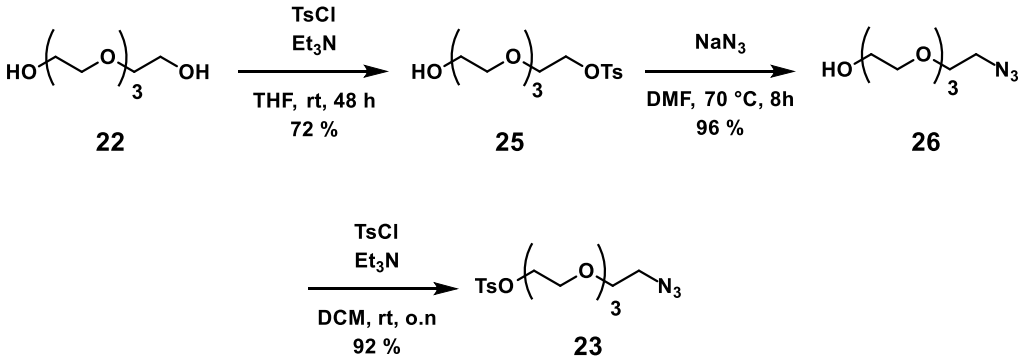

Scheme 2.3: Synthesis of the Azido-PEG$_3$-OTs linker **23**.

The carboxylic acid picolyl azide building block **16** was coupled here again using HATU to *N*-Boc- 2,2′-(ethylenedioxy)diethylamine **27** (Scheme 2.4). The Boc protecting group on the second amine was removed by a treatment with 2 M HCl to provide the short linker picolylazide-PEG$_2$-amine **21**.

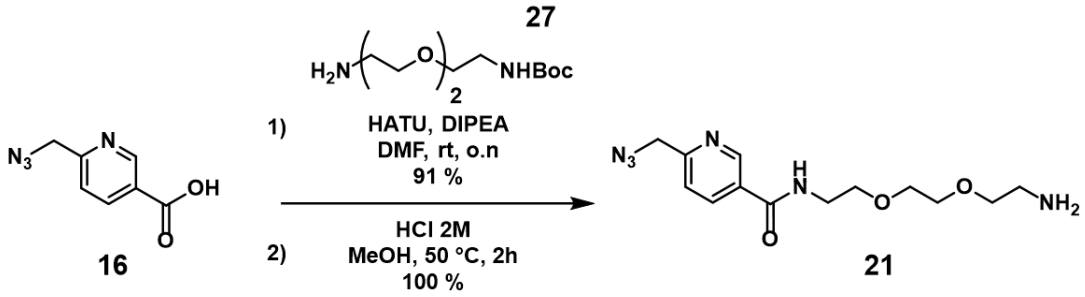

Scheme 2.4: Synthesis of Picolyl azide-PEG$_2$-amine **21**.

The first step towards the synthesis of the picolyl azide/bis-azide linker from methyl 3,5-dihydroxybenzoate was the conjugation on the hydroxyl groups of the azido-PEG$_3$-OTs linker **24**. This was achieved by deprotonating the two hydroxyl groups which could thus substitute each the tosylate of one azido-PEG$_3$-OTs linker **23**. Potassium carbonate was used as a base instead of sodium or lithium hydroxide to prevent the hydrolysis of the methyl ester. This double conjugation was performed with a yield of 77 %. The carboxylic acid on the core was subsequently deprotected by saponification with sodium hydroxide. Finally, the carboxylic

acid was activated by HATU and was further coupled to the picolylazide-PEG_2-amine linker to provide the Picolyl azide/bis-azide linker **19**.

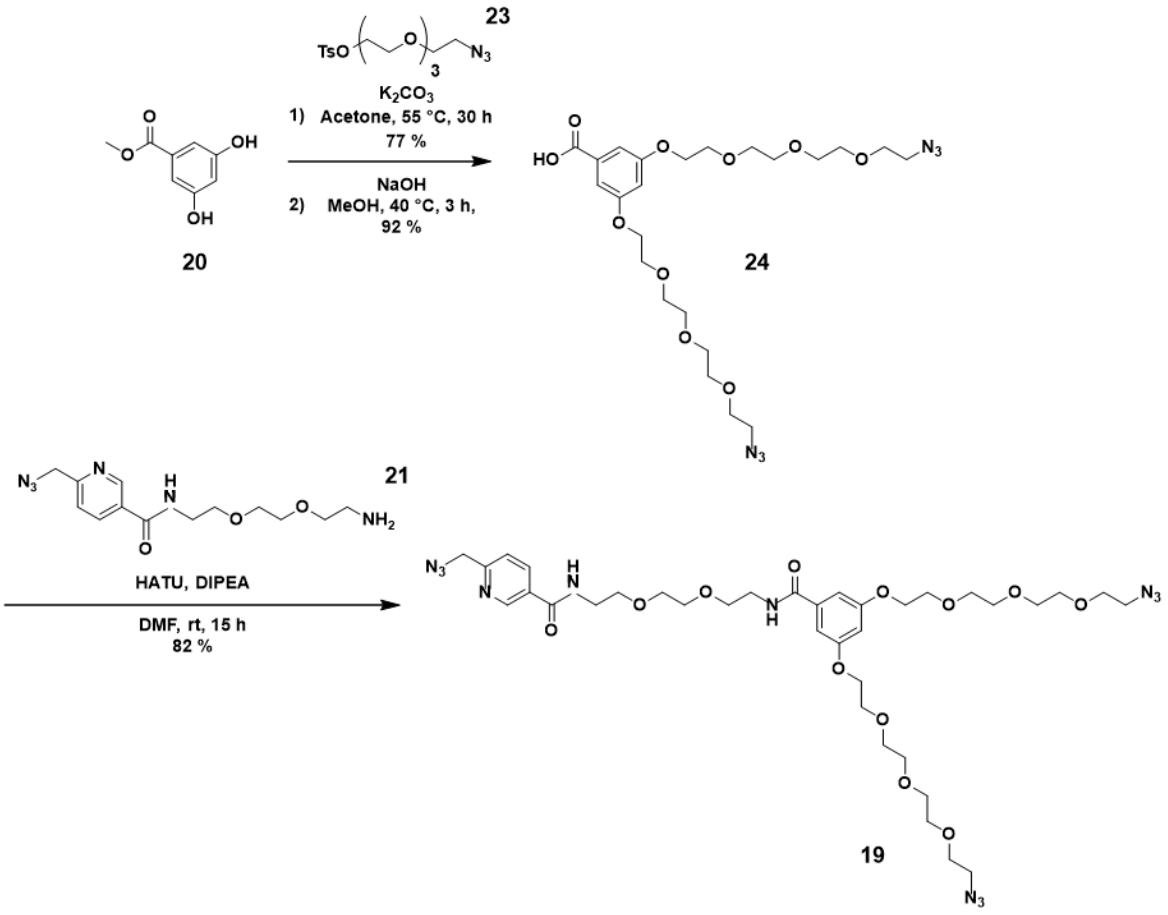

Scheme 2.5: Synthesis of the picolyl azide/bis-azide linker **19**.

2.2.3 Click experiments

The ability of the picolyl azide-PEG_{10}-azide linker **17** to be clicked in a chemoselective protocol was assessed with a 11-mer oligodeoxyribonucleotide containing one C8-alkyne-dU nucleoside. Several stoichiometric ratios of copper catalyst/alkyne-carrying ODN and linkers/ alkyne-carrying ODN were tested in order to find the best conditions for:

1- Performing the reaction until full completion;

2- Achieve the highest possible chemoselectivity and prevent side reaction on the non-chelating azido group.

The different conditions tested are listed in Table 2.1. The reactions were performed in parallel, over the same time and at the same temperature. The final concentration of the DNA strand was identical in each sample.

Table 2.1: Click screening with the picolyl azide-PEG_{10}-azide linker **17**. [*] The percentage of completion of the reactions were determined by integration of the HPLC trace of the crude product at 260 nm.

Sample entry	Sequence	Stoichiometric ratio linker/alkyne	Stoechiometric ratio copper/alkyne	Calcd [M-H]-	Found [M-H]-	Completion [%]*
1	5' GGCCGCT-**MonoAz**-TTG 3'	10	2	4114.5	4111.1	**84.9**
2		20	2			**97.4**
3		50	2			**98.8**
4		10	5			**90.2**
5		20	5			**97.0**
6		50	5			**98.8**
7		10	10			**87.8**
8		20	10			**96.7**
9		50	10			**97.6**

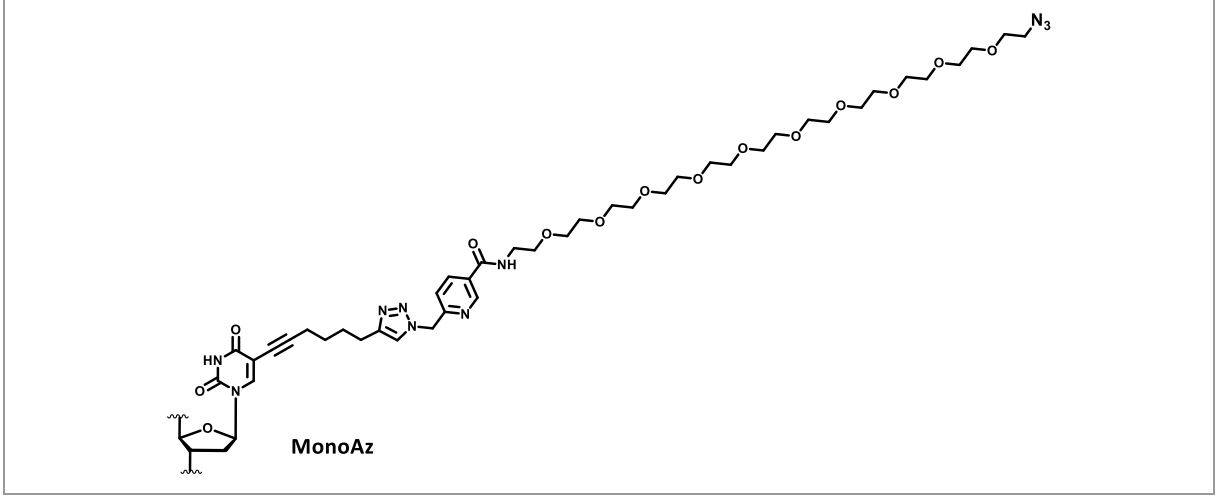

The HPLC chromatograms of the crude products from the samples 1, 4 and 7 show a small signal corresponding to the unclicked alkyne-ODN. The starting material was also detected in the crude product of these samples by measuring their MALDI-TOF spectra. For all the other samples, the completion seems to be total as no signal from the unclicked ODN was detected in the crude products neither by HPLC nor by MALDI-TOF (Figure 2.3). In addition, the approximate calculations of the percentage of completion of these reaction provided all data superior up to 95 %. For all the sample crude products, no other signal than the ones corresponding to the linker in excess and the target product were detected. Based on this analytics, we decided to choose the condition of the sample 2 (2 equivalents of copper catalyst; 20 equivalents of linker) for further click reactions of the picolyl azide-PEG_{10}-azide linker **17** on alkyne ODN. Indeed, these conditions provided a full completion while requiring the smallest amounts of catalyst and reactant.

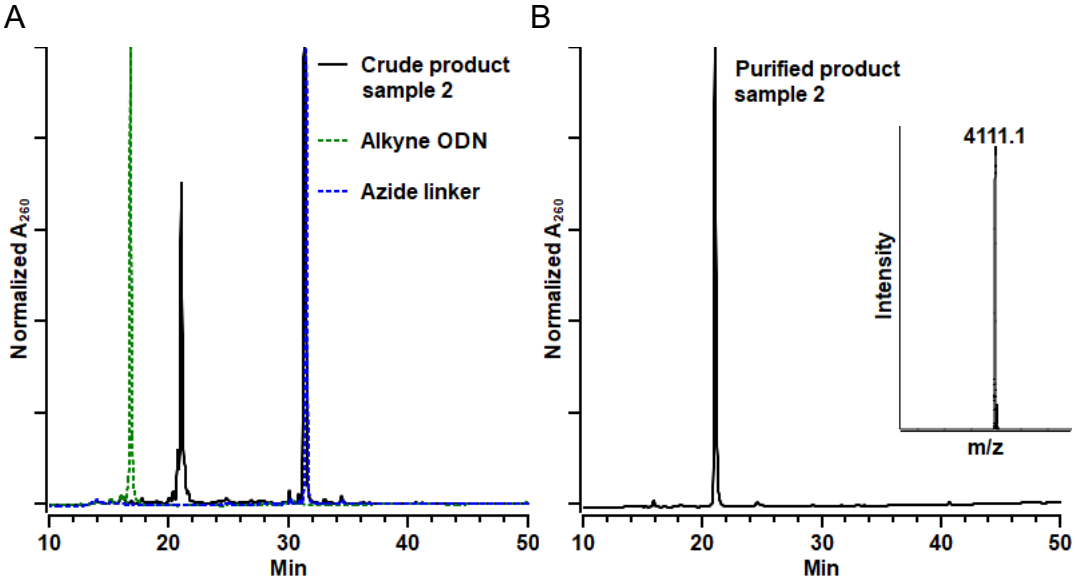

Figure 2.3: (A) HPLC profile of the crude product from the sample 2 (see Tab. 2.1). The starting materials, alkyne-carrying ODN (green dotted) and the picolyl azide-PEG_{10}-azide linker **17** (blue dotted) are depicted for comparison. (B) HPLC profile of the purified product from sample 2 and the corresponding MALDI-TOF spectrum (inset).

We performed a similar click screen with the picolyl azide/bis-azide linker **19**. We chose again an 11-mer oligodeoxyribonucleotide containing one C8-alkyne-dU nucleoside (Table 2.2). The different stoichiometric ratios of copper catalyst/alkyne-carrying ODN and linkers/ alkyne-carrying ODN tested are shown in the Table 2.2. Based on the results from the screening with the picolyl azide-PEG_{10}-azide linker **17**, we narrowed down the number of conditions to test

this time. Indeed, it did not seem necessary to investigate higher excess of respectively 5 for the copper catalyst and 20 for the linker.

Table 2.2: Click screening with the picolyl azide/bis-azide linker **19**. [*] The percentage of completion of the reactions were determined by integration of the HPLC trace of the crude product at 260 nm.

Sample entry	Sequence	Stoichiometric ratio linker/alkyne	Stoechiometric ratio copper/alkyne	Calcd [M-H]-	Found [M-H]-	Completion [%]*
1	5' CGGGA-**BisAz**-CGTCA 3'	10	2	4292.6	4288.4	**99.2**
2		20	2			**>99.9**
3		10	5			**99.3**
4		20	5			**>99.9**

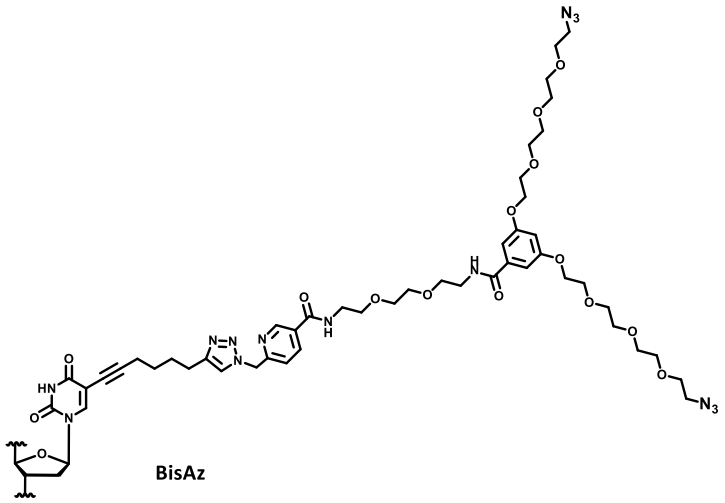

The HPLC chromatograms of the crude product of every sample show a full conversion as well as the crude MALDI-TOF spectra where no unclicked ODN was detected. This was verified after integrating the area of the chromatograms corresponding to the starting ODN and the target clicked product. However, for every condition tested, an additional signal appearing shortly before the elution of the target product was detected. The ratio of the trace of this side product to the trace of the target product was about 25/75 and constant for every sample. No additional signal were detected in the MALDI-TOF spectra of the crude products. After isolating this HPLC trace from the crude product by preparative HPLC and measuring its MALDI-TOF spectrum we found that it had the same mass of the target product. Therefore, we hypothesized that on some ODN, one of non-chelating the azido-group of the linker reacted instead of the picolyl azide giving as a result the same mass as the target clicked product.

Nevertheless, since this side reaction never accounted for more than a fourth of the target product and did not prevent the isolation of this last species in sufficient amount for the next experiments, no effort was further made to prevent its formation by screening other conditions.

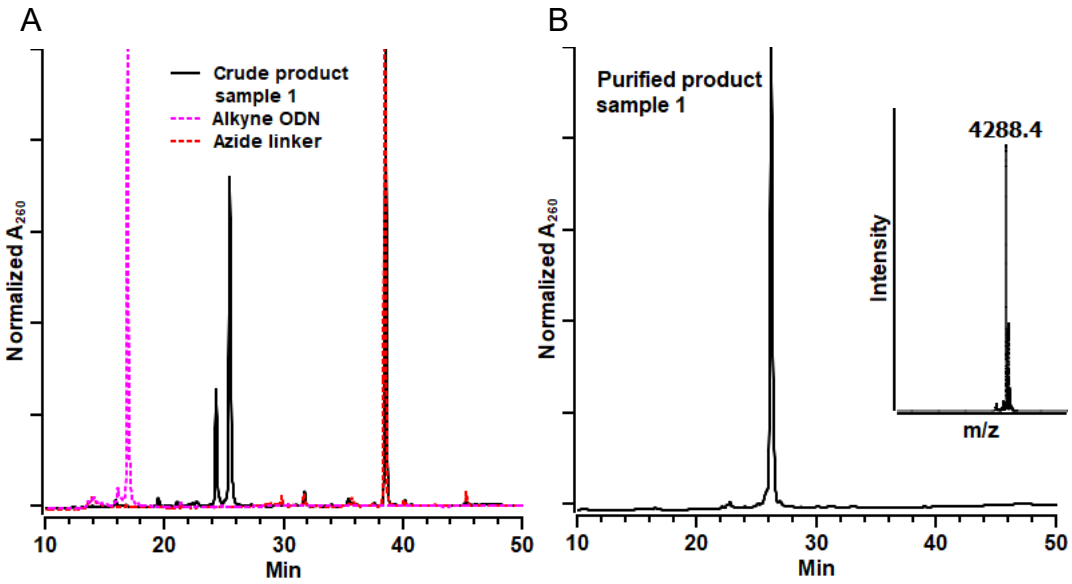

Figure 2.4: (A) HPLC profile of the crude product from the sample 1 (see Tab. 2.2). The starting materials, alkyne-carrying ODN (pink dotted) and the picolyl azide/bis-azide linker **19** (red dotted) are depicted for comparison. (B) HPLC profile of the purified product from sample 1 and the corresponding MALDI-TOF spectrum (inset).

2.3 Synthesis of alkyne functionalized ODN

2.3.1 Strategy

The next step of this thesis project was to develop a strategy towards the functionalization of DNA strands with alkyne groups at the end of long spacers, here again for the needs of the CLICKPLA. As well as for the synthesis of azide functionalized ODN described in the previous section, we decided to rely on the incorporation of the C8-alkyne-dU nucleoside by solid phase synthesis.[91] The alkyne group present on the C8-alkyne-dU needing to be extended. We envisioned a sequential strategy as described by Leigh et al. and previously applied in our group to successively click different labels on one single oligonucleotide.[48, 100] In this method, a first alkyne is clicked while a second one remains protected by a silyl group. Upon the first click, the second alkyne is deprotected and clicked in turn, with another azide label (Figure 2.5). Therefore, we decided to synthesize bifunctional linkers bearing one azide moiety as well as one or two alkyne ones. Once again and for the same reasons mentioned previously, poly(ethylene glycol) chains were chosen as the backbone structures of the linkers to be synthesized. Considering the very high coupling efficiency demonstrated in the previous section by the chelating azido group, we designed syntheses towards linkers bearing picolyl azides rather than non-chelating azides.

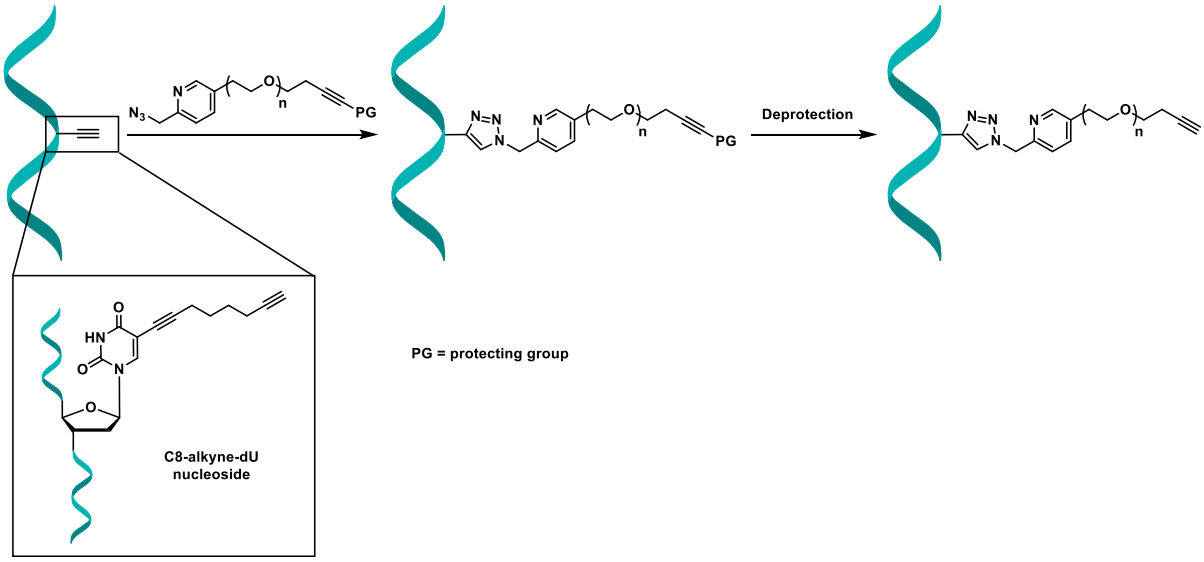

Figure 2.5: Sequential strategy towards the synthesis of alkyne functional DNA strands. The chelating azido group of an unsymmetrical azide/protected alkyne linker is conjugated by CuAAC to an oligodeoxynucleotide containing a C8-alkyne-dU artificial nucleoside. The alkyne of the linker is be subsequently deprotected.

2.3.2 Synthesis of picolyl azide/alkyne-TMS linkers

At first we considered the synthesis of a linker bearing a trimethylsilyl (TMS) protected alkyne. Indeed this protecting group presents the advantage that it can be removed under mild conditions.[48] This property of the TMS protecting group to be easily cleaved off also makes the synthesis of molecules attached to it challenging. Indeed, TMS are unstable towards many conditions.[101] Thus, once introduced during a synthesis, the protected molecule should not undergo any harsh synthetic step in order to keep the TMS in place. The most reliable method, in our opinion, is to introduce the TMS group during the last step of the synthesis of the molecule of interest.

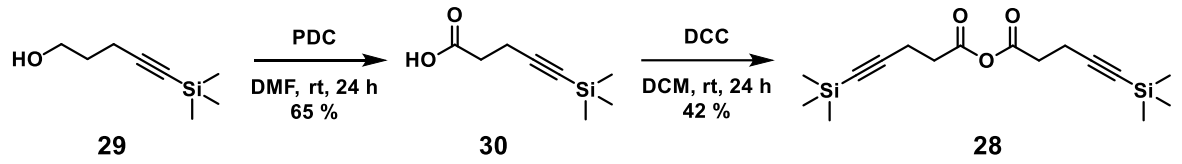

Scheme 2.6: Synthesis of 5-(Trimethylsilyl)pent-4-ynoic anhydride **28**.

Based on a procedure described by Boons et al., we synthesized a symmetric acid anhydride with two TMS protected alkynes **28** (Scheme 2.6).[102] This molecule can readily react with an amino group under conditions in which the TMS is stable. The next step was then the synthesis of a long unsymmetrical PEG linker respectively terminated on its two respective extremities by a picolyl azide and a free amino group **31** (Scheme 2.7).

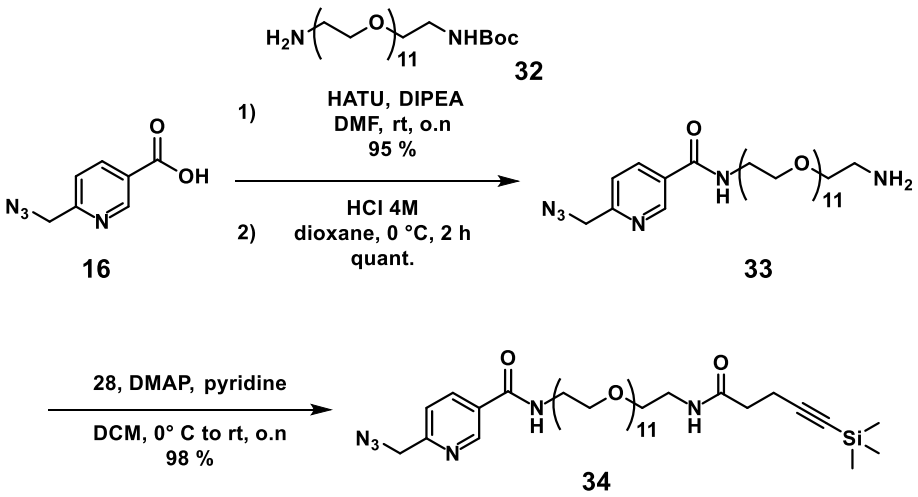

Scheme 2.7: Synthesis of the picolyl azide-PEG_{11}-TMS protected alkyne linker **34**.

The synthesis of such linker was already achieved as described during the section 2.2.2 (Scheme 2.4) with a short linker. Here we substituted the Boc-PEG_2-amine **27** by a Boc-PEG_{11}-amine **32** and applied the same synthetic procedure (Scheme 2.7). First, the PEG linker was conjugated to the picolyl azide carboxylic acid reactant **16** via an amide coupling. The second amine of the PEG chain was then deprotected from its Boc group by acid hydrolysis. At last, the acid anhydride **28** was coupled to the linker **33** here again through an amide linkage providing the picolyl azide-PEG_{11}-TMS protected alkyne linker **34** in an excellent yield (98 %).

2.3.3 Click experiments

Before performing a click screen, as previously described and in order to optimize the couplings efficiency, we made a quick test regarding reaction between a 15-mer alkyne oligodeoxyribonucleotide and the picolyl azide-PEG_{11}-TMS protected alkyne linker **34** with standard click conditions:

- Copper sulfate as the source of metal catalyst;
- Sodium ascorbate as the reducing agent;
- BTTAA as the copper (I) stabilizing ligand.

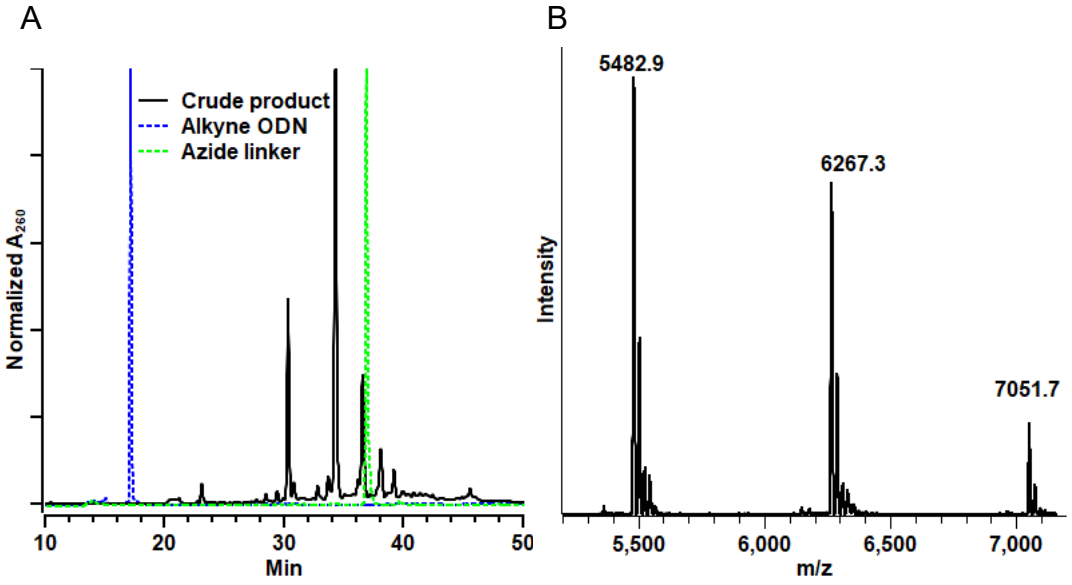

Figure 2.6: Analysis of the crude product from the click reaction (A) HPLC profile. The starting materials, alkyne-carrying ODN (blue dotted) and the the picolyl azide-PEG_{11}-TMS protected alkyne linker **34** (green dotted) are depicted for comparison. (B) MALDI-TOF spectrum.

However, to our disbelief, the analysis of the crude product by HPLC provided a profile with several signals (Figure 2.6). If the starting alkyne ODN seemed to be fully reacted, it appeared several by-products had been generated during the click reaction. Further analysis by MALDI-TOF mass spectrometry confirmed that in addition to the target product, at least two side-products had been formed. We hypothesized that the TMS protecting group might be removed during the click reaction after conjugation to the ODN. We thought that the linker being in excess (10 equivalents), it could happen that unreacted linkers might have clicked onto the already conjugated but deprotected ones. Calculations of the intrinsic molecular weights of such ODN with several linkers successively clicked provided indeed the values found in the MALDI-TOF spectrum of the crude product thus confirming this hypothesis (Table 2.3).

Table 2.3: Mass spectrometric data of the click crude product with the picolyl azide-PEG_{11}-TMS protected alkyne linker **34**.

Sequence	Calcd [M-H]-	Found [M-H]-
5' CATTAAAGGTGAA-**X1**-T 3'	5488.5	**5482.9**
5' CATTAAAGGTGAA-**X2**-T 3'	6272.9	**6267.3**
5' CATTAA AGGTGAA-**X3**-T 3'	7057.3	**7051.7**

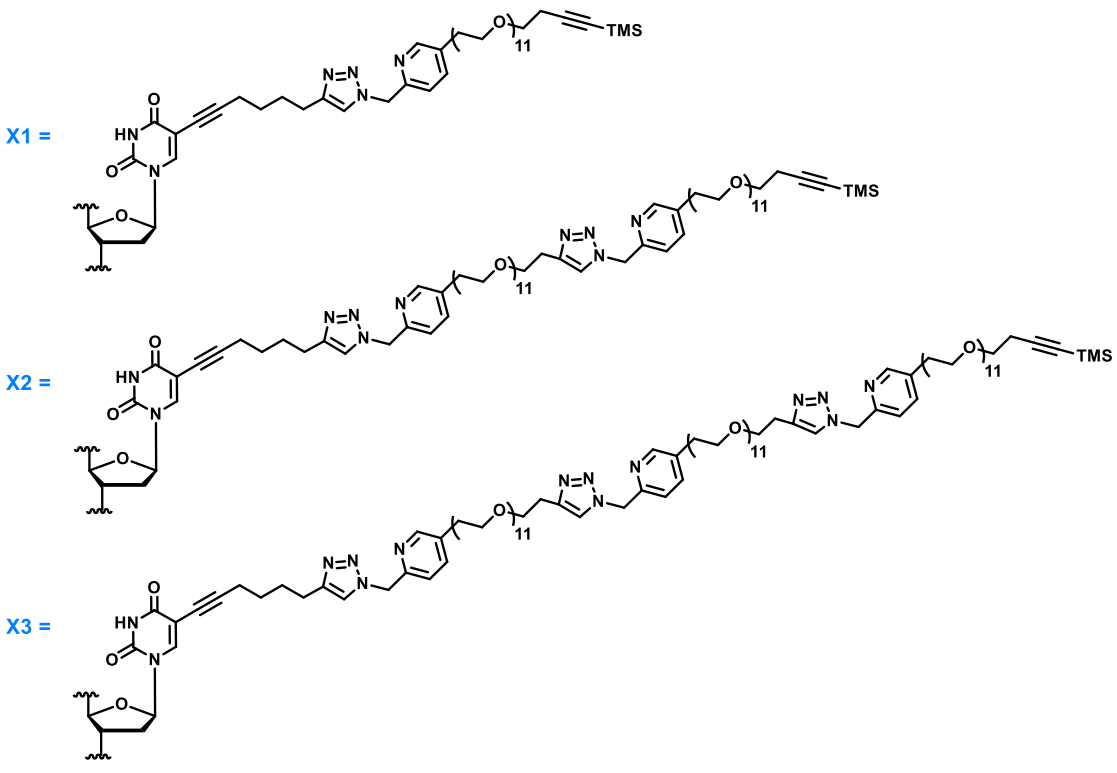

2.3.4 Synthesis of picolyl azide/alkyne-TES linkers

Since the TMS alkyne protecting group was not stable enough for our purposes, we decided to replace it by a triethylsilyl (TES) protecting group which is notably less labile than TMS and can be cleaved off by fluoride ions from water soluble salts such as potassium fluoride or sodium fluoride.[103] We developed a synthesis similar to the one which provided the picolyl azide-PEG_{11}-TMS protected alkyne linker **34**. Starting from the readily protected 5-triethylsilyl-4-pentyn-1-ol **35**, we oxidized it into a carboxylic acid **36** with pyridinium dichromate. Since TES is not as sensitive as TMS, we conjugated directly the TES carboxylic acid **36** to the picolyl azide-PEG_{11}-amine linker **33** in a one-pot HATU mediated coupling to obtain the picolyl azide-PEG_{11}-TES protected alkyne linker **37** (Scheme 2.8).

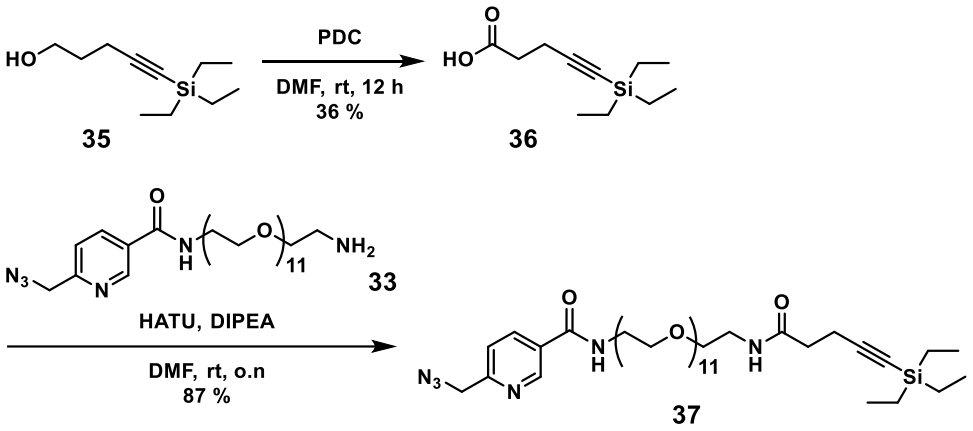

Scheme 2.8: Synthesis of the picolyl azide-PEG_{11}-TES protected alkyne linker **37**.

In parallel to the synthesis of the mono-TES protected alkyne linker, we undertook the challenge of designing and achieving the synthesis of an unsymmetrical linker bearing one picolyl azide and two TES protected alkyne. A similar approach as the one that allowed the synthesis of the picolyl azide/bis-azide linker **19** and based on the starting building block methyl 3,5-dihydroxybenzoate **20** was adopted. The first step was the conjugation of the two hydroxyl groups present on the starting core with a PEG linker bearing a Boc-protected amino group **38**. To this aim, the azide of the azido-PEG_3-OTs linker **23** was reduced into an amine by catalytic hydrogenation with palladium on carbon, which was directly reacted with Boc anhydride in a one pot procedure (Scheme 2.9).

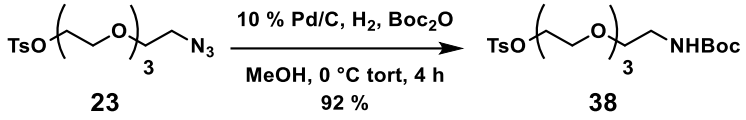

23 38

Scheme 2.9: Synthesis of the Boc-PEG_3-OTs **38**.

The two hydroxyl groups of methyl 3,5-dihydroxybenzoate **20** were deprotonated with potassium carbonate in order to substitute the tosyl group of the linkers **38** (Scheme 2.10). The double conjugated product was obtained with a 70 % yield. The methyl ester on the core was hydrolysed with sodium hydroxide. This deprotection proceeded orthogonally and the two Boc protecting groups remained on the molecule **39**. Once free, the carboxylic acid of the core was activated by the tandem HATU/DIPEA and coupled to the picolylazide-PEG_2-amine linker **21**. Eventually, the two Boc protecting group were removed by a hydrochloric acid solution in dioxane and the two amino groups were reacted in an amide coupling to the TES carboxylic acid **36**. The picolyl azide/bis-TES protected alkyne linker **40** was provided in a quasi-quantitative yield.

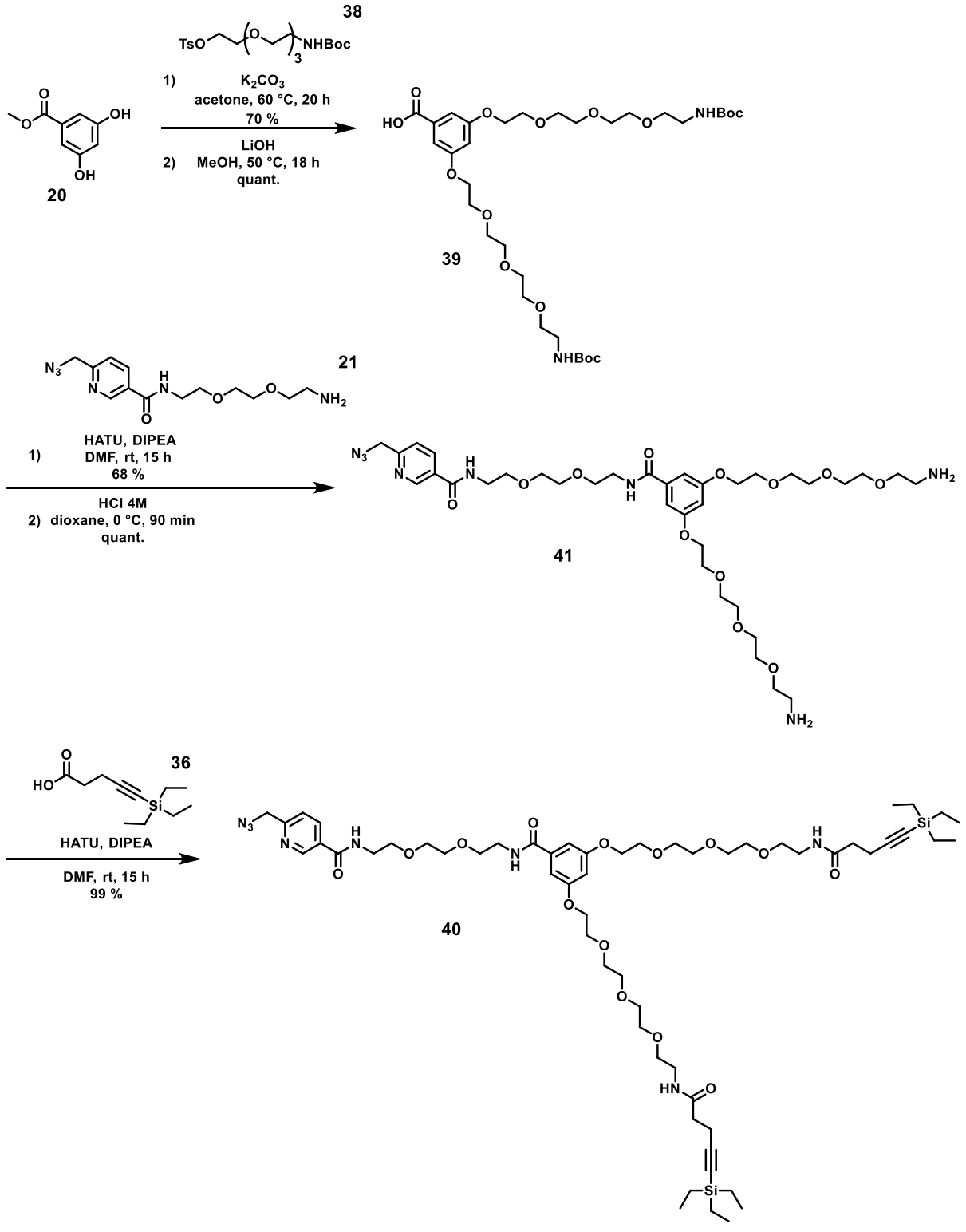

Scheme 2.10: Synthesis of the picolyl azide/bis-TES protected alkyne linker **40**.

2.3.5 Click experiments and deprotection

We first tried to click the picolyl azide-PEG_{11}-TES protected alkyne linker **37** onto a 11-mer ODN containing one C8-alkyne-dU modified nucleoside. As for the TMS linker **34**, we used standard click reagents (copper sulfate as source of metal catalyst; sodium ascorbate as reducing agent; BTTAA as a copper (I) stabilizing ligand). In order to optimize the reaction, we tested several stoichiometric ratios of copper (2, 5 and 10 equivalents) and linker (5, 10 and 20 equivalents) to the alkyne-bearing ODN (Table 2.4). This optimization was done in order to perform the reaction with the highest conversion possible while using the minimal amount of reactant and catalyst. This is particularly important regarding the copper reagent in order to prevent metal induced catalytic cleavage of the DNA strand.[104] Every reaction was performed in parallel, for the same time duration and at the same temperature. The final concentration of the DNA strand was identic in each sample.

Table 2.4: Click screening with the picolyl azide-PEG_{11}-TES protected alkyne linker **37**. [*] The percentage of completion of the reactions was determined by integration of the HPLC trace of the crude product at 260 nm.

Sample entry	Sequence	Stoichiometric ratio linker/alkyne	Stoechiometric ratio copper/alkyne	Calcd [M-H]-	Found [M-H]-	Completion [%]*
1	5' GGCCGCT-**MonoTES**-TTG 3'	5	2	4326.7	4322.7	**79.8**
2		10	2			**65.2**
3		20	2			**77.2**
4		5	5			**>99.9**
5		10	5			**>99.9**
6		20	5			**86.6**
7		5	10			**>99.9**
8		10	10			**>99.9**
9		20	10			**>99.9**

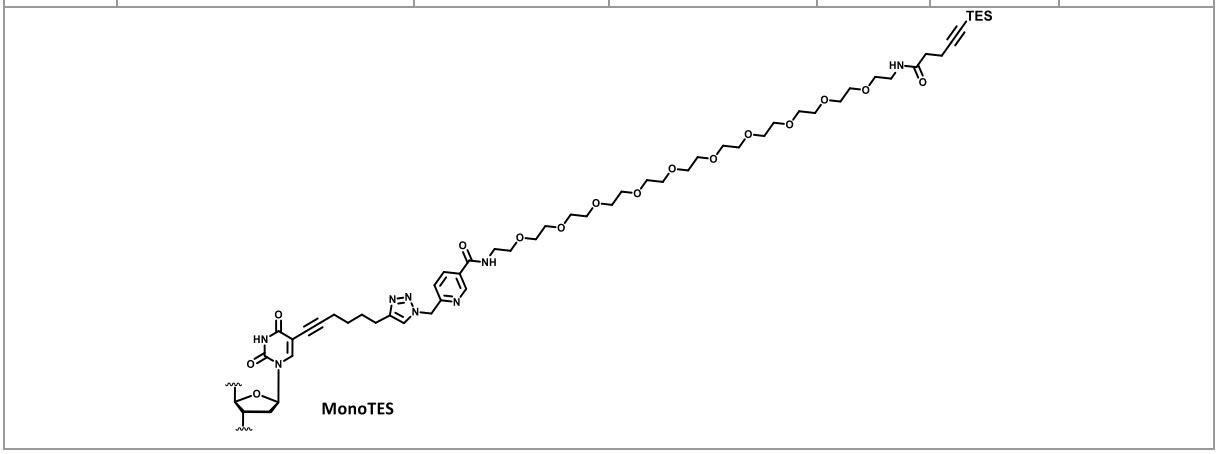

From 5 equivalents of copper to the alkyne ODN, almost every reaction proceeded in a quantitative manner with percentages of conversion higher than 95 %. In this regard, the stoichiometric rates of the sample 4 were chosen as the references since they were the one using the least amount of linker (5 equivalents as well). While the HPLC profile of the crude products show some additional signals than the one corresponding to the target product, this last one was nevertheless easily isolated and purified by preparative HPLC (Figure 2.7).

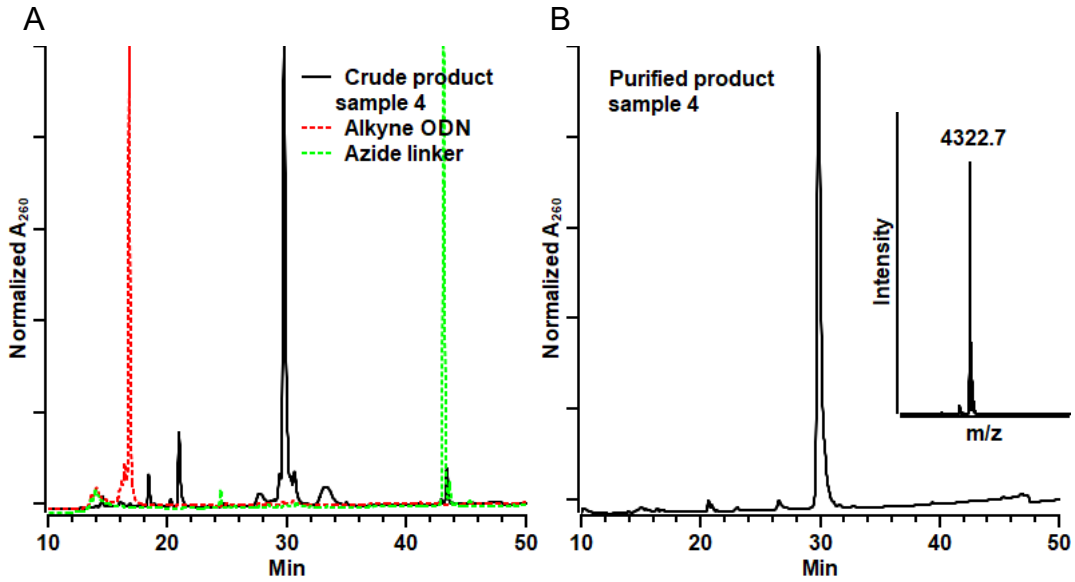

Figure 2.7: (A) HPLC profile of the crude product from the sample 4 (see Tab. 2.4). The starting materials, alkyne-carrying ODN (red dotted) and the the picolyl azide-PEG_{11}-TES protected alkyne linker **37** (green dotted) are depicted for comparison. (B) HPLC profile of the purified product from sample 4 and the corresponding MALDI-TOF spectrum (inset).

Once purified, the DNA strand clicked with the picolyl azide-PEG_{11}-TES protected alkyne linker **37** was subsequently treated with a sodium fluoride aqueous solution in order to free the alkyne from its protecting group. The deprotection was completed in 48 hours at 40 °C and provided the deprotected ODN as the only product of the reaction (Figure 2.8). This was confirmed by analysing the crude product by MALDI-TOF mass spectrometry. The spectrum obtained, shows only one signal corresponding to the target product. The HPLC profile of the crude product showing a quite clean product, we decided that this procedure does not require an additional purification by preparative HPLC. The functionalized ODN was only desalted on a centrifugal membrane filter to get rid of the salts from the deprotection reaction before further experiments.

A

Sequence	Calcd [M-H]-	Found [M-H]-
5' GGCCGCT-**MonoAlk**-TTG 3'	4212.6	4208.7

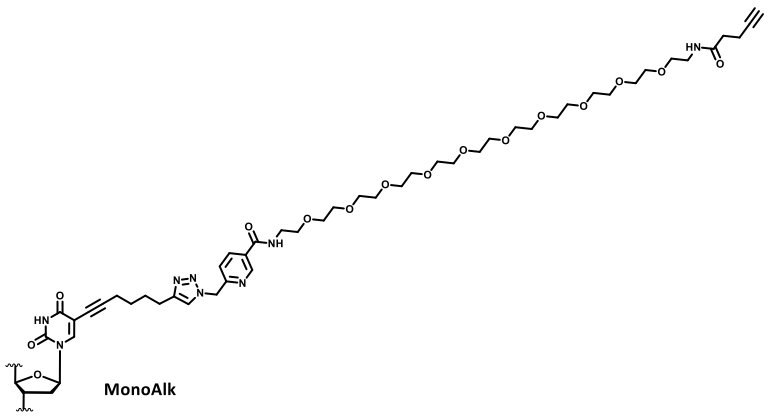

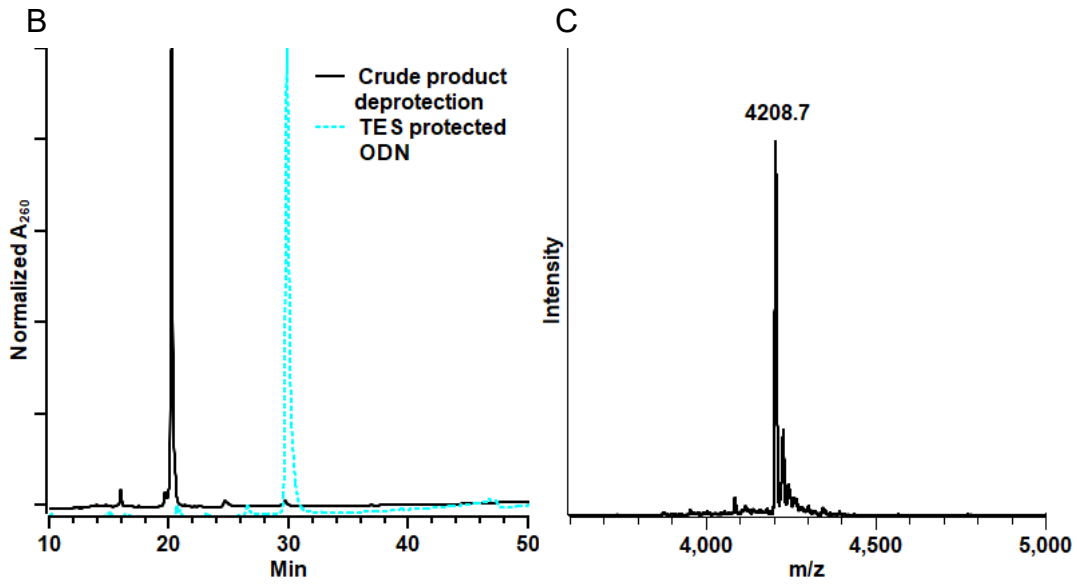

Figure 2.8: Analysis of the crude product from the deprotection of the TES protected alkyne ODN. (A) Mass spectrometric data. (B) HPLC profile. The starting material, TES protected alkyne ODN, is depicted for comparison (blue dotted). (C) MALDI-TOF spectrum.

We subsequently investigated the clicking ability of the picolyl azide/bis-TES protected alkyne linker **40**. As previously, the linker was clicked to a 11-mer ODN containing one C8-alkyne-dU modified nucleoside with standard click reagents (copper sulfate as source of metal catalyst; sodium ascorbate as reducing agent; BTTAA as a copper (I) stabilizing ligand). For the screening of this linker we kept a stoichiometric ratio of copper (I) to alkyne ODN constant and equal to 10 equivalents for all the samples. Only the effect of the ratio of linker (from 5 to 50 equivalents) on the reaction was studied in this test (Table 2.5). Again, every reaction was performed in parallel, for the same time duration and at the same temperature. The final concentration of DNA strand was also identical in each sample.

Table 2.5: Click screening with the picolyl azide/bis-TES protected alkyne linker **40**. [*] The percentage of completion of the reactions were determined by integration of the HPLC trace of the crude product at 260 nm.

Sample entry	Sequence	Stoichiometric ratio linker/alkyne	Stoechiometric ratio copper/alkyne	Calcd [M-H]-	Found [M-H]-	Completion [%]*
1	5' CGGGA-**BisTES**-CGTCA 3'	5	10	4628.9	4627.0	**2.9**
2		10	10			**18.9**
3		20	10			**33.1**
4		50	10			**45.2**

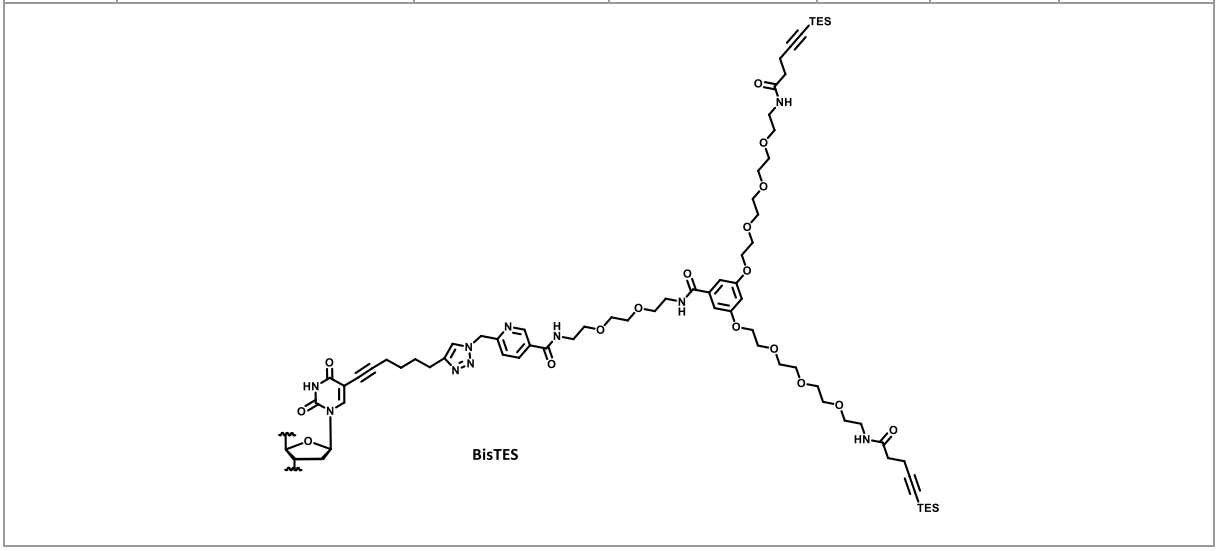

BisTES

Unfortunately, the coupling efficiency of this linker upon click reaction remained relatively low despite the higher stoichiometric ratios tried. The highest percentage of conversion obtained was of 45 % and it required 50 equivalents of linker. Indeed, analysis of the HPLC profile of the crude product shows that most of the alkyne ODN remained unclicked. (Figure 2.9). Likewise, if the MALDI-TOF spectrum of the crude product enables the detection of the

target compound, the main signal came from the unclicked alkyne ODN (Calcd $[M-H]^-$ = 3346.2; Found $[M-H]^-$ = 3341.6). One plausible explanation for the lack of efficiency of this linker in comparison to the other linkers previously studied could be a lower water solubility. Indeed, we observe upon its addition to the aqueous reaction mixture that this reaction mixture became slightly cloudy. This indicates a precipitation. In addition, in the click reactions described in the previous sections, the unclicked linkers in excess were eluted during the elution with a gradient of 0 to 90 % of buffer B over 45 minutes. However, the picolyl azide/bis-TES protected alkyne linker did not appear on the HPLC profiles of the crude products from the click reactions. Since the samples are filtered before being injected in the HPLC, if the linker was precipitated, it would have stayed inside the filter and thus would not be in the injected samples.

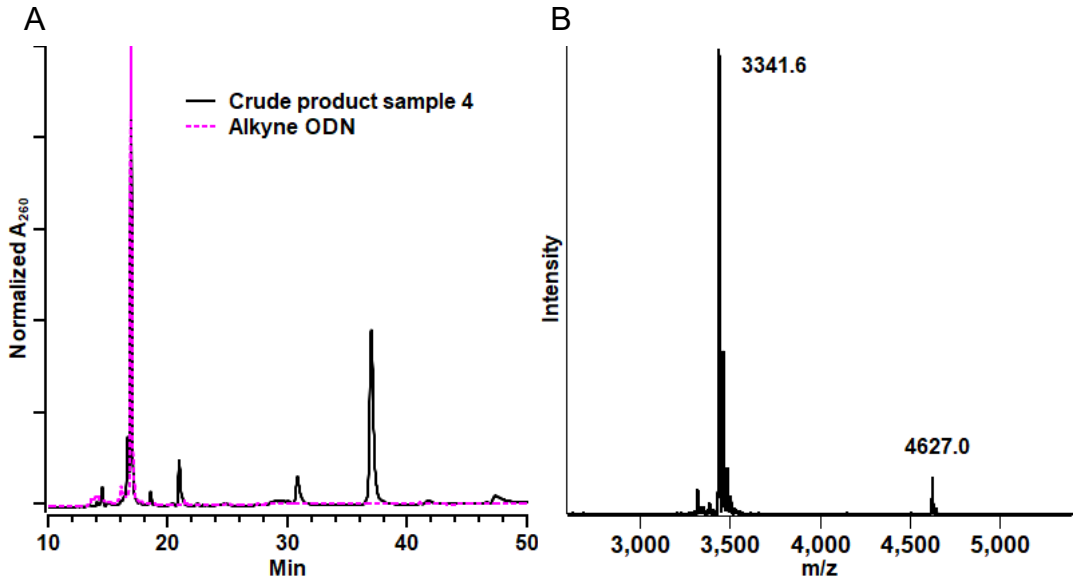

Figure 2.9: Analysis of the crude product from the sample 4. (A) HPLC profile. The starting material, alkyne ODN, is depicted for comparison (pink dotted). (C) MALDI-TOF spectrum.

2.4 ODN design and synthesis

2.4.1 Design parameters

As described in the objectives section, the CLICKPLA features four oligodeoxyribonucleotides: one long template and three smaller strands. The first step of the CLICKPLA being the simultaneous hybridization of the three probes on the template, we had to design complementary DNA strands with optimal hybridization potentials. In this regard, several parameters such as the length of the oligonucleotides needed to be optimal.[105] Too short probes would result in unspecific hybridization. Too long probes might require longer hybridization time. Too long probes could also increase the risk of having complementary regions within the probes themselves, which could result in the formation of hairpin structures inhibiting the hybridization with the target strand. The base composition of the oligonucleotides should be about 40 to 60 % of G-C to keep the duplex more stable. Eventually, sequences with long stretches of a same base should be avoided. The step following the hybridization of the three probes on their template is to conjugate them by click chemistry. In order to make this conjugation likely to take place and since the modifications bearing the clickable chemical functions will be remoted from each other, the modifications need to be smartly placed within each probes. The double helix formed by the hybridization of DNA strands is a three-dimensional structure with a pitch of 10.5 base pairs.[21] Therefore, it has been shown that coupling across one complete turn of the double helix is possible since the modifications will be placed on the same side of the helix (Figure 2.10).[106, 107]

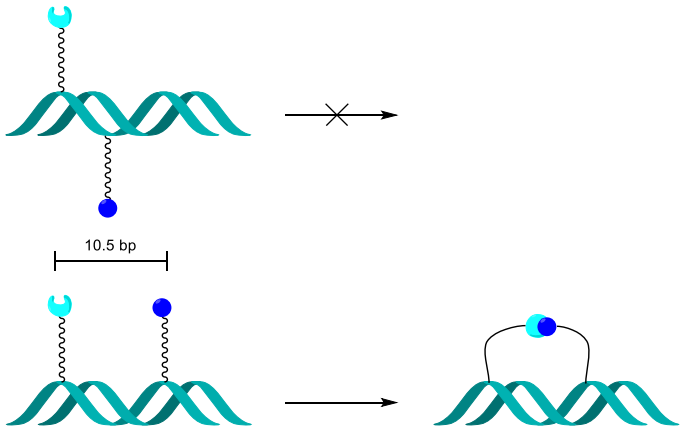

Figure 2.10: Coupling across the DNA double helix.

2.4.2 ODN synthesized

Based on the parameters previously described, we designed two sets of oligonucleotides for the CLICKPLA with each set including three functionalized probes and one template strand (Figure 2.11). We chose 11-mer probes for the first set of oligonucleotides (ODN-1, ODN-2 and ODN-3) and a 39 base pairs long complementary template (ODN-4). For the second set, three 15-mer probes were designed (ODN-5, ODN-6 and ODN-7) and a corresponding template strand of 45-mer (ODN-8). The sequences of the template were taken from the single stranded plasmid M13mp18. The incorporation site of the C8-alkyne-dU nucleoside within the sequence of each probe was chosen in order to have an 8 bp distance until the next modification once the probes hybridized in order to increase the chances of conjugation between the probes.

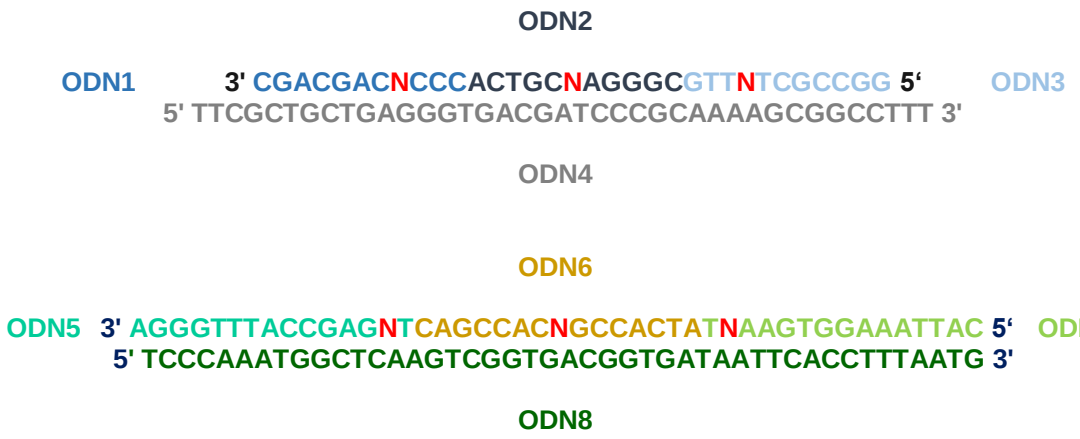

Figure 2.11: Sequences of the two sets of DNA strands designed for the CLICKPLA. The base N (in red) is the modified nucleoside.

In the objectives part of this chapter, two versions of the CLICKPLA had been envisioned. In the first one, the two side probes would each carry an azide function and the middle probe would bear two alkynes. In the second version, the side probes would carry the alkyne functions whereas the middle probe would be the azides bearing one. Considering the coupling efficiencies of the different linkers synthesized, we decided to focus on the latter one (Figure 2.12).

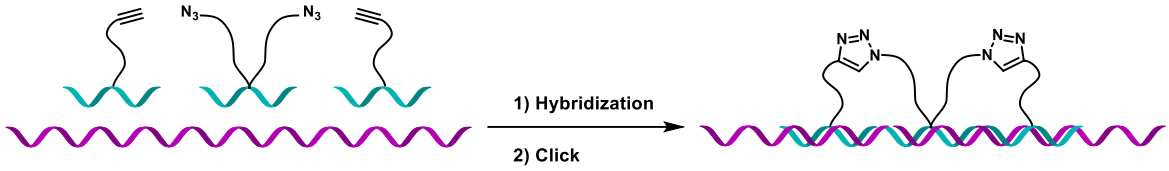

Figure 2.12: Schematic representation of the CLICKPLA version selected. The oligonucleotide probes are represented in green. The oligonucleotide templates is in purple. At first, three probes are hybridized to the complementary template. In a second time, the click reaction between the alkyne side probes and azide middle probe can be initiated and the three probes are conjugated to each other.

Indeed, both the picolyl azide-PEG_{11}-TES protected alkyne linker **37** and the picolyl azide/bis-azide linker **19** provided high coupling efficiencies upon click reaction with alkyne-modified oligonucleotides. Therefore, we decided to functionalize the side side probes of each set (respectively ODN-1and ODN-3 for the first set and ODN-5 and ODN-7 for the second set) with the picolyl azide-PEG_{11}-TES protected alkyne linker **37**. The middle probes were functionalized with the picolyl azide/bis-azide linker **19** in order to bear two azides. All the oligonucleotides synthesized and functionalized for both sets are recapitulated in the following table (Table 2.6)

Table 2.6: Mass spectrometric data of the oligonucleotides synthesized for the CLICKPLA. [*] The strands containing only the canonical bases were purchased.

Entry	Sequence	Calcd [M-H]-	Found [M-H]-
ODN-**1**	5' CCC-**C8-Alk-dU**-CAGCAGC 3'	3351.1	3347.2
ODN-**2**	5' CGGGA-**C8-Alk-dU**-CGTCA 3'	3346.2	3441.6
ODN-**3**	5' GGCCGCT-**C8-Alk-dU**-TTG 3'	3428.2	3424.8
ODN-**4***	5' TTCGCTGCTGAGGGTGACGATCCCGCAAAAGCGGCCTTT 3'	11998.8	-
ODN-**5**	5' T-**C8-Alk-dU**-GAGCCATTTGGGA 3'	4712.0	4710.6
ODN-**6**	5' ATCACCG-**C8-Alk-dU**-CACCGAC 3'	4571.0	4567.6
ODN-**7**	5' CATTAAAGGTGAA-**C8-Alk-dU**-T 3'	4704.1	4699.6
ODN-**8***	5' TCCCAA ATGGCTCAAGTCGGTGACGGTGATAATTCACCTTTAATG 3'	13840	-
ODN-**2-BisAz**	5' CGGGA-**BisAz-**CGTCA 3'	4292.6	4288.0
ODN-**6-BisAz**	5' ATCACCG-**BisAz-**CACCGAC 3'	5417.3	5415.1
ODN-**1-TES**	5' CCC-**TES-**CAGCAGC 3'	4249.7	4246.5
ODN-**3-TES**	5' GGCCGCT-**TES-**TTG 3'	4326.7	4322.7
ODN-**5-TES**	5' T-**TES-**GAGCCATTTGGGA 3'	5610.5	5610.0
ODN-**7-TES**	5' CATTAAAGGTGAA-**TES-**T 3'	5602.6	5596.5
ODN-**1-Alk**	5' CCC-**Alk-**CAGCAGC 3'	4135.6	4129.9
ODN-**3-Alk**	5' GGCCGCT-**Alk-**TTG 3'	4212.6	4208.7
ODN-**5-Alk**	5' T-**Alk-**GAGCCATTTGGGA 3'	5496.5	5491.0
ODN-**7-Alk**	5' CATTAAAGGTGAA-**Alk-**T 3'	5488.5	5483.2

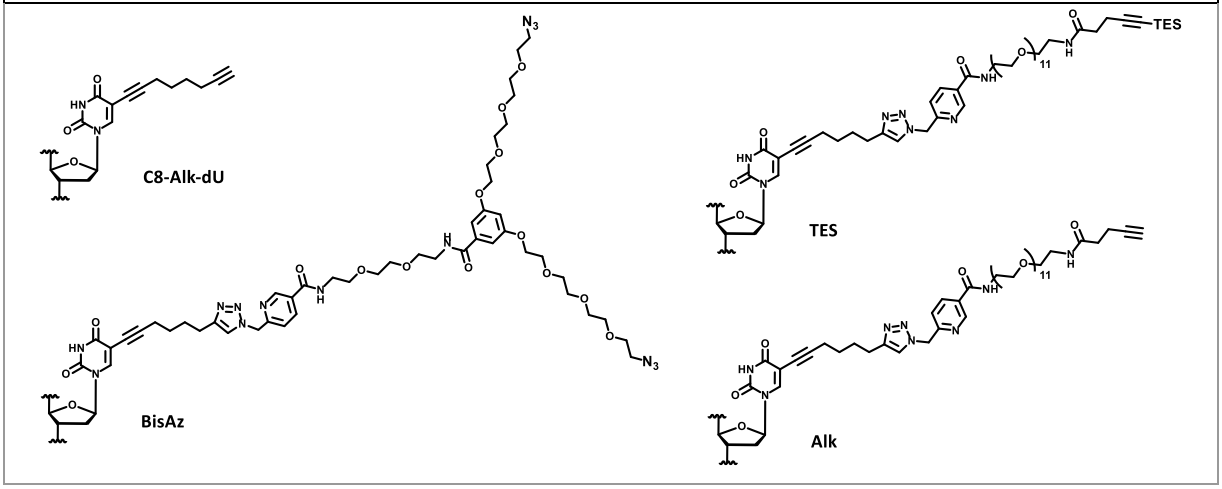

2.4.3 Melting temperature (Tm) measurement

Each functionalized probe was added alone in solution to its corresponding template and the melting temperature was measured by following the UV-vis signal at 260 nm upon several cycles of heating and cooling. The resulting absorption profiles and the temperatures determined from them are shown in the figure 2.13. This experiment was performed in order to control that every oligo probe functionalized with a linker was able to form properly a hybridized duplex with its associated template strand.

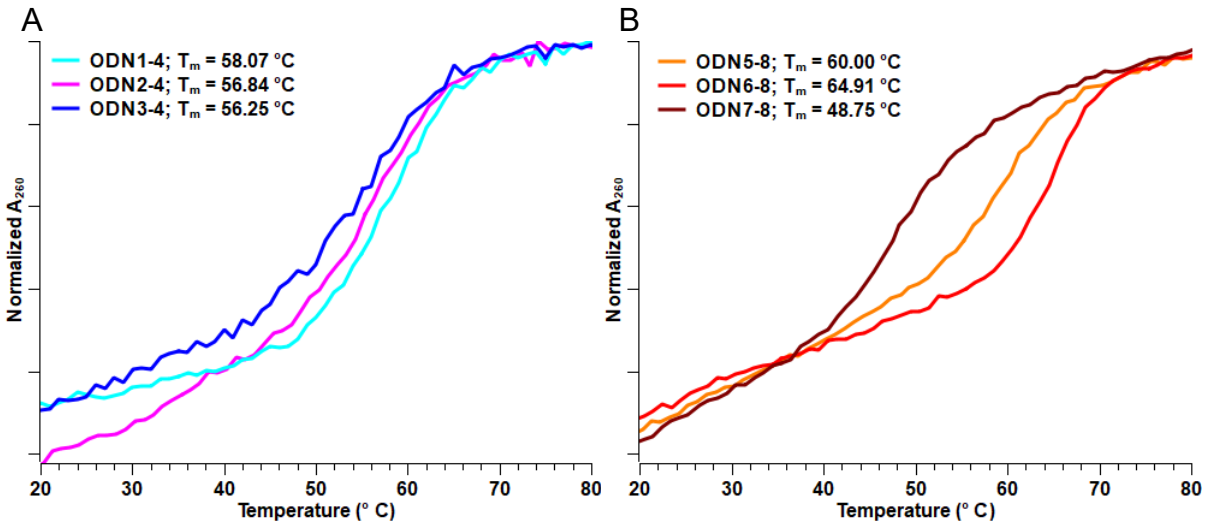

Figure 2.13: Melting profiles of (A) ODN-1-Alk, ODN-2-BisAz and ODN-3-Alk with the template ODN-4; (B) ODN-5-Alk, ODN-6-BisAz and ODN-7-Alk with the template ODN-8.

The melting temperatures were also measured as an indication of within which range of temperatures, the click reaction of the CLICKPLA could be performed. Indeed, the probes designed being relatively short and particularly for the ones from the 11-mer set, it was important to ensure that the hybridized duplex would remain stable during the click conjugation. All the profiles obtained provided melting temperatures superior than 45 °C. We assumed therefore that the duplex of both sets should remain hybridized at the usual room temperature condition used for click reaction with oligonucleotide.

2.4.4 Click test with dyes

In order to test that the synthesized and functionalized oligonucleotides are indeed functional towards further click reactions, we conjugated them with organic dyes. Thus, coumarin azide **41** and fluorescein alkyne **42** were clicked respectively on the strands bearing the alkyne linker and the strands bearing the bis-azide linker. This test had no other purpose than assessing the formation of the clicked adduct. We therefore investigated the crude reaction products only by MALDI-TOF mass spectrometry (Table 2.7). Indeed, every functional oligonucleotide, only the target product was detected confirming so the expected reactivity of the probes synthesized for the CLICKPLA.

Table 2.7: Mass spectrometric data of the oligonucleotides synthesized for the CLICKPLA.

Entry	Sequence	Calcd [M-H]-	Found [M-H]-
ODN-**1 Coumarine**	5' CCC-**AlkCoumarin**-CAGCAGC 3'	4338.6	4334.5
ODN-**3-Coumarine**	5' GGCCGCT-**AlkCoumarin**-TTG 3'	4415.6	4411.3
ODN-**5-Coumarine**	5' T-**AlkCoumarin**-GAGCCATTTGGGA 3'	5699.5	5695.3
ODN-**7-Coumarine**	5' CATTAAAGGTGAA-**AlkCoumarin**-T 3'	5691.5	5686.5
ODN-**2-BisFluoresceine**	5' CGGGA-**BisAzFluoresceine**-CGTCA 3'	5118.8	5116.4
ODN-**6-BisFluoresceine**	5' ATCACCG-**BisAzFluoresceine**-CACCGAC 3'	6243.5	6239.6

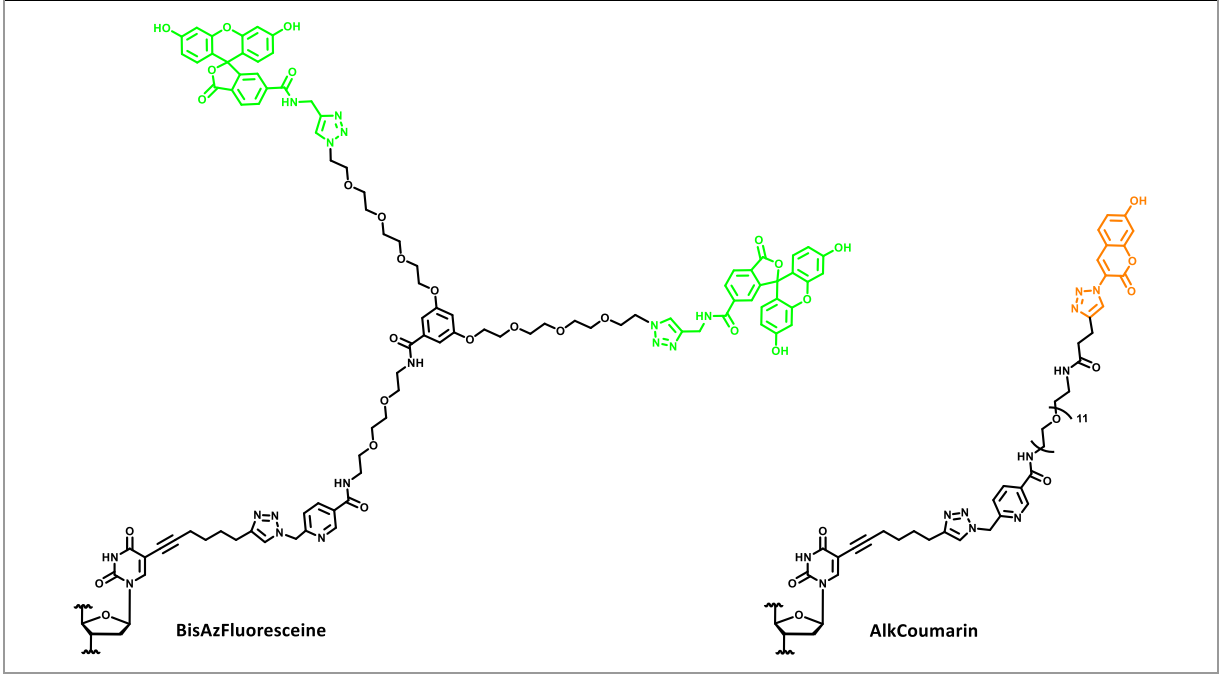

2.5 CLICKPLA experiments

2.5.1 Double conjugation experiments

Once all the oligonucleotides probes had been synthesized, functionalized and tested regarding their ability to form a duplex with their templates and their click reactivity, we performed the first CLICKPLA experiments. To do so, all the ODN of a given set were mixed together and concentrated. After hybridizing the three probes on the respective template, a sample was taken out as a negative control and the click catalyst Master Mix containing copper sulphate, sodium ascorbate and the chelating agent BTTAA was added (see Experimental part). In parallel, a second reaction tube containing only the three probes without the template was prepared and reacted in the same way.

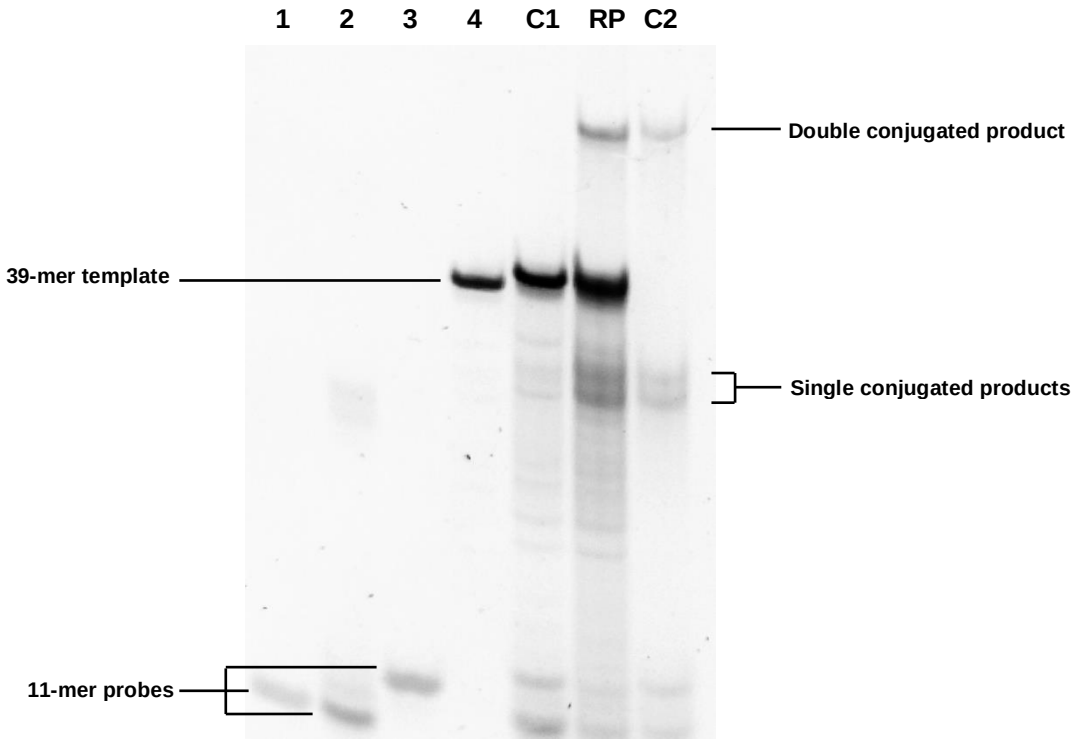

Figure 2.14: 20% denaturing PAGE from the CLICKPLA experiment with the 11-mer probes. Lanes 1 to 4 contain respectively ODN-1-Alk, ODN-2-BisAz, ODN-3-Alk and ODN-4. The lane C1 is a control with all the ODN from the 11-mer set hybridized but not clicked. The lane RP is the click reaction product with all the ODN from the 11-mer set. C2 is a control with the 11-mer probes clicked in the absence of template. C1 = control 1; C2= control 2; RP = reaction product.

The click reactions were analysed by denaturing urea polyacrylamide gel electrophoresis. Figure 2.13 shows the results for the 11-mer set consisting of ODN-1-Alk, ODN-2-BisAz, ODN3-Alk and ODN-4. Lane C1 contains the sample that was taken out of the reaction tube containing all the ODN of the set prior to the addition of the click catalyst Master Mix. As no click reaction took place and since the reaction products were analysed on a denaturing gel, we can expectedly observe the three probes and the template separated from each other at their respective running distances as verified by the individual strands applied in lanes 1-4. In the lane RP, which corresponds to the complete 11-mer set after the click, we can again observe a band from the template ODN-4. However, the bands corresponding to the three probes have significantly faded and three new bands are visible instead. The first two new bands have similar electrophoretic mobilities, which are slightly higher than the 39-mer template and lower than the ones of the 11-mer probes. Therefore, we assumed that these two bands correspond to the single conjugated products of ODN-1-Alk/ODN-2-BisAz and ODN-3-Alk/ODN-2-BisAz. More interestingly, the third new band in the reaction product lane has an even lower mobility than the template indicating a higher size. The modified ODNs being bulkier than normal DNA, we expected that their conjugate would run significantly slower on the gel. Thus, we assigned this band as the target double conjugated product of the three probes and thus that the template assisted click conjugation between the three functionalized oligonucleotides was successful. Eventually, the lane C2 shows the product of the control reaction in the absence of template. While the bands assigned to the single conjugated products and more important the one assigned to the target double conjugated product can still be observed, their intensity is lower, even though approximately the same amount of material was loaded in each lane. This indicates that although the double click reaction can happen in the absence of template and within the conditions employed here ([ODN] = 10 µM; reaction time: 3 hours at room temperature), the presence of a template provides a major enhancement to the efficiency of the reaction.

The same experiments were also performed with the 15-mer set of probes consisting of ODN-5-Alk, ODN-6-BisAz, ODN-7-Alk and ODN-8. The analysis of these samples using denaturing PAGE is shown in Figure 2.15.

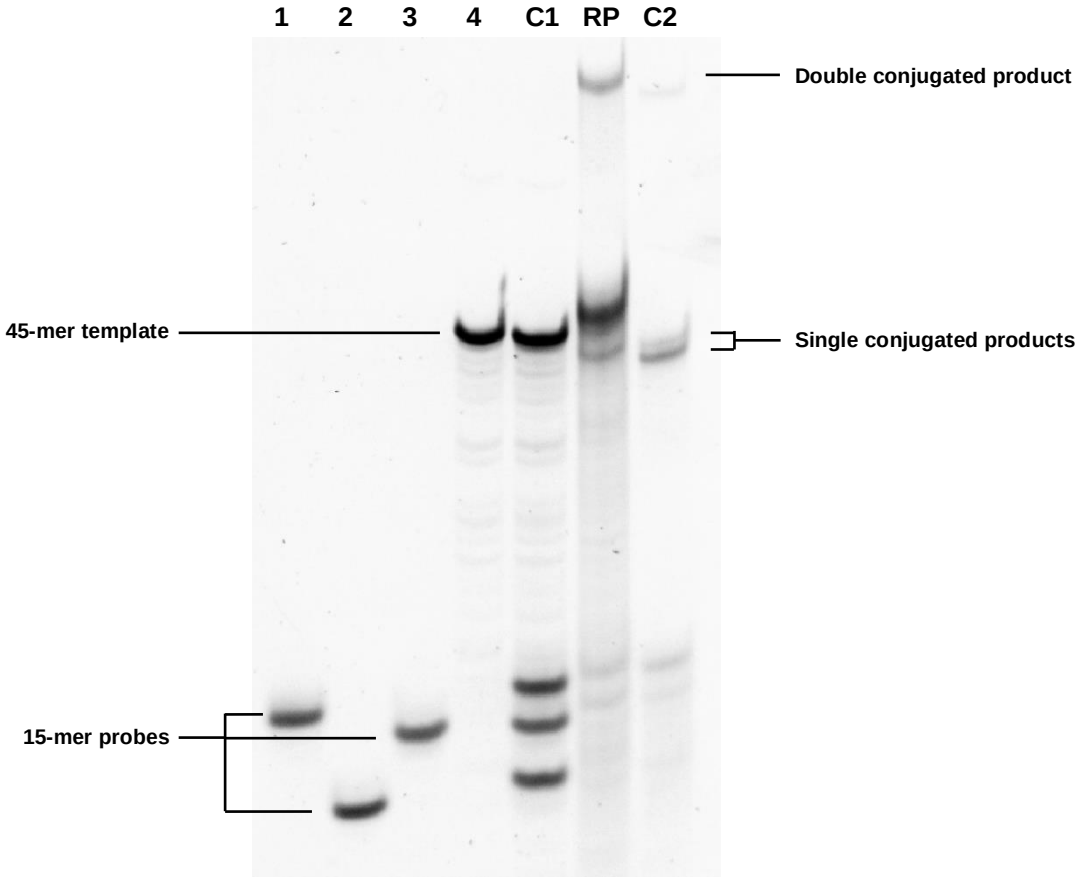

Figure 2.15: 20% denaturing PAGE from the CLICKPLA experiment with the 15-mer probes. Lanes 1 to 4 contain respectively ODN-5-Alk, ODN-6-BisAz, ODN-7-Alk and ODN-8. The lane C1 is a control with the all the ODN from the 15-mer set hybridized but not clicked. The lane RP is the click reaction product with all the ODN from the 15-mer set. C2 is a control with the 15-mer probes clicked in the absence of template. C1 = control 1; C2= control 2; RP = reaction product.

In lane, C1, which contains the complete 15-mer set without click, we can observe clearly and well resolved the three bands of ODN-5-Alk, ODN-6-BisAz and ODN-7-Alk as well as the one of the template ODN-8. Analogous to the results for the 11-mer set, while the template is equally visible in the lane where the actual click reaction product was applied (lane RP), the lanes of the 15-mer probes are only faintly visible and three new bands can be observed. Although not as well resolved as on the gel of the 11-mer set (Figure 2.13), there are still two bands with similar electrophoretic mobility as the template. These bands are assumed to be the single conjugated products of ODN-5-Alk clicked to ODN-6-BisAz and ODN-7-Alk with ODN-6-BisAz. The third new band, higher again on the gel than the 45-mer template is attributed to the target double conjugated product. The reaction control without template shows clearly the formation of the single conjugated products. However, the band assigned to the

double conjugated product is almost not visible this time. To the longer probe ODNs seem to correspond less unwanted conjugation in the absence of the template. This result confirms that the template assisted double click reaction is very effective. On the other hand, the probability for the middle probe to be clicked with both side probes remains very low without the proximity effect provided by the template and placing them next to each other upon hybridization.

2.5.2 Concentration experiments

Encouraged by the template assisted double conjugation results with both the 11-mer set and the 15 mer set, we decided to investigate if the template assistance can enable the reaction to proceed at lower concentrations. The reactions described in the previous section were performed at a final concentration of oligonucleotides of 10 µM. For the following experiments, we used the 11-mer probes (ODN-1-Alk, ODN-2-BisAz and ODN-3-Alk) as well as their template (ODN-4) and several reactions were carried out with different concentrations of oligonucleotides ranging from 10 µM down to 0.1 µM. For every reaction, a reaction control without the template was performed in parallel. The reaction products were again analysed by denaturing PAGE (Figure 2.16).

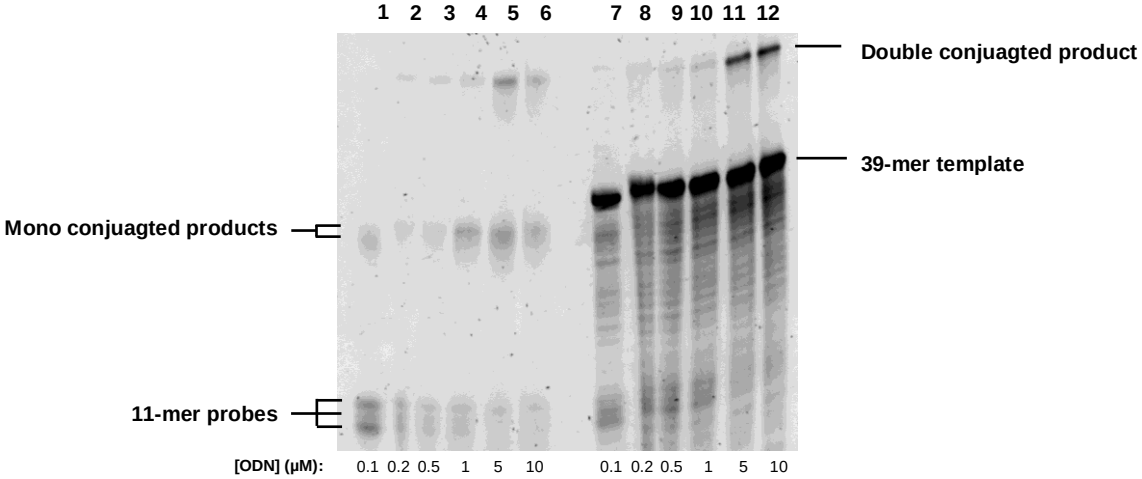

Figure 2.16: 20% denaturing PAGE from the CLICKPLA experiments with the 11-mer probes at different concentration. Lanes 1 to 6 contain the reaction controls with ODN-1-Alk, ODN-2-BisAz, ODN-3-Alk and without template. The lanes 7 to 12 contain the reaction with ODN-1-Alk, ODN-2-BisAz, ODN-3-Alk and ODN-4.

In lanes 11 and 12, which correspond to the reactions performed at 5 and 10 µM respectively, we can observe a very strong band for the target double conjugated product. At lower concentration than 5 µM, this band can still be observed but its intensity decreases along with the concentration. The same is observed for the reaction controls, although as expected the target double conjugated product band is less strong than the one corresponding to the reactions in the presence of template.

2.5.3 Reaction time experiments

After testing different final concentrations of oligonucleotides, we envisioned to perform the double click conjugation with different durations. Indeed, so far every reaction performed had been ran for 3 hours. Here, we decided to test whether the reaction could be achieved within 15, 30 or 60 minutes. In addition, we decided to use a different reaction temperature for these tests by heating the reaction at 40 °C whereas the previous reactions had been performed room temperature. As shown in section 2.4.3, all the ODN probes have a melting temperature higher than 45 °C. Therefore, we assumed that a reaction at 40 °C should not cause stability issue to the duplex formed by the probes with the template. On the other hand, we were curious to test if slightly increasing the reaction temperature while running the reaction for shorter times could prevent the formation of the double conjugated product in the absence of template. For these experiments, we used the 15-mer probes (ODN-5-Alk, ODN-6-BisAz and ODN-7-Alk) and the corresponding template (ODN-8). The reactions were ran in parallel and stopped at different intervals. In order to stop the reactions at defined times, the reaction mixtures were diluted in water by a factor 100 and directly desalted on a centrifuge membrane filter in order to wash the copper catalyst away. For every reaction, a control was performed simultaneously without the template. The ODN concentration was the same in every reaction tube and equal to 10 µM. The denaturing PAGE obtained from analysis of these samples is shown in figure 2.17. In the lane 4 to 6, where the reaction mixtures in presence of template were applied, we can observe an intense band for the double conjugated product. Quite impressively, it seems that the double click reaction is already effective after 15 minutes. This is even more striking considering the low concentration at which the reactions took place. Moreover, in the lanes where the products from the reaction controls without template were applied, we could barely observe, if at all, the formation of the double conjugated product. On the other hand, the

unclicked probes were still clearly observable in these lanes. These results confirm that the proximity effect of the template greatly enhances the double conjugation by CuAAC.

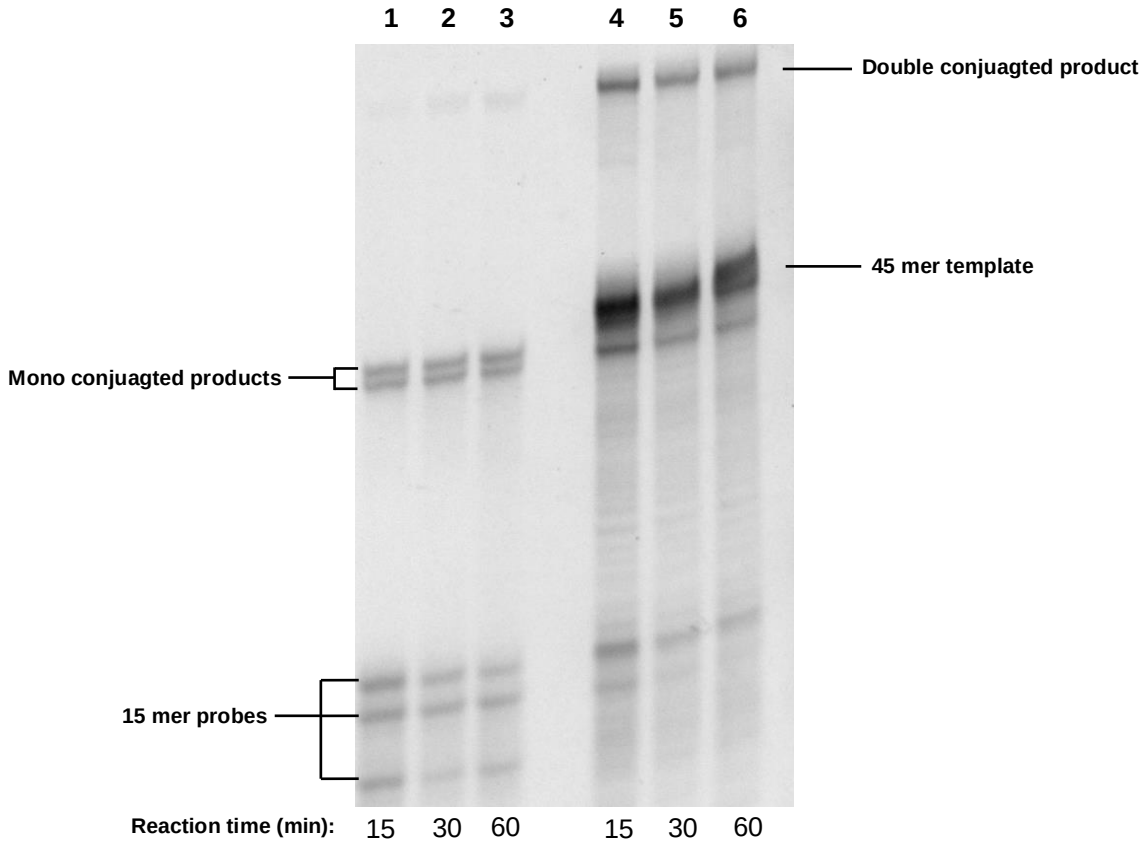

Figure 2.17: 20% denaturing PAGE from the CLICKPLA experiments with the 15 mer probes clicked with different reaction times. Lanes 1, 2 and 3 contain the reaction controls with ODN-5-Alk, ODN-6-BisAz, ODN-7-Alk and without template. The lane 4, 5 and 6 contain the reaction with ODN-5-Alk, ODN-6-BisAz, ODN-7-Alk and ODN-8.

2.6 Conclusions and Outlook

Proximity ligation assay is a very sensitive method developed for the detection of proteins and based on DNA amplification.[1] Since the original proof of concept reported by Landegren et al. in 2002, the PLA and variation of the original concept have been employed in a wide range of applications.[80]

The project presented in this chapter aimed at investigating if the CuAAC reaction could in theory enhance the existing PLA methods. As a proof of concept, we designed a model where three click functional oligonucleotide probes are hybridized next to each other on a single longer oligonucleotide. The latter one, acting as a template, would enable the probes to be hybridized next to each other and facilitate further conjugation by click chemistry.

The first part of the project was to synthesize linkers enabling the desired functionalization of oligonucleotides. At first, we synthesized two unsymmetrical linkers with respectively one picolyl azide/one non-chelating azide and one picolyl azide/two non-chelating azides. These linkers could be chemoselectively clicked on alkyne modified DNA strand thanks to the picolyl azide and thus leaving the non-chelating azide(s) free for subsequent reactions. Next, we synthesized unssymetrical linkers with a picolyl azide and one or two protected alkyne groups. After clicking these linkers to alkyne modified DNA strands thanks to their picolyl azide moiety, the alkyne of the linker was freed from its protecting group rendering it functional towards further click reactions.

The strategies thus developed enabled the synthesis of two sets of oligonucleotide probes with 11- and 15- mer strands respectively. Each set featured three probes, two single alkyne functionalized side probes and one double azide middle probe as well as a complementary oligonucleotide template. Both sets of probes were hybridized on their respective template and conjugated to each other by click reaction. Analysis by denaturing PAGE showed the successful formation of the double conjugated product with both sets of probes. Moreover, we demonstrated that the proximity effect created by the hybridization of the probes on their template was an essential component to the double conjugation between the three probes.

In conclusion, an oligonucleotide template was used to mimic the proximity effect found in PLAs. After hybridization on this template, three beforehand functionalized oligonucleotide probes were conjugated to each other by click chemistry. This model based on three probes could be applied in a Triple Proximity Ligation Assay in the future as following. After recognition of a three-protein complex by three proximity probes, three click functional

oligonucleotides are added and hybridized to the oligonucleotides on the proximity probes. After washing the non-hybridized clickable oligonucleotides, addition of a copper catalyst solution will result in the formation of a double conjugated product between the three hybridized proximity probes. This double conjugated product will then serve as a template in its turn for the circularization of three linear oligonucleotide connectors by enzymatic ligation. In theory, the circular strand thus generated could be formed only in the presence of the double conjugated product which itself accounts for the presence of the protein (or protein complex) of interest. One of the extremities of the double conjugated product will serve as a primer and the circular strand will be amplified by RCA upon addition of a DNA polymerase. The amplification product will eventually be detected by fluorescence *in situ* hybridization (FISH) with complementary fluorescence-labelled oligonucleotides.

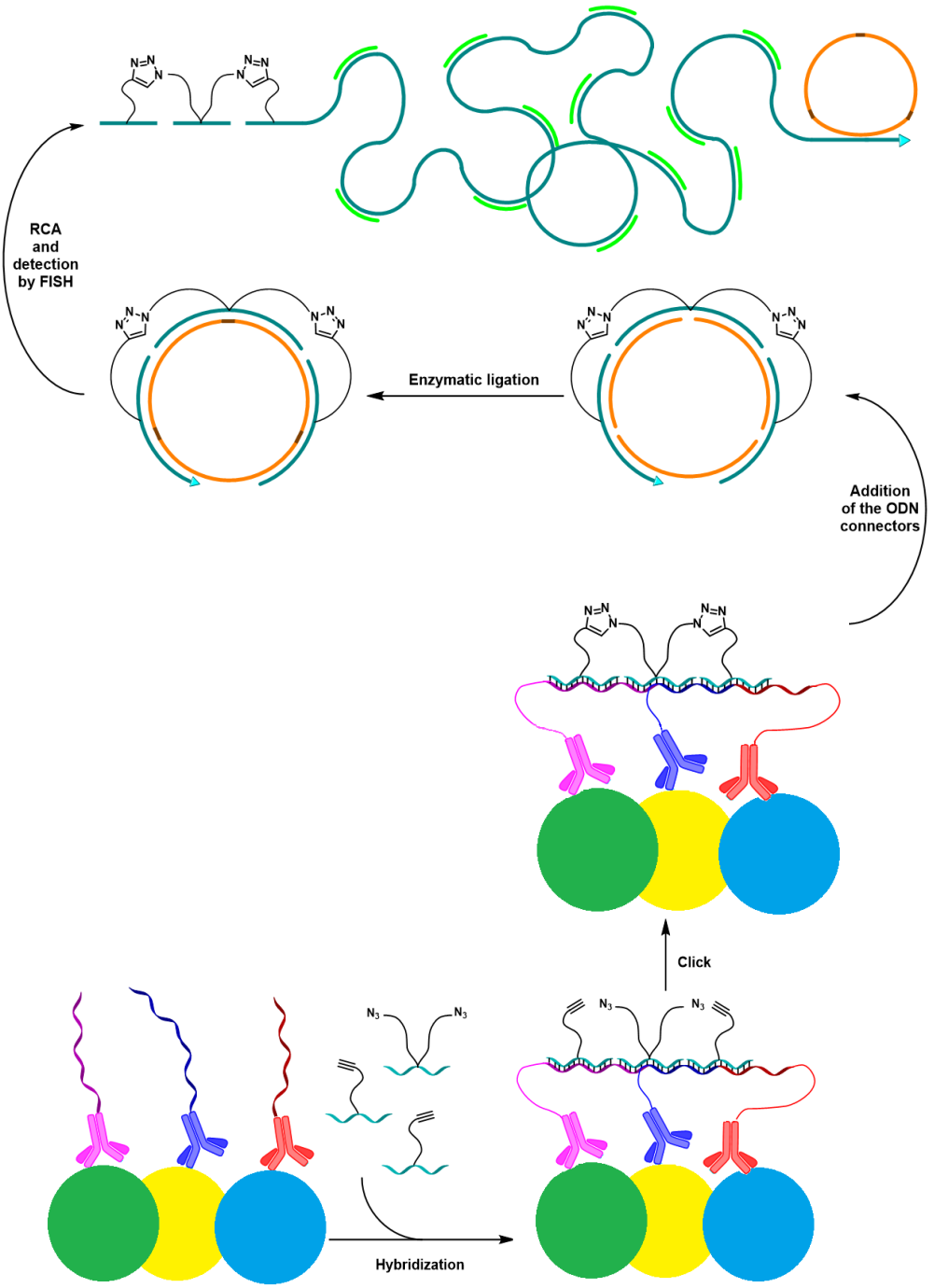

Scheme 2.11: Presentation of a triple proximity ligation assay based on click chemistry. If three proximity probes are close to each other (pink, blue, red), by binding a same three-protein complex (green, yellow, bright blue), then subsequently added click functional ODN probes (green) can be hybridized to the proximity probes and conjugated to each others by CuAAC. The double conjugated product can further act as a template to linear ODN connector (orange) to form a circular structure covalently joined by enzymatic DNA ligation. RCA is then initiated by using the double conjugated product as a primer. The RCA product is detected by FISH.

3. SYNTHESIS AND INCORPORATION OF 5-CARBOXYCYTIDINE PHOSPHORAMIDITE IN SYNTHETIC RNA

3.1 Objectives

5-Hydroxymethyl-[108, 109], 5-formyl-[110], and 5-carboxycytidine[111] bases (respectively abbreviated hmdC, fdC and cadC) are modified bases that were discovered in the DNA of higher eukaryotes. Since their discovery, it has been established that these bases are dynamically generated and removed to regulate the transcriptional activity of genes and therefore possess an epigenetic role. Indeed, they are oxidized derivatives of mdC, which is well known for silencing the gene transcription in the promoters where it is found.[112, 113, 114, 115, 116, 117]

More recently, mC[9], fC[10, 11, 12] and caC[13] have also been found in messenger RNA of mammalian cells. It was recently proven that the so-called ten-eleven translocation (TET) enzymes, the protein family responsible for the oxidation of the DNA base mdC, can also oxidize the RNA base mC subsequently into hmC, fC [11] and caC [118]. In theory, this could indicate a link between DNA and RNA epigenetics[11, 118], as well as a role from these bases in the regulation of the biosynthesis of proteins.[119, 120] Overall, their actual functions remain to to be elucidated and in order to do so, it is necessary to develop phosphoramidite building blocks and their corresponding automated solid-phase synthesis procedures.

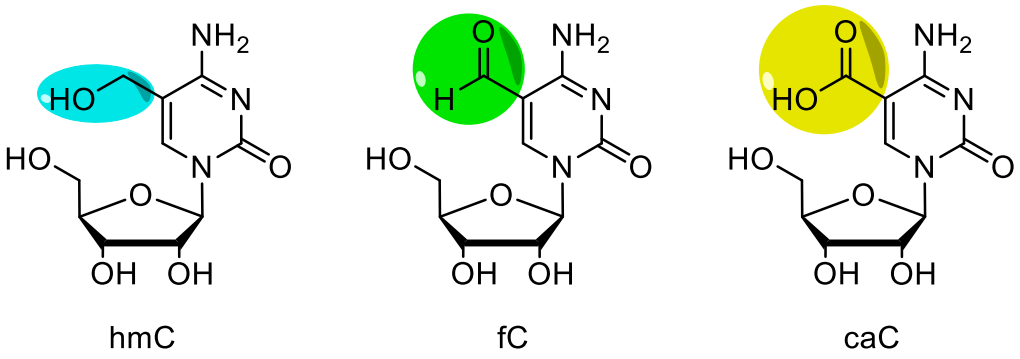

Figure 3.1: Depiction of the three RNA nucleoside modifications hmC, fC and caC.

Indeed, this would provide access to synthetic RNA strands with one or several of these modifications, which could in turn be used in studies aiming at deciphering the functional consequences of hmC, fC and caC in RNA. Phosphoramidite building blocks for hmC and fC have already been reported by respectively Micura[121, 122] and Deiters[123]. However, these building blocks require specific conditions for their incorporation into RNA strands. Therefore, phosphoramidite building blocks for hmC, fC as well as caC able to be incorporated with standard solid-phase RNA synthesis conditions still needed to be developed. Moreover, such building blocks would enable the incorporation of the three modifications in a one single strand. The goal of this project was therefore the development of a synthesis route towards a caC RNA phosphoramdite building block compatible with standard RNA solid-phase synthesis. In parallel to the synthesis of the caC building block, described in the present chapter, the synthesis routes towards a fC RNA phosphoramidite building block as well as a hmC one were developed by co-members of the Carell Group, Dr. Nobuhiro Tago and Dr. Iacovos Michaelides. In a joint effort, we further aimed at incorporating all the three C modification phosphoramidite building blocks in a single synthetic RNA strand.

3.2 Design and protecting group strategy

In order to synthesize a caC RNA phosphoramidite, we needed to develop an alternative protecting group strategy to the one employed for the corresponding DNA building block.
The RNA molecule is intrinsically more sensitive than the DNA one due to the 2'-OH on the ribose. The latter, upon deprotonation, can attack as a nucleophile the adjacent phosphorous in the phosphodiester bond leading to the cleavage of the RNA backbone. Because of this chemical instability, silyl groups usually protect the 2'-OH RNA phosphoramidite building blocks and their removal by a fluoride source (commonly with the trimethylamine trihydrofluoride reagent[124]) is the last treatment that the synthetic RNA strand undergoes. Here we chose to use a TBS group for the protection of 2'-OH position of the ribose. For the protection of the exocyclic amine N4, we decided to use a *p*-methoxybenzoyl group, which can be easily removed at the same time as the cleavage of the strands from the solid support during the ammonolysis step. The carboxylic acid on the position 5 of the caC DNA phosphoramidite is generally protected by alkyl ester groups such as trifluoroethyl ester[125] or methyl ester[126]. Once the building block is incorporated inside the synthetic strand, these protecting groups are removed by hydrolysis with aqueous NaOH instead of ammonolysis, which could result in the formation a 5-carboxamide side product. However, we assumed that such harsh condition are not compatible with RNA synthesis. The silyl protecting group of the 2'-OH on the ribose could be removed as well during this treatment, resulting in the cleavage of the synthetic RNA strand. Therefore, we chose instead to protect the carboxylic acid group with a *p*-nitrophenylethylester group. The latter can be cleaved in milder condition using DBU in THF at room temperature prior to the ammonolysis and thus preventing the formation of a 5-carboxyamide side product. The caC RNA phosphoramidite **42** thus envisioned is depicted in scheme 3.1.

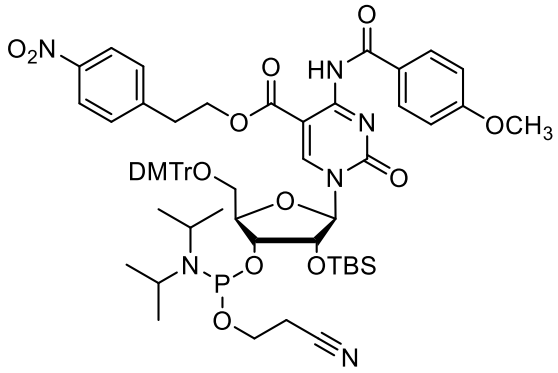

Scheme 3.1: Structure of the caC RNA phosphoramidite building block **42** designed.

After the incorporation of one or several caC phosphoramidite by automatic solid phase synthesis, we imagined the deprotection of the different moieties according to the following sequence:

1- Phosphodiester bonds;
2- 5-carboxilic acid;
3- N4-amine deprotection // cleavage from the solid support;
4- 2'-OH deprotection.

A non-nucleophilic base could simultaneously remove the cyanoethyl group and the p-nitrophenylethylester group, respectively protecting the phosphodiester bond and the 5-carboxilic acid. However, in order to avoid potential Michael-type addition, the 5-carboxilic acid was deprotected after the phosphodiester linkage. Indeed the deprotection of the latter generates acrylonitrile, which could add itself to the base of the nucleoside, and the Michael-System in the nucleobase will be stronger once the carboxylic acid unmasked.[127, 128, 129, 130, 131, 132]

3.3 Synthesis of a caC RNA phosphoramidite building block

Starting from 3´,5´-*O*-(di-*tert*-butylsilanediyl)-2´-*O*-*tert*-butyldimethylsilyl-cytidine **43**, the nucleoside moiety was iodinated in position 5 by a treatment with iodine in the presence of ceric ammonium nitrate. The iodinated product **44** was obtained with a 49 % yield. Following a procedure from Nomura *et al*.[133], **44** was subsequently converted into the corresponding *p*-nitrophenylethylester **45** in 52 % yield. This was achieved by the mean of a palladium catalyzed carbon monoxide insertion in the presence of *p*-nitrophenethylalcohol. The N4-amine was reacted in turn with the acylating agent *p*-anisoyl chloride leading to its protection as a methoxybenzoyl amide **46**. The latter compound **46** was obtained in a 81 % yield. The following reaction consisted in the cleavage of the silyl group protecting simultaneously the 3' and 5' position of the nucleoside. This cleavage was achieved with a solution of HF in pyridine and provided the compound **47** with 89 % yield. The nucleoside was eventually DMT-protected (95 % yield) and phosphorylated (75 % yield) with standard nucleoside chemistry procedures[134, 135]. The caC RNA phosphoramidite building block **42** was thus obtained ready for use with an automatic oligonucleotide synthesizer.

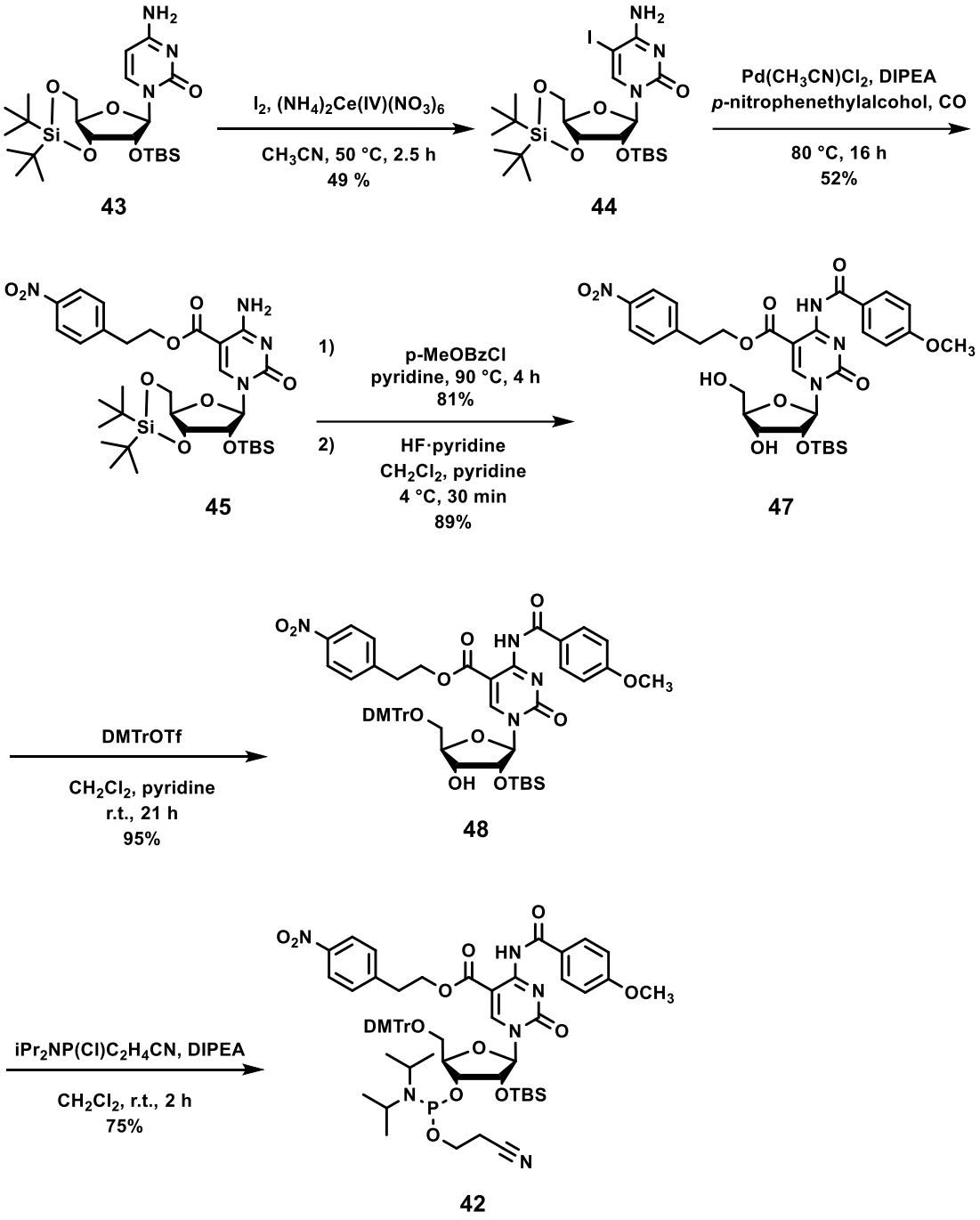

Scheme 3.2: Synthesis of the caC RNA phosphoramidite building block **42**.

3.4 Solid phase synthesis of RNA strands containing caC

Following the synthesis of the caC RNA phosphoramidite buiding bock **42**, we aimed at testing its compatibility with automated solid phase synthesis and validating the deprotection protocol designed for this building block. Therefore, we incorporated the caC phosphoramidite synthesized **42** in two different RNA strands. A short one (13mer) and a long one (21mer) respectively designated ON-1 and ON-2 (Table 3.1).

Table 3.1: Mass spectrometric data of the oligonucleotides synthesized containing the caC modification.

Entry	Sequence	Calcd [M-H]-	Found [M-H]-
ON-**1**	5' CCUAC**caC**GCAUUAC 3'	4061.6	4057.7
ON-**2**	5' UCUGAGUCCCUAUUA**caC**AAGAG 3'	6696.9	6690.9

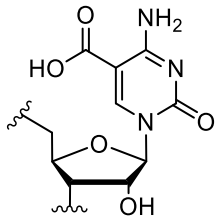

caC

During the solid phase synthesis, the coupling time of the special caC phosphoramidite **42** was extended to 20 minutes (instead of 10 minutes for the standard RNA phosphoramidites) in order to ensure the highest possible coupling yield. According to the deprotection strategy envisioned in the section 3.2, once the synthesis achieved, the solid support was treated with DBU in acetonitrile for 1 to 3 minutes to cleave the cyanoethyl group protecting the phosphodiester bound. This solution was then replaced by one with DBU in THF and the deprotection of the carboxyl group was achieved after 2 hours. The oligonucleotides were further treated with standard deprotection conditions to remove the remaining labile groups. Thus, cleavage from the solid support and cleavage of the N4 amino protecting group were achieved by exposure to an ammonium hydroxide solution in ethanol. Eventually, the TBS group was removed from the 2'-OH with a trimethylamine trihydrofluoride solution in DMSO. The crude products of ON-1 and ON-2 synthesis were analysed by MALDI-TOF mass

spectrometry and it was possible to detect the mass corresponding to both full-length strands containing the caC modification. Both oligonucleotides were further purified and successfully isolated by HPLC (see Figure 3.2).

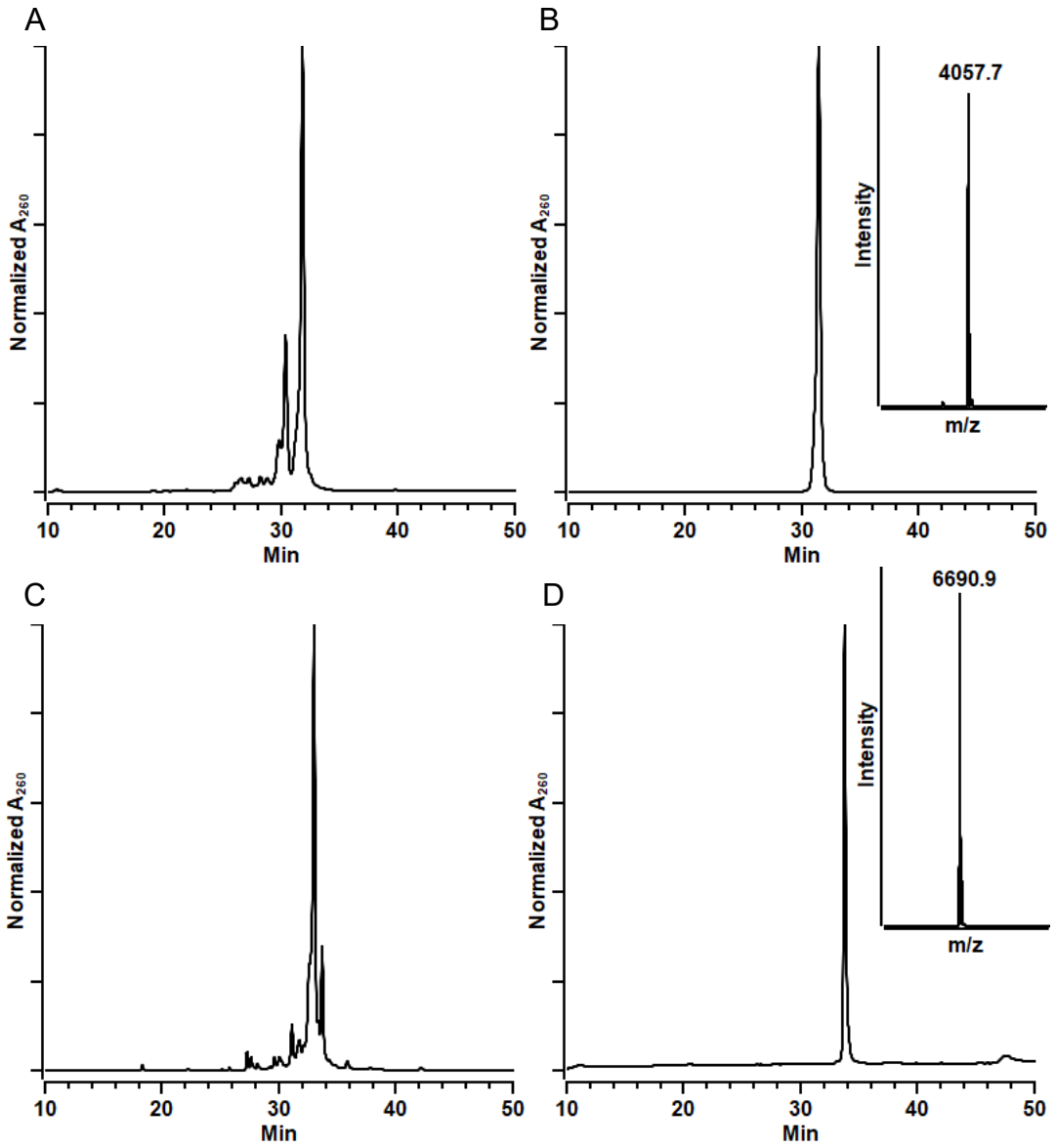

Figure 3.2: (A) HPLC profile of the crude product from the synthesis and deprotection of ON-1. (B) HPLC profile of the purified product from the synthesis and deprotection of ON-1 and the corresponding MALDI-TOF spectrum (inset). (C) HPLC profile of the crude product from the synthesis and deprotection of ON-2. (B) HPLC profile of the purified product from the synthesis and deprotection of ON-2 and the corresponding MALDI-TOF spectrum (inset).

3.5 Solid phase synthesis of a RNA strand containing all the C modifications

As mention in the objectives part of the present chapter, new RNA phosphoramidite building blocks for the fC **49** and hmC **50** modifications were prepared along in the Carell Group (see Scheme 3.3). Like the caC building block **42** here reported, these two fC **49** and hmC **50** building blocks have been designed in order to be compatible with standard RNA solid phase synthesis and deprotection. Therefore, the three newly synthesized C modifications building blocks should be compatible with each other and we decided to investigate this eventuality by incorporating the three of them in one single RNA strand.

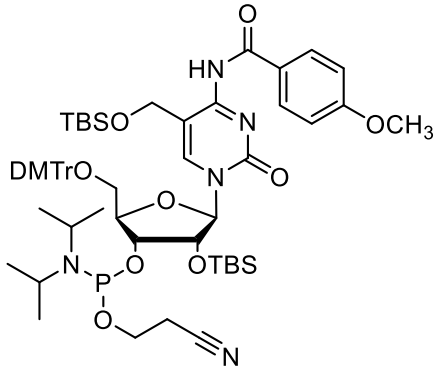

50

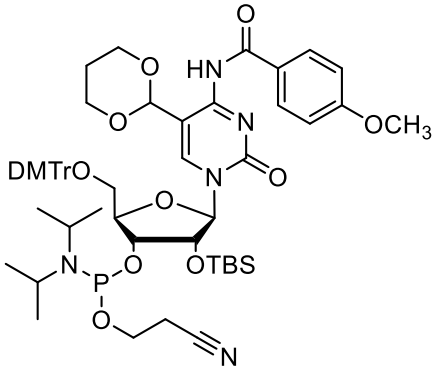

49

Scheme 3.3: Structure of the hmC **50** and fC **49** RNA phosphoramidite building block incorporated together in the same RNA strand with the caC one **42**.

The sequence of the oligonucleotide containing one of each C modification is depicted in the Table 3.2. The coupling time for the special C modifications phosphoramidites was extended to 20 minutes, here again in order to maximise the synthesis yield. Subsequent to the solid phase synthesis, we applied to this strand the same deprotection protocol as the one described previously for the caC containing strands ON-1 and ON-2. The oligonucleotide underwent a final treatment with citric acid-sodium citrate buffer at pH 4 to eventually remove the acetal protecting the carbonyl group of the fC modified nucleoside.

Table 3.2: Mass spectrometric data of the oligonucleotide synthesized containing hmC, fC and caC modifications.

Entry	Sequence	Calcd [M-H]-	Found [M-H]-
ON-**3**	5' UCUGAGU**caC**C**fC**UAUUA**hmC**AAGAG 3'	6754.9	6749.8

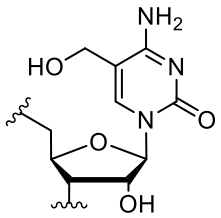

hmC

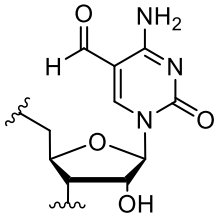

fC

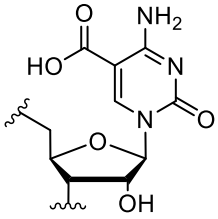

caC

MALDI-TOF analysis of the crude product from the deprotection of ON-3 allowed the detection of the correct mass of the full-length synthetic RNA strand with the three C modified nucleosides. Moreover, analysis of the crude product by HPLC provided a relatively clean profile (Figure 3.3). This can be attributed to an effective synthesis and incorporation of all the three special phosphoramidite building blocks as well as an effective deprotection protocol preventing the formation of any major side products. Finally, the synthetic RNA strand containing caC, fC and hmC nucleosides was successfully purified and isolated by HPLC (see Figure 3.3).

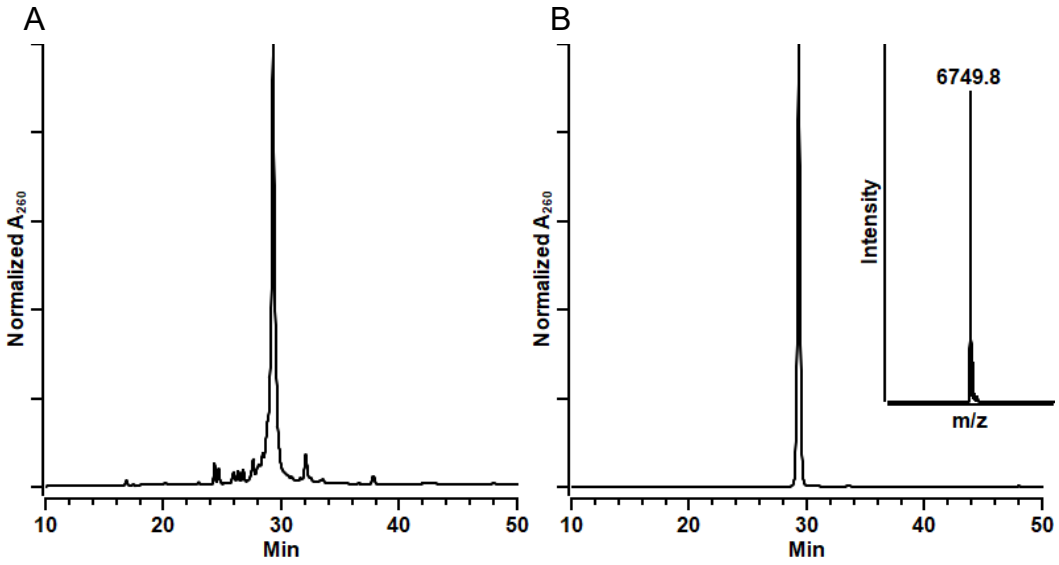

Figure 3.3: (A) HPLC profile of the crude product from the synthesis and deprotection of ON-3. (B) HPLC profile of the purified product from the synthesis and deprotection of ON-3 and the corresponding MALDI-TOF spectrum (inset).

3.6 Enzymatic digestion and uHPLC-MS analysis

In order to confirm the identity and the integrity of the C modifications incorporated by solid phase synthesis, the RNA strand ON-3 containing hmC, fC and caC was enzymatically digested to cleave the strand into single nucleosides. The resulting mixture was subsequently analysed by UHPLC-MS and allowed the detection of all the nucleosides present in the strand (Figure 3.4). In addition to the four canonical nucleosides, we were able to detect the three C modified nucleosides. Moreover, the HPLC profile obtained shows only the four signals corresponding to the canonical nucleosides and the three signals corresponding to hmC, fC and caC. Thus, the absence of additional signal confirms that the incorporation of the special phosphoramidites and deprotection of the resulting RNA strand proceeded effectively and without the formation of side-product or degradation of the oligonucleotide.

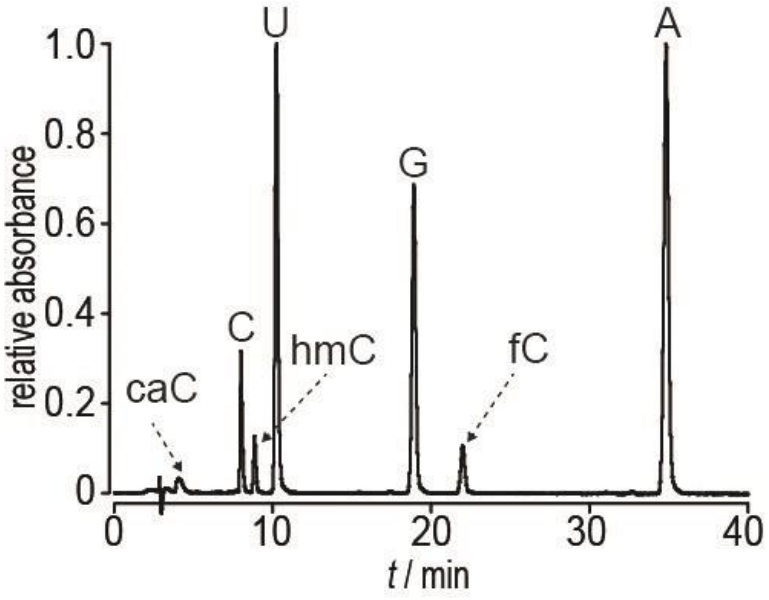

Figure 3.4: UHPLC profile of the enzymatically digested ON-3 allowing the detection of hmC, fC and caC in addition to the four canonical nucleosides A, C, G and U.

3.7 Conclusions and Outlook

In a team effort from the Carell Group, we synthesized new RNA phosphoramidite building block of hmC **50**, fC **49** and caC **42**. Well-designed deprotection strategies enabled efficient incorporation of these building blocks by automated solid phase synthesis inside RNA strands of different lengths. The newly developed modified cytosine building blocks have indeed allowed the synthesis of a strand containing all the three epigenetic bases at specific sites.

It will now be possible to start investigating the role of these modifications inside RNA by performing biochemical studies based on synthetic RNA material containing one or several of the C(5) modified cytosine bases. We envisioned for example similar experiments to those previously performed in our group to study the role of hmC, fC and caC in the context of DNA.[136] In short, we could incubate nuclear extracts from selected cell-line with RNA strands containing the modified bases. The proteins interacting with the modified bases could be further isolated in a pull-down assay and analysed by quantitative mass spectrometry. The identification and study of the proteins recognizing hmC, fC and caC in RNA could thus lead to decipher how these bases are dynamically formed and their intrinsic exact functions.

4. EXPERIMENTAL

4.1 General Methods and Materials for Synthesis

Chemicals were purchased from *Sigma Aldrich*, *ABCR*, *Alfa Aesar*, *Acros Organics*, *Tokyo Chemical Industry Co.* or *Carbosynth* and used without further purification. The solvents for organic synthesis were of reagent grade and purified by distillation. Dry solvents were bought from *Sigma Aldrich* and *Acros Organics.* Acetonitrile for HPLC purification was purchased from *VWR*. ddH_2O refers to double distilled water and was obtained by a *Milli-Q® Plus* purification system from *Merck Millipore* using a *QPAK® 2* cartridge.

All reactions were carried out with *Heidolph MR3001K* magnetic stirring hotplates, and if moisture and air sensitive, in oven-dried glassware (>12 h, 110 °C) under nitrogen or argon. The temperature of reactions (except room temperature) was adjusted with an acetone/dry ice mixture, a water/ice-mixture or an oil bath and the temperature monitored with a *Heidolph ETK 3001* contact thermometer. *In vacuo* solvent removals and solution reconcentrations were performed with a *Heidolph Laborota 4000* rotary evaporator with a *Vario PC2001* diaphragm pump from *Vacuumbrand*. For the removal of water and acetonitrile by freeze-drying, a *Christ Alpha 2-4 LD plus* lyophilizer was used. Alternatively, a centrifugal evaporator *Savant SpeedVac® Plus SC110A* was used.

Chromatographic purification of products was accomplished using flash column chromatography on *Merck Geduran* Si 60 (40 – 63 μm) silica gel (normal phase) or by reversed-phase high-performance liquid chromatography (RP-HPLC). Thin layer chromatography (TLC) was performed on *Merck* 60 (silica gel F_{254}) plates and visualized under UV light (λ = 254 and 366 nm) and staining with ninhydrin solution (0.3 g ninhydrin, 3 mL acetic acid in 100 mL n-Butanol), potassium permanganate (1.5 g $KMnO_4$, 10.0 g K_2CO_3, 125 mg NaOH in 200 mL water) or ceric ammonium molybdate (10.0 g ammonium molybdate tetrahydrate, 2 g $Ce(SO_4)_2 \cdot 4H_2O$, 180 mL ddH_2O, 20 mL conc. H_2SO_4).

^{1}H-, ^{13}C-, and ^{31}P-NMR spectra were recorded in deuterated solvents purchased from *Eurisotop* on *Varian Oxford 200*, *Bruker ARX 300*, *Varian VXR400S*, *Varian Inova 400*, *Brucker* Avance III (cryoprobe) 400, *Brucker AMX 600* and *Brucker Avance III HD* (cryoprobe) 800 spectrometers and calibrated to the residual solvent peak using reported values.[137] The chemical shifts (d) are given in ppm, the coupling constants (J) in Hz. Multiplicities are

abbreviated as follows: s = singlet, d = doublet, t = triplet, q = quartet, m = multiplet, br = broad and combinations of these. For assignment of the structures, additional 2D NMR spectra (COSY, HSQC and HMBC) were measured. High resolution electrospray ionization mass spectra (HRMS-ESI) were recorded on a *Thermo Finnigan LTQ-FT* (ESI-FTICR), and high resolution electron impact ionization mass spectra (HRMS-EI) were recorded on a *Thermo Finnigan* MAT 95. Matrix-assisted laser desorption/ionization-time-of-flight (MALDI-TOF) mass spectra were recorded on a *Brucker Autoflex II*. For MALDI-TOF measurements, the samples were dialyzed on a 0.025 µm *VSWP* filter (*Merck Millipore*) against ddH_2O for 1 h and then co-crystallized in a 3-hydroxypicolinic acid matrix (HPA: 25 mg 3-hydroxypicolinic acid, 5 mg ammonium citrate, 5 µL 15-crown-5 in 0.5 mL H_2O/MeCN = 1:1). IR spectra were recorded on a *Perkin Elmer spectrum BX instrument* and are reported as follows: wavenumber $\tilde{\upsilon}$ in cm^{-1}. The pH values of buffers were adjusted using a *MP 220* pH meter (*Mettler Toledo*). UV spectra and melting profiles were measured on a *Jasco V-650* spectrometer using quartz glass cuvettes with 1 cm path length. The concentration of purified oligonucleotide was determined in triplicate with a *NanoDrop ND-1000* spectrophotometer from *Thermo Scientific* using calculated extinction coefficient from *OligoAnalyzer 3.0* (*Integrated DNA Technologies*: https://eu.idtdna.com/calc/analyzer). For strands containing artificial bases, the extinction coefficient of their corresponding control strand was employed without correction.

Reversed-Phase High-Performance Liquid Chromatography (RP-HPLC)

The following devices were used for the analysis and purification of the synthetic DNA/RNA strands and the linkers synthesized. In order to remove insoluble particles, samples for preparative HPLC were filtered through a 0.2 µm GHP filter membrane (*Acrodisc®*), and samples for analytical HPLC were centrifuged at maximum speed, prior to loading.

Analytical RP-HPLC was performed on an analytical HPLC *Waters Alliance* (2695 Separation Module, 2996 Photodiode Array Detector) equipped with the column Nucleosil 120-3 C18 from *Macherey Nagel*. Using a flow of 0.5 mL/min, gradients of 0–50 % B in 45 min or 0–90 % B over 45 minutes were applied. Preparative RP-HPLC was performed on a HPLC *Waters Breeze* (2487 Dual λ Array Detector, 1525 Binary HPLC Pump) equipped with the columns Nucleosil 100-7 C18, VP 250/10 C18 from Macherey Nagel. Using a flow of 5 mL/min, a gradient of 0–90 % B over 45 minutes was applied

Buffer systems: Buffer A: 0.1 M triethylammonium acetate in water;

Buffer B: 0.1 M triethylammonium acetate in 80% (v/v) acetonitril

4.2 Chemical synthesis

4.2.1 Synthesis of the picolyl azide-PEG$_{10}$-azide linker (17)

6-Hydroxymethyl-nicotinic acid methyl ester[47]

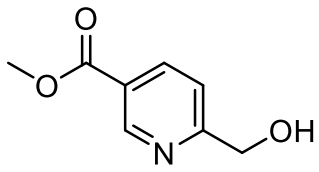

$C_8H_9NO_3$
MW: 167.16 g/mol

2,5-pyridinedicarboxylic acid dimethyl ester (5.23 g, 26.8 mmol, 1.0 eq.) was dissolved in dry MeOH/dry THF (2:1, 300 mL) and cooled down to 0 °C. $NaBH_4$ (2.03 g, 53.6 mmol, 2.0 eq.) was then added portionwise over 20 minutes. The reaction was stirred at 0 °C for 3 hours before being quenched by the addition of a saturated NH_4Cl-solution (~ 100 mL). The solvent was removed *in vacuo* and the aqueous layer was extracted with DCM (3 × 100 mL). The combined organic layers were dried over $MgSO_4$, filtered and the solvent was removed *in vacuo*. 6-hydroxymethyl-nicotinic acid methyl ester was obtained as a colorless solid (3.95 g, 23.6 mmol, 88 %).

R_f (*i*Hex/EtOAc, 1/1) = 0.3.

^{1}H-NMR (400 MHz, $CDCl_3$): δ (ppm): 9.15 (d, *J* = 2 Hz, 1H), 8.29 (dd, *J* = 8.1, 1.9 Hz, 1H), 7.36 (d, *J* = 8.1 Hz, 1H), 4.83 (s, 2H), 3.95 (s, 3H).

^{13}C-NMR (101 MHz, $CDCl_3$): δ (ppm): 165.6, 163.4, 149.9, 137.8, 125.0, 120.0, 64.2, 52.5.

Methyl 5-(azidomethyl)nicotinate

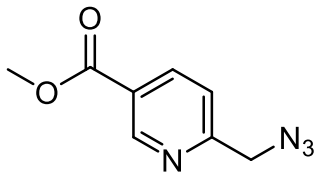

$C_8H_8N_4O_2$
MW: 192.18 g/mol

The synthesis is based on a modified procedure from *C. Uttamapinant et al*.[47]
6-hydroxymethyl-nicotinic acid methyl ester (1.00 g, 5.98 mmol) was dissolved in dry DCM (40 mL). Triethylamine (1.67 mL, 1.21 g, 12.0 mmol, 2.0 eq.) was added and the reaction was cooled to 0 °C. Subsequently, mesyl chloride (695 µL, 1.03 g, 8.97 mmol, 1.5 eq.) was added and the reaction was stirred over night at room temperature. The solvent was removed *in vacuo* and water was added (30 mL). The aqueous layer was extracted with DCM (3 × 30 mL), the combined organic layers were dried over $MgSO_4$ and reconcentrated *in vacuo*. The residue was dissolved again in 60 mL THF and sodium azide (3.89 g, 59.8 mmol, 10.0 eq.) was added. The reaction was further stirred at room temperature for 48 h before being diluted with water and ethyl acetate (100 mL). The aqueous layer was extracted with ethyl acetate (3 × 100 mL) and the combined organic layers were dried over $MgSO_4$ and filtered. The solvent was removed *in vacuo* to provide methyl 5-(azidomethyl)nicotinate as a pale yellow solid (705 mg, 3.67 mmol, 62 %).

R_f (*i*Hex/EtOAc, 1/1) = 0.8.

^{1}H-NMR (400 MHz, $CDCl_3$): δ (ppm): 9.19 (d, *J* = 2.1 Hz, 1H), 8.33 (dd, *J* = 8.1, 2.1 Hz, 1H), 7.46 (d, *J* = 8.1 Hz, 1H), 4.58 (s, 2H), 3.96 (s, 3H).

^{13}C-NMR (101 MHz, $CDCl_3$): δ (ppm): 165.2, 160.6, 150.5, 138.2, 125.2, 121.3, 55.6, 52.4.

6-Azidomethylnicotinic acid (16)[47]

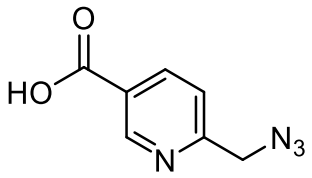

$C_7H_6N_4O_2$
MW: 178.15 g/mol

Methyl 5-(azidomethyl)nicotinate (703 mg, 3.66 mmol) was dissolved in methanol (15 mL) and 2.0 M LiOH solution in water was added (6.5 mL). The reaction was stirred for 1 hour at room temperature and subsequently quenched with HCl (2.0 M in water, 6.5 mL). The solvent was removed *in vacuo* and the residue was extracted with DCM (2 × 20 mL) and EtOAc (2 × 20 mL). The combined organic layers were dried over $MgSO_4$, filtered and the solvent was removed *in vacuo*. 6-azidomethylnicotinic acid **16** was obtained as a dark yellow solid (621 mg, 3.49 mmol, 95 %).

R_f (EtOAc) = 0.4.

^{1}H-NMR (400 MHz, $CDCl_3$): δ (ppm): 9.31 (m, 1H), 8.47 (dd, *J* = 8.1, 2.1 Hz, 1H), 7.68 (d, *J* = 8.1 Hz, 1H), 4.81 (s, 2H).

^{13}C-NMR (101 MHz, $CDCl_3$): δ (ppm): 168.9, 160.9, 150.6, 139.4, 125.5, 122.8, 54.9.

HR-MS (ESI): calc. for $C_7H_7O_2N_4^+$ $[M+H]^+$: 179.0564; found: 179.0559.

***O*-(2-(6-(Azidomethyl)nicotinamidoethyl)-*O′*-(2-azidoethyl)nonaethylene glycol (17)**

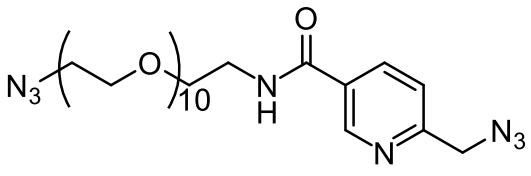

$C_{29}H_{50}N_8O_{11}$
MW: 686.76 g/mol

6-Azidomethylnicotinic acid **16** (20.3 mg, 114 µmol) and HATU (52.0 mg, 137 µmol, 1.2 eq.) were dissolved in dry DMF (0.4 mL) and DIPEA (40.0 µL, 29.5 mg, 228µmol, 2.0 eq.) were added. The mixture was stirred for 15 minutes at room temperature and *O*-(2-Aminoethyl)-*O′*-

(2-azidoethyl)nonaethylene glycol (60.0 mg, 114 µmol, 1.0 eq.) was added. The reaction was stirred over night at room temperature and the solvent was removed *in vacuo*. The residue was taken up in DCM (15 mL) and washed with brine (15 mL). The aqueous layer was reextracted one time with DCM (15 mL) and the combined organic layers were dried over $MgSO_4$ and filtered. The solvent was removed *in vacuo* and the residue was purified by flash column chromatography (Silica, DCM/MeOH, 100/0 → 95/5). **17** was obtained as a colourless oil (63 mg, 92 µmol, 81 %).

$\mathbf{R_f}$ (DCM/MeOH, 10/1) = 0.6.

^{1}H-NMR (400 MHz, $CDCl_3$): δ (ppm): 9.01 (d, *J* = 2.3 Hz, 1H, CH_{arom}), 8.20 (dd, *J* = 8.1, 2.3 Hz, 1H, CH_{arom}), 7.42 (d, *J* = 8.1 Hz, 1H, CH_{arom}), 4.53 (s, 2H, $C_{arom}CH_2N_3$), 3.78 – 3.46 (m, 42H, 21×$C_{linker}H_2$), 3.37 (t, *J* = 5.1 Hz, 2H, $CH_2CH_2N_3$).

^{13}C-NMR (101 MHz, $CDCl_3$): δ (ppm): 165.2 (*C*=O), 158.4 (C_{arom}), 148.3 (C_{arom}), 136.4 (CH_{arom}), 129.5 (CH_{arom}), 121.5 (CH_{arom}), 70.7 ($C_{linker}H_2$), 70.7 ($C_{linker}H_2$), 70.6 ($C_{linker}H_2$), 70.6 ($C_{linker}H_2$), 70.5 ($C_{linker}H_2$), 70.3 ($C_{linker}H_2$), 70.0 ($C_{linker}H_2$), 69.6 ($C_{linker}H_2$), 55.3 ($C_{arom}CH_2N_3$), 50.7 ($CH_2CH_2N_3$), 40.0 (CH_2CH_2NH).

HR-MS (ESI): calc. for $C_{29}H_{51}O_{11}N_8^+$ $[M+H]^+$: 687.3673; found: 687.3682.

4.2.2 Synthesis of the picolyl azide/bis-azide linker (19)

***tert*-butyl (2-(2-(2-(6-(Azidomethyl)nicotinamido)ethoxy)ethoxy)ethyl)carbamate**

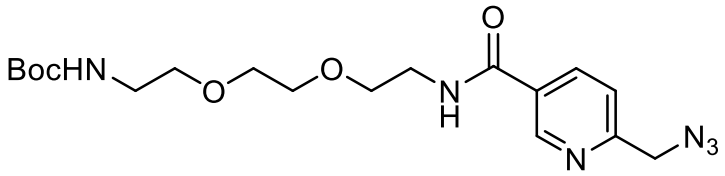

$C_{18}H_{28}N_6O_5$
MW: 408.46 g/mol

6-Azidomethylnicotinic acid **16** (947 mg, 5.32 mmol, 1.0 eq.) and HATU (2.20 g, 5.80 mmol, 1.2 eq.) were dissolved in dry DMF (5.0 mL) and DIPEA (1.68 mL, 1.25 g, 9.66 mmol, 2.0 eq.) was added. The mixture was stirred for 30 minutes at room temperature and *tert*-Butyl 2-(2-(2-aminoethoxy)ethoxy)ethylcarbamate (1.14 mL, 1.20 g, 4.83 mmol, 0.9 eq.) was added. The reaction was stirred overnight at room temperature and the solvent was removed *in vacuo*. The residue was taken up in DCM (50 mL) and washed with brine (50 mL). The combined organic layers were dried over $MgSO_4$, filtered and the solvent was removed *in vacuo*. The residue was purified by flash column chromatography (Silica, DCM/MeOH, 100/0 → 96/4). Tert-butyl (2-(2-(2-(6-(azidomethyl)nicotinamido)ethoxy)ethoxy)ethyl)carbamate was obtained as a brown oil (1.78 g, 4.36 mmol, 91 %).

R_f (DCM/MeOH, 10/1) = 0.8.

^{1}H-NMR (400 MHz, $CDCl_3$): δ (ppm): 8.97 (d, *J* = 2.3 Hz, 1H, C*H*$_{arom}$), 8.15 (dd, 1H, *J* = 8.1, 2.3 Hz, 1H, C*H*$_{arom}$), 7.40 (d, *J* = 7.9 Hz, 1H, C*H*$_{arom}$), 4.50 (s, 2H, $C_{arom}CH_2N_3$), 3.77 – 3.55 (m, 10H, 5×$C_{linker}H_2$), 3.28 – 3.22 (m, 2H, $C_{linker}H_2$), 1.37 (s, 9H, 3×CH_3).

^{13}C-NMR (101 MHz, $CDCl_3$): δ (ppm): 165.4 (*C*=O), 158.5 (*C*=O), 156.1 (*C*$_{arom}$), 148.2 (*C*$_{arom}$), 136.3 (*C*H$_{arom}$), 129.4 (*C*H$_{arom}$), 121.6 (*C*H$_{arom}$), 79.4 (*C*$_{tert}$), 70.2 (OCH_2CH_2O), 70.1 (OCH_2CH_2O), 69.5 (OCH_2CH_2NHBoc), 55.6 ($C_{arom}CH_2N_3$), 40.3 (OCH_2CH_2NHBoc), 39.8 (OCH_2CH_2NHCO), 28.4 ($C(CH_3)_3$).

HR-MS (ESI): calc. for $C_{18}H_{29}O_5N_6^+$ $[M+H]^+$: 409.2194; found: 409.2191.

***N*-(2-(2-(2-Aminoethoxy)ethoxy)ethyl)-6-(azidomethyl)nicotinamide (21)**

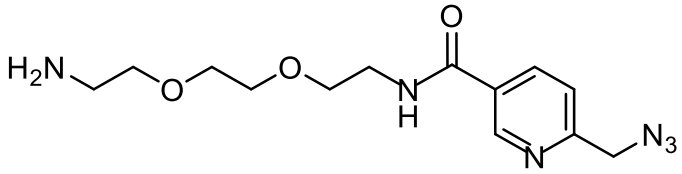

$C_{13}H_{20}N_6O_3$
MW: 308.34 g/mol

Tert-butyl (2-(2-(2-(6-(azidomethyl)nicotinamido)ethoxy)ethoxy)ethyl)carbamate (1.78 g, 4.36 mmol, 1.0 eq.) was dissolved in methanol (6mL) and an aqueous solution of HCl was added (2.0 M, 3.0 mL, 20.0 eq.). The reaction was stirred at 50 °C for 2 hours before being quenched by addition of a solution of NaOH (1.0 M in water, 6 mL). The solvent was removed in vacuo and the aqueous layer was extracted with DCM (2 × 15 mL) and EtOAc (1 × 15 mL). The organic layers were combined, dried over $MgSO_4$ and filtered. The solvent was removed *in vacuo* and **21** was obtained as an orange oil (955 mg, 3.10 mmol, 72 %).

R_f (DCM/MeOH, 10/1) = 0.3.

^{1}H-NMR (599 MHz, $CDCl_3$): δ (ppm): 9.01 (d, *J* = 2.3 Hz, 1H, C*H*$_{arom}$), 8.19 (dd, 1H, *J* = 8.1, 2.3 Hz, 1H, C*H*$_{arom}$), 7.42 (d, *J* = 8.1 Hz, 1H, C*H*$_{arom}$), 4.53 (s, 2H, $C_{arom}CH_2N_3$), 3.72 – 2.75 (m, 12H, 6×$C_{linker}H_2$).

^{13}C-NMR (151 MHz, $CDCl_3$): δ (ppm): 165.3 (*C*=O), 158.5 (*C*$_{arom}$), 148.2 (*C*$_{arom}$), 136.3 (*C*H$_{arom}$), 129.5 (*C*H$_{arom}$), 121.5 (*C*H$_{arom}$), 73.0 (O*C*$H_2CH_2NH_2$), 70.3 (O*C*H_2CH_2O), 70.0 (O*C*H_2CH_2O), 69.7 (O*C*H_2CH_2NHCO), 55.3 ($C_{arom}CH_2N_3$), 41.5 ((O$CH_2CH_2NH_2$), 39.9 (OCH_2CH_2NHCO).

HR-MS (ESI): calc. for $C_{13}H_{21}O_3N_6^+$ $[M+H]^+$: 309.1673; found: 309.1673.

14-Hydroxy-3,6,9,12-tetraoxatetradecyl-4'-methylbenzolsulfonat (25)

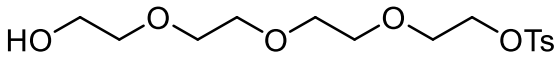

$C_{15}H_{24}O_7S$
MW: 348.41 g/mol

Tetraethylenglycole **22** (29.25 g, 150.6 mmol, 1.0 eq.) was dissolved in dry THF (100 mL) and triethylamine (122 g, 1.20 mol, 8.0 eq.) was added. The reaction was cooled down to 0 °C and a solution of tosylchloride (28.71 g, 150.6 mmol, 1.0 eq.) in dry THF (50 mL) was added over a period of 1 hour. After 48-hour stirring at room temperature the solvent was removed *in vacuo*. The mixture was taken up in HCl (2 M, 150 mL) and extracted with DCM (4 × 150 mL). The combined organic layers were dried over $MgSO_4$ and filtered. After removal of the solvent *in vacuo* the crude product was purified by flash column chromatography (Silica, DCM → DCM/MeOH (99 /1 → 0/1)). The product **25** was obtained as a colourless oil (48.27 g, 138.6 mmol, 92 %).

^{1}H-NMR (400 MHz, $CDCl_3$): δ (ppm): 7.82-7.76 (m, 2H, C*H*$_{arom.}$), 7.37-7.30 (m, 2H, C*H*$_{arom.}$), 4.20-4.12 (m, 2H, C*H*$_2$), 3.73-3.52 (m, 14H, 7×C*H*$_2$), 2.42 (s, 3H, C*H*$_3$), 2.38-2.31 (s, 1H, O*H*).

^{13}C-NMR (101 MHz, $CDCl_3$): δ (ppm): 144.9 (*C*$_{arom.}$), 133.2 (*C*$_{arom.}$), 130.0 (2×CH$_{arom.}$), 128.1 (2×*C*H$_{arom.}$), 72.6 (*C*H$_2$), 70.9 (*C*H$_2$), 70.8 (*C*H$_2$), 70.6 (*C*H$_2$), 70.5 (*C*H$_2$), 69.4 (*C*H$_2$), 68.9 (*C*H$_2$), 61.9 (*C*H$_2$), 21.8 (*C*H$_3$).

HR-MS (ESI): $C_{15}H_{25}O_7S^+$ $[M+H]^+$, calc.: 349.1315, found: 349.1316.

2-(2-(2-(2-Azidoethoxy)ethoxy)ethoxy)ethan-1-ol (26)

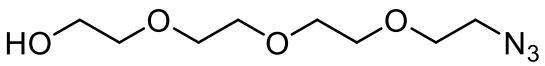

$C_8H_{17}N_3O_4$
MW: 219.24 g/mol

To **25** (8.08 g, 23.19 mmol, 1.0 eq.) in solution in dry DMF (100 mL) was added NaN_3 (7.54 g, 116 mmol, 5.0 eq.). The mixture was stirred at 70 °C for 8 hours and the solvent was removed *in vacuo*. The residue was retaken in water (100 mL), extracted with DCM (2 × 100 mL) and

the combined organic layers were dried over $MgSO_4$ and filtered. The solvent was removed *in vacuo* and 2-(2-(2-(2-azidoethoxy)ethoxy)ethoxy)ethan-1-ol **26** was obtained as a colourless oil (4.87 g, 22.2 mmol, 96 %).

^{1}H-NMR (400 MHz, $CDCl_3$): δ (ppm): 3.76 – 3.68 (m, 2H, CH_2), 3.68 – 3.62 (m, 10H, 5×CH_2), 3.63 – 3.58 (m, 2H, CH_2), 3.39 (t, *J* = 5.2 Hz, 2H, CH_2).

^{13}C-NMR (101 MHz, $CDCl_3$): δ (ppm): 72.5 (*C*H_2), 70.7 (*C*H_2), 70.7 (*C*H_2), 70.6 (*C*H_2), 70.4 (*C*H_2), 70.1 (*C*H_2), 61.7 (*C*H_2), 50.7 (*C*H_2).

HR-MS (ESI): $C_8H_{18}O_4N_3^+$ $[M+H]^+$, calc.: 220.1292, found: 220.1293.

2-(2-(2-(2-Azidoethoxy)ethoxy)ethoxy)ethyl 4-methylbenzenesulfonate (23)

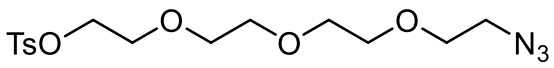

$C_{15}H_{23}N_3O_6S$
MW: 373.42 g/mol

26 (4.75 g, 21.67 mmol) was dissolved in dry DCM (50 mL). Triethylamine (8.92 mL, 6.51 g, 65.0 mmol, 3.0 eq.) was added and the reaction was cooled to 0 °C. Subsequently tosylchloride (12.39 g, 65.00 mmol, 3.0 eq.) was added and the reaction was stirred over night at room temperature. The solvent was removed *in vacuo* and the residue was taken up in HCl (2.0 M in water, 50 mL). After extraction with DCM (5 × 50 mL), the combined organic layers were dried over $MgSO_4$, filtered and the solvent was remved *in vacuo*. The crude product was purified by flash column chromatography (Silica, *i*-Hex/EtOAc 1/0 → 3/7). 2-(2-(2-(2-azidoethoxy)ethoxy)ethoxy)ethyl 4-methylbenzenesulfonate **23** was obtained as a colourless oil (7.42 g, 20.0 mmol, 92 %).

^{1}H-NMR (400 MHz, $CDCl_3$): δ (ppm): 7.80 (d, *J* = 7.9 Hz, 2H, CH_{arom}), 7.34 (d, *J* = 7.9 Hz, 2H, CH_{arom}), 4.16 (t, *J* = 4.9 Hz, 2H, CH_2), 3.72 – 3.58 (m, 12H, 6×CH_2), 3.38 (t, *J* = 5.0 Hz, 2H, CH_2), 2.45 (s, 3H, CH_3).

^{13}C-NMR (101 MHz, $CDCl_3$): δ (ppm): 144.9 (*C*$_{arom.}$), 133.2 (*C*$_{arom.}$), 130.0 (2×*C*H$_{arom.}$), 128.1 (2×*C*H$_{arom.}$), 70.9 (*C*H_2), 70.8 (*C*H_2), 70.8 (*C*H_2), 70.2 (*C*H_2), 69.4 (*C*H_2), 68.9 (*C*H_2), 50.8 (*C*H_2), 21.8 (*C*H_3).

HR-MS (ESI): $C_{15}H_{27}O_6N_4S^+$ $[M+NH_4]^+$, calc.: 391.1646, found: 391.1649.

Methyl-3, 5-bis(2-(2-(2-(2-azidoethoxy)ethoxy)ethoxy)ethoxy)benzoate

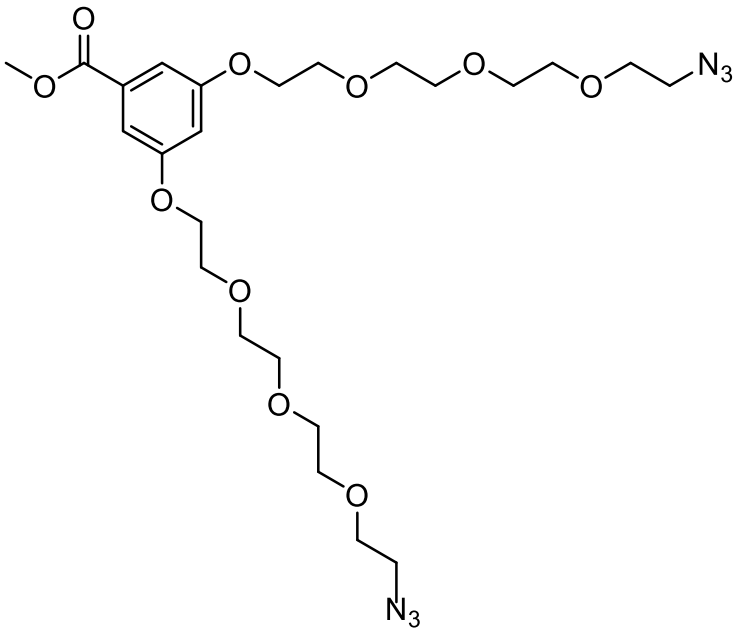

$C_{24}H_{38}N_6O_{10}$
MW: 570.60 g/mol

To a solution of methyl 3,5-dihydroxybenzoate (30 mg, 178.41 µmol, 1.0 eq.) **20** in acetone (1.7 mL), **23** (147 mg, 392.51 µmol, 2.2 eq.) and K_2CO_3 (123.29 mg, 892.07 µmol, 5.0 eq.) were added. The reaction was stirred at 55 °C for 30 hours and the solvent was removed. The residue was taken up in water (5 mL) and DCM (5 mL) and extracted with DCM (3 × 5 mL). The combined organic layers were dried over $MgSO_4$, filtered and the solvent removed *in vacuo*. The crude product was purified by flash column chromatography (Silica, DCM/MeOH 100/0 → 96/4) and the product was obtained as a yellow oil (78.0 mg, 137 µmol, 77 %).

^{1}H-NMR (400 MHz, $CDCl_3$): δ (ppm): 7.19 – 7.05 (m, 2H, 2×CH_{arom}), 7.12 – 7.05 (m, 1H, CH_{arom}), 4.17 – 4.05 (m, 4H, 2×CH_2), 3.90 – 3.79 (m, 7H, 2×CH_2+CH_3), 3.75 – 3.56 (m, 20H, 10×CH_2), 3.36 (t, *J* = 5.0 Hz, 4H, 2×CH_2).

^{13}C-NMR (101 MHz, $CDCl_3$): δ (ppm): 166.8 (*C*=O), 159.7 (2×$C_{arom.}$), 131.8 ($C_{arom.}$), 108.0 (2×*C*H$_{arom}$), 106.9 (*C*H$_{arom}$), 70.8 (*C*H$_2$), 70.7 (*C*H$_2$), 70.7 (*C*H$_2$), 70.6 (*C*H$_2$), 70.0 (*C*H$_2$), 70.0 (*C*H$_2$), 69.6 (*C*H$_2$), 69.6 (*C*H$_2$), 67.7 (*C*H$_2$), 67.7 (*C*H$_2$), 52.2 (*C*H$_3$), 50.7 (*C*H$_2$N$_3$).

HR-MS (ESI): $C_{24}H_{42}O_{10}N_7^+$ $[M+NH_4]^+$, calc.: 588.2987, found: 588.2976.

3,5-bis(2-(2-(2-(2-Azidoethoxy)ethoxy)ethoxy)ethoxy)benzoic acid (24)

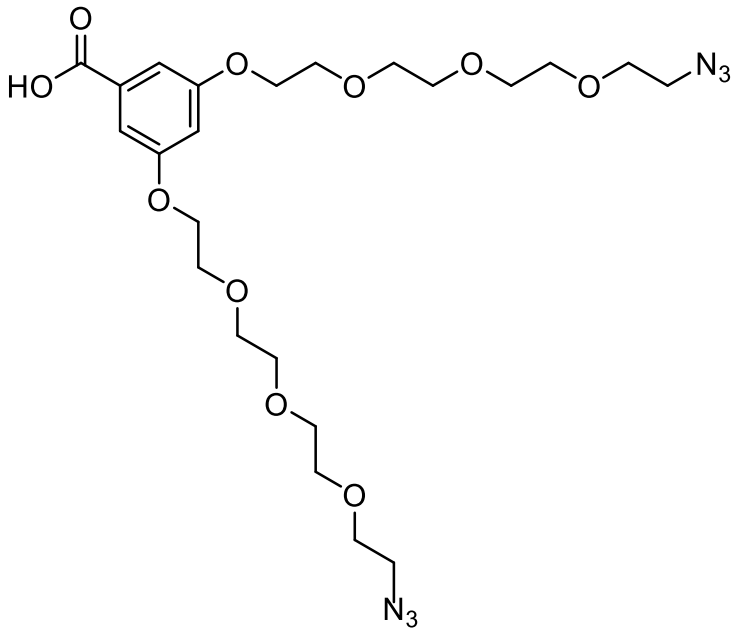

$C_{23}H_{36}N_6O_{10}$
MW: 556.57 g/mol

Methyl 3,5-bis(2-(2-(2-(2-azidoethoxy)ethoxy)ethoxy)ethoxy)benzoate (56 mg, 98.14 µmol, 1.0 eq.) was dissolved in methanol (2 mL) and NaOH (1.0 M in water, 491 µL, 5.0 eq.) was added. The reaction was stirred at 40 °C for 3 hours and cooled to room temperature. It was subsequently quenched by adding dropwise HCl (2.0 M, 250 µL) and the solvent was removed *in vacuo*. The residue was taken up in water (10 mL) and extracted with EtOAc (3 × 10 mL). The combined organic layers were dried over $MgSO_4$, filtered and **24** was obtained as a colourless liquid (50 mg, 90 µmol, 92 %).

^{1}H-NMR (400 MHz, $CDCl_3$): δ (ppm): 7.23 – 7.18 (m, 2H, 2×C*H*$_{arom}$), 6.73 – 6.67 (m, 1H, C*H*$_{arom}$), 4.18 – 4.05 (m, 4H, 2×C*H*$_2$), 3.90 – 3.62 (m, 24H, 12×C*H*$_2$), 3.37 (t, *J* = 5.0 Hz, 4H, 2×C*H*$_2$) .

^{13}C-NMR (101 MHz, $CDCl_3$): δ (ppm): 170.5 (*C*=O), 159.8 (2×*C*$_{arom.}$), 131.2 (*C*$_{arom.}$), 108.4 (2×*C*H$_{arom}$), 107.5 (*C*H$_{arom}$), 70.8 (*C*H$_2$), 70.7 (*C*H$_2$), 70.7 (*C*H$_2$), 70.6 (*C*H$_2$), 70.0 (*C*H$_2$), 69.6 (*C*H$_2$), 67.7 (*C*H$_2$), 50.7 (*C*H$_2$N$_3$).

HR-MS (ESI): $C_{23}H_{40}O_{10}N_7^+$ $[M+NH_4]^+$, calc.: 574.2831, found: 574.2821.

6-(Azidomethyl)-N-(2-(2-(2-(3,5-bis(2-(2-(2-(2-azidoethoxy)ethoxy)ethoxy)ethoxy)benzamido)ethoxy)ethoxy)ethyl)nicotinamide (19)

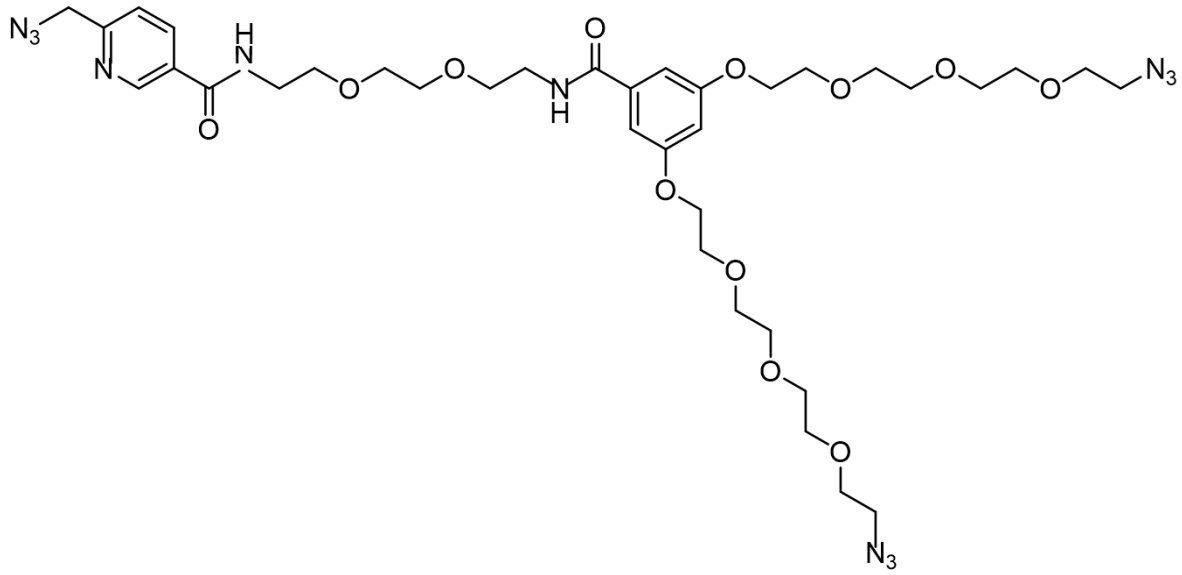

$C_{36}H_{54}N_{12}O_{12}$
MW: 846.90 g/mol

24 (25 mg, 44.92 µmol, 1.0 eq.) was dissolved in dry DMF (0.5 mL). HATU (21 mg, 54 µmol, 1.2 eq.) and DIPEA (15.7µL, 11.6 mg, 89.8 µmol, 2 eq.) were added and the mixture was stirred 45 minutes at room temperature. A solution of **21** (15 mg, 49.4 µmol, 1.1 eq.) in DMF (0.5 mL) was added and the reaction was stirred 12 hours at room temperature. The solvent was removed *in vacuo* and the residue was taken up in DCM (10 mL) and washed with brine (10 mL). The aqueous layer was reextracted one time with DCM (15 mL) and the combined organic layers were dried over $MgSO_4$ and filtered. The solvent was removed *in vacuo* and the residue was purified by flash column chromatography (Silica, DCM/MeOH, 100/0 → 95/5). **19** was obtained as an orange oil (31 mg, 37 µmol, 82 %).

^{1}H-NMR (400 MHz, $CDCl_3$): δ (ppm): 8.98 (d, *J* = 2.1 Hz, 1H, C*H*$_{arom}$N$_{arom}$), 8.15 (dd, *J* = 8.1, 2.1 Hz, 1H, C*H*$_{arom}$), 7.40 (d, *J* = 8.0 Hz, 1H, C*H*$_{arom}$), 7.14 – 7.04 (m, 1H, C*H*$_{arom}$), 6.91 (d, *J* = 2.3 Hz, 2H), 4.53 (s, 2H, C$_{arom}$C*H*$_2$N$_3$), 4.26 – 3.20 (m, 40H, 20×CH_2), 1.58 – 1.16 (m, 4H, 2×CH_2).

^{13}C-NMR (101 MHz, $CDCl_3$): δ (ppm): 167.3 (*C*=O), 165.2 (*C*=O), 159.8 (2×*C*$_{arom}$), 158.4 (*C*$_{arom}$HN$_{arom}$), 147.8 (*C*H$_{arom}$N$_{arom}$), 136.6 (*C*H$_{arom}$), 129.5 (*C*$_{arom}$), 121.7 (*C*H$_{arom}$), 106.0 (*C*H$_{arom}$), 104.3 (*C*H$_{arom}$), 77.4 (*C*H_2), 77.0 (*C*H_2), 76.7 (*C*H_2), 70.7 (*C*H_2), 70.7 (*C*H_2), 70.6 (*C*H_2), 70.3 (*C*H_2), 70.2 (*C*H_2), 70.0 (*C*H_2), 69.7 (*C*H_2), 69.6 (*C*H_2), 69.5 (*C*H_2), 67.6 (*C*H_2), 55.1 (C$_{arom}$*C*H$_2$N$_3$), 50.7 (CH$_2$*C*H$_2$N$_3$), 39.8 (OCH$_2$*C*H$_2$NH), 39.7 (OCH$_2$*C*H$_2$NH).

HR-MS (ESI): $C_{36}H_{55}O_{12}N_{12}^+$ $[M+H]^+$, calc.: 847.4057, found: 847.4056.

4.2.3 Synthesis of the picolyl azide-PEG$_{11}$-TMS protected alkyne linker (34)

5-(Trimethylsilyl)pent-4-ynoic acid (30)[102]

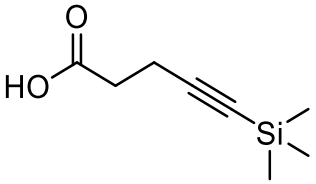

$C_8H_{14}O_2Si$
MW: 170.28 g/mol

5-(Trimethylsilyl)pent-4-yn-1-ol **29** (4.97 g, 31.8 mmol) was dissolved in dry DMF (40 mL). PDC (29.91 g, 79.49 mmol, 2.5 eq.) was added and the reaction was stirred 24 hours at room temperature. The residue was diluted with water (180 mL) and extracted with diethyl ether (3×100 mL). The combined organic layers were washed with HCl (1 M in water, 2×100 mL), brine (100 mL), dried over $MgSO_4$ and filtered. The solvent was removed *in vacuo* and the crude product was purified by flash column chromatography (Silica, *i*-Hex/EtOAc 1/0 → 2:3). 5-(Trimethylsilyl)pent-4-ynoic acid **30** was obtained as a white oil (2.2 g, 12.9 mmol, 41 %).

^{1}H-NMR (400 MHz, $CDCl_3$): δ (ppm): 2.68 – 2.48 (m, 4H, C*H*$_2$), 0.14 (s, 9H, Si(C*H*$_3$)$_3$).
^{13}C-NMR (101 MHz, $CDCl_3$): δ (ppm): 176.7 (*C*=O), 104.9 (CH$_2$*C*≡C), 85.4 (CH$_2$C≡*C*), 33.4 (*C*H$_2$CH$_2$C≡C), 15.6 (CH$_2$*C*≡C), 0.0 (Si(*C*H$_3$)$_3$).

5-(Trimethylsilyl)pent-4-ynoic anhydride (28)[102]

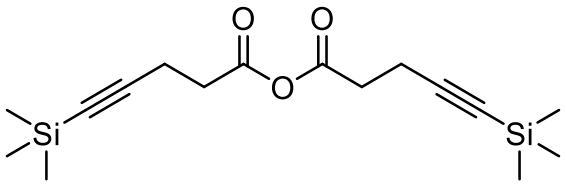

$C_{16}H_{26}O_3Si_2$
MW: 322.55

5-(Trimethylsilyl)pent-4-ynoic acid **30** (434 mg, 2.55 mmol, 1.0 eq.) was dissolved in DCM (10 mL) and DCC (263 mg, 1.27 mmol, 0.5 eq.) was added. The reaction was stirred over night at room temperature and was filtered. The filtrate was stored at -20 °C for 2 hours and filtered again. This step was repeated two times and the solvent was removed *in vacuo* to provide 5-(Trimethylsilyl)pent-4-ynoic anhydride **28** as a colourless oil (335 mg, 1.04 mmol, 42 %).
^{1}H-NMR (400 MHz, $CDCl_3$): δ (ppm): 2.99 – 2.24 (m, 8H, 2×CH_2), 0.14 (s, 18H, 2×Si(CH_3)$_3$).
^{13}C-NMR (101 MHz, $CDCl_3$): δ (ppm): 167.3 (2×*C*=O), 103.8 (2×CH_2*C*≡C), 86.2 (2×CH_2C≡*C*), 34.6 (2×*C*$H_2$$CH_2$C≡C), 15.2 (2×$CH_2$*C*≡C), 0.0 (2×Si(*C*$H_3$)$_3$).
HR-MS (ESI): $C_{16}H_{30}O_3NSi_2$ $[M+NH_4]^+$, calc.: 340.1758, found: 340.1760.

***tert*-butyl(1-(6-(Azidomethyl)pyridin-3-yl)-1-oxo-5,8,11,14,17,20,23,26,29,32,35-undecaoxa-2-azaheptatriacontan-37-yl)carbamate**

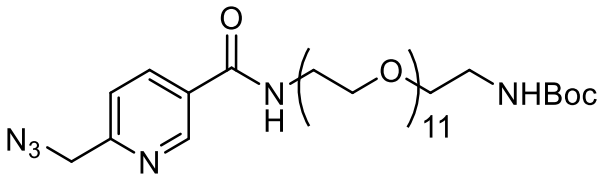

$C_{36}H_{64}N_6O_{14}$
MW: 804.94 g/mol

6-Azidomethylnicotinic acid **16** (50.0 mg, 281 µmol, 1.0 eq.) was dissolved in dry DMF (500 µL). HATU (128 mg, 337µmol, 1.2 eq.) and DIPEA (97.8 µL, 72.6 mg, 561 µmol, 2.0 eq.) were added and the reaction mixture was stirred 10 minutes at room temperature. *O*-(2-Aminoethyl)-*O'*-(2-(Boc-amino)ethyl)decaethylene glycol (180.97 mg, 280.66 µmol, 1.0 eq.)

in solution in dry DMF (500 µL) was added. The reaction was stirred over night and the solvent was removed *in vacuo*. The residue was taken up in DCM (5 mL), washed with brine and dried over $MgSO_4$ and filtered. The crude product was concentrated *in vacuo* and purified by flash column chromatography (Silica, DCM/MeOH, 100/0 → 96/4). Tert-butyl(1-(6-(azidomethyl)pyridin-3-yl)-1-oxo-5,8,11,14,17,20,23,26,29,32,35-undecaoxa-2-azaheptatriacontan-37-yl)carbamate was obtained as a brown oil (213 mg, 265 µmol, 95 %).

^{1}H-NMR (400 MHz, $CDCl_3$): δ (ppm): 9.02 (d, *J* = 2.2 Hz, 1H, $C_{arom}HN_{arom}$), 8.21 (dd, *J* = 8.1, 2.2 Hz, 1H, CH_{arom}), 7.42 (d, *J* = 8.1 Hz, 1H, CH_{arom}), 4.53 (s, 2H, $C_{arom}CH_2N_3$), 3.71 – 3.56 (m, 44H, 22×$C_{linker}H_2$), 3.51 (t, *J* = 5.2 Hz, 2H, $C_{linker}H_2$), 3.29 (q, *J* = 5.4 Hz, 2H, $C_{linker}H_2$), 1.42 (s, 9H, 3×CH_3).

^{13}C-NMR (101 MHz, $CDCl_3$): δ (ppm): 165.2 (*C*=O), 158.3 (C_{arom}), 156.0 (*C*=O), 148.3 ($C_{arom}HN_{arom}$), 136.5 ($C_{arom}H$), 129.5 (C_{arom}), 121.5 ($C_{arom}H$), 79.1 (C_{tert}), 70.6 (CH_2), 70.5 (CH_2), 70.5 (CH_2), 70.5 (CH_2), 70.5 (CH_2), 70.3 (CH_2), 70.2 (CH_2), 69.7 (CH_2), 55.2 ($C_{arom}CH_2N_3$), 40.3 (OCH_2CH_2NHCO), 40.0 (OCH_2CH_2NHCO), 28.4 ($C(CH_3)_3$).

HR-MS (ESI): $C_{36}H_{65}O_{14}N_6$ $[M+H]^+$, calc.: 805.4554, found: 805.4556.

N-(35-amino-3,6,9,12,15,18,21,24,27,30,33-undecaoxapentatriacontyl)-6-(azidomethyl)nicotinamide hydrochloride (33)

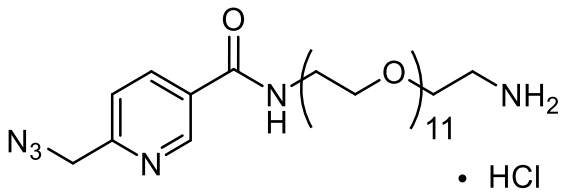

$C_{31}H_{57}ClN_6O_{12}$
MW: 741.28 g/mol

Tert-butyl(1-(6-(azidomethyl)pyridin-3-yl)-1-oxo-5,8,11,14,17,20,23,26,29,32,35-undecaoxa-2-azaheptatriacontan-37-yl)carbamate (100 mg, 124.23 µmol, 1.0 eq.) was dissolved in HCl (4.0 M in dioxane, 500 µL, 73 mg, 16.1 eq.) and stirred at 0 °C for 2 hours. The solvent was removed in vacuo and *N*-(35-amino-3,6,9,12,15,18,21,24,27,30,33-undecaoxapentatriacontyl)-6-(azidomethyl)nicotinamide **33** was obtained as a yellow oil (92.0 mg, 124 µmol, quant.).

^{1}H-NMR (400 MHz, $CDCl_3$): δ (ppm): 8.98 (d, *J* = 1.8 Hz, 1H, $C_{arom}HN_{arom}$), 8.82 (dd, *J* = 8.4, 1.8 Hz, 1H, CH_{arom}), 7.53 (d, *J* = 8.3 Hz, 1H, CH_{arom}), 4.71 (s, 2H, $C_{arom}CH_2N_3$), 3.38 – 2.97 (m, 46H, 23×$C_{linker}H_2$), 2.75 – 2.63 (m, 2H, $C_{linker}H_2$).
^{13}C-NMR (101 MHz, $CDCl_3$): δ (ppm): 161.6 (*C*=O), 152.5 (C_{arom}), 145.5 ($C_{arom}HN_{arom}$), 141.5 ($C_{arom}H$), 133.0 (C_{arom}), 125.2 ($C_{arom}H$), 70.5 (CH_2), 70.4 (CH_2), 70.3 (CH_2), 70.3 (CH_2), 70.2 (CH_2), 70.2 (CH_2), 70.2 (CH_2), 70.1 (CH_2), 70.0 (CH_2), 70.0 (CH_2), 70.0 (CH_2), 69.9 (CH_2), 69.2 (CH_2), 66.9 (CH_2), 49.9 ($C_{arom}CH_2N_3$), 40.2 ($OCH_2CH_2NH_2$), 40.1 (OCH_2CH_2NHCO).
HR-MS (ESI): $C_{31}H_{57}O_{12}N_6$ $[M+H]^+$, calc.: 705.4028, found: 705.4026.

6-(Azidomethyl)-N-(2,2-dimethyl-7-oxo-11,14,17,20,23,26,29,32,35,38,41-undecaoxa-8-aza-2-silatritetracont-3-yn-43-yl)nicotinamide (34)

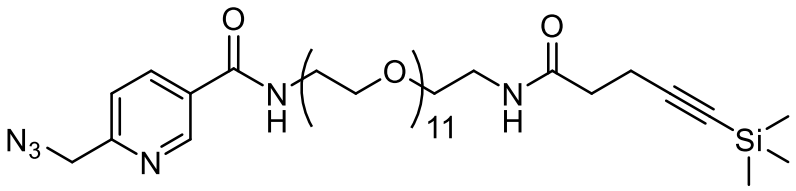

$C_{39}H_{68}N_6O_{13}Si$
MW: 857.09 g/mol

N-(35-amino-3,6,9,12,15,18,21,24,27,30,33-undecaoxapentatriacontyl)-6-(azidomethyl)nicotinamide **33** (40 mg, 51 µmol, 1.0 eq.) was dissolved in dry DCM (1 mL). Pyridine (83 µL, 81 mg, 1.0 mmol, 20.0 eq.) and DMAP (6 mg, 51.4 µmol, 1.0 eq) were added and the reaction mixture was cooled to 0 °C. A solution of 5-(Trimethylsilyl)pent-4-ynoic anhydride (50 mg, 154.3 µmol, 3.0 eq.) in DCM (1 mL) was added dropwise and the reaction was stirred over night while being allowed to warm to room temperature. Subsequently, the residue was dissolved in DCM (20 mL) and washed with water (20 mL), $NaHCO_3$ saturated aqueous solution (20 mL) and $CuSO_4$ saturated aqueous solution (20 mL). The organic layer was dried over $MgSO_4$, filtered and concentrated *in vacuo*. The crude product was purified by flash column chromatography (Silica, DCM/MeOH, 100/0 → 85/15) and the product **34** was obtained as a yellow oil (43 mg, 50 µmol, 98 %).
^{1}H-NMR (400 MHz, $CDCl_3$): δ (ppm): 9.05 (s, 1H, $C_{arom}HN_{arom}$), 8.23 (dd, *J* = 8.0, 1.8 Hz, 1H, CH_{arom}), 7.41 (d, *J* = 6.9 Hz, 1H, CH_{arom}), 4.52 (s, 2H, $C_{arom}CH_2N_3$), 3.68 – 3.50 (m, 46H,

23×$C_{linker}H_2$), 3.46 – 3.40 (m, 2H, $C_{linker}H_2$), 2.57 – 2.49 (m, 2H, $CH_2CH_2C{\equiv}C$), 2.43 – 2.34 (m, 2H, $CH_2CH_2C{\equiv}C$), 0.11 (s, 9H, $Si(CH_3)_3$).

^{13}C-NMR (101 MHz, $CDCl_3$): δ (ppm): 171.2 (*C*=O), 165.3 (*C*=O), 158.2 (C_{arom}), 148.4 ($C_{arom}HN_{arom}$), 140.4 (C_{arom}), 136.4 ($C_{arom}H$), 121.4 ($C_{arom}H$), 105.9 ($CH_2C{\equiv}C$), 85.3 ($CH_2C{\equiv}C$), 70.5 (CH_2), 70.5 (CH_2), 70.5 (CH_2), 70.5 (CH_2), 70.5 (CH_2), 70.5 (CH_2), 70.4 (CH_2), 70.4 (CH_2), 70.2 (CH_2), 70.2 (CH_2), 69.9 (CH_2), 69.8 (CH_2), 55.3 ($C_{arom}CH_2N_3$), 40.0 (OCH_2CH_2NHCO), 39.3 (OCH_2CH_2NHCO), 35.4 ($CH_2CH_2C{\equiv}C$), 16.3 ($CH_2CH_2C{\equiv}C$), 0.1 ($Si(CH_3)_3$).

HR-MS (ESI): $C_{39}H_{72}O_{13}N_7Si$ $[M+NH_4]^+$, calc.: 874.4952, found: 874.4957.

4.2.4 Synthesis of the picolyl azide-PEG$_{11}$-TES protected alkyne linker (37)

5-(Triethylsilyl)pent-4-ynoic acid (36)

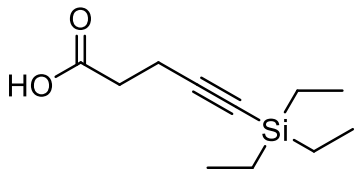

$C_{11}H_{20}O_2Si$
MW: 212.36 g/mol

5-Triethylsilyl-4-pentyn-1-ol **35** (4.55 g, 22.9 mmol, 1.0 eq.) was dissolved in dry DMF (50 mL). PDC (21.57 g, 57.34 mmol, 2.5 eq.) was added and the reaction was stirred overnight at room temperature. Diethyl ether was added and the reaction mixture was filtered over celite. The residue was concentrated *in vacuo* and purified by flash column chromatography (Silica, *i*-Hex/EtOAc 1/0 → 1/1). 5-(triethylsilyl)pent-4-ynoic acid **36** was obtained as colourless oil (1.74 g, 8.19 mmol, 36 %).

^{1}H-NMR (400 MHz, $CDCl_3$): δ (ppm): 2.66 – 2.51 (m, 4H, 2×CH_2), 0.97 (t, *J* = 7.9 Hz, 9H, $Si(CH_2CH_3)_3$), 0.56 (q, *J* = 7.8 Hz, 6H, $Si(CH_2CH_3)_3$).

^{13}C-NMR (101 MHz, $CDCl_3$): δ (ppm): 178.0 (*C*=O), 105.6 ($CH_2C{\equiv}C$), 82.9 ($CH_2C{\equiv}C$), 33.6 ($CH_2CH_2C{\equiv}C$), 15.6 ($CH_2CH_2C{\equiv}C$), 7.4 ($Si(CH_2CH_3)_3$), 4.4 ($Si(CH_2CH_3)_3$).

HR-MS (ESI): $C_{11}H_{19}O_2Si$ $[M-H]^-$, calc.: 211.1160, found: 211.1160.

6-(Azidomethyl)-N-(42,42-diethyl-37-oxo-3,6,9,12,15,18,21,24,27,30,33-undecaoxa-36-aza-42-silatetratetracont-40-yn-1-yl)nicotinamide (37)

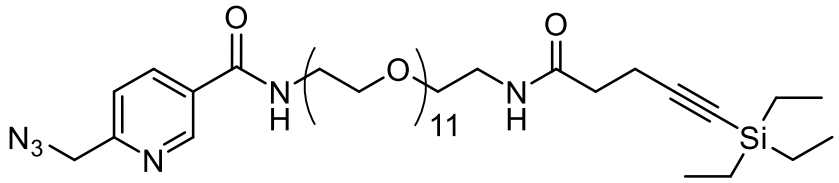

$C_{42}H_{74}N_6O_{13}Si$
MW: 899.17 g/mol

5-(triethylsilyl)pent-4-ynoic acid **36** (6.63 mg, 31.2 µmol, 1.1 eq.) was dissolved in dry DMF (300 µL). DIPEA (9.9 µL, 7.3 mg, 57 µmol, 2.0 eq.) and HATU (12.95 mg, 34.05 µmol, 1.2 eq.) were added and the reaction mixture was stirred 30 minutes at room temperature. A solution of *N*-(35-amino-3,6,9,12,15,18,21,24,27,30,33-undecaoxapentatriacontyl)-6-(azidomethyl)nicotinamide **33** (20 mg, 28 µmol in DMF (300 µL) was added and the reaction was stirred overnight at room temperature. The solvent was removed *in vacuo* and the residue was taken up in DCM (10 mL) and washed with brine (10 mL). The organic layer was dried over $MgSO_4$, filtered, concentrated *in vacuo* and purified by flash column chromatography (Silica, DCM/MeOH, 100/0 → 90/10). The product **37** was obtained as a pale yellow oil (22 mg, 24 µmol, 87 %).

^{1}H-NMR (400 MHz, $CDCl_3$): δ (ppm): 9.03 (dd, *J* = 2.3, 0.8 Hz, 1H, $C_{arom}HN_{arom}$), 8.22 (dd, *J* = 8.1, 2.3 Hz, 1H, CH_{arom}), 7.41 (d, *J* = 8.1 Hz, 1H, CH_{arom}), 4.52 (s, 2H, $C_{arom}CH_2N_3$), 3.71 – 3.54 (m, 44H, 22×$C_{linker}H_2$), 3.52 (dd, *J* = 5.6, 4.5 Hz, 2H, $C_{linker}H_2$), 3.46 – 3.38 (m, 2H, $C_{linker}H_2$), 2.59 – 2.34 (m, 4H, 2×CH_2), 0.94 (t, *J* = 7.9 Hz, 9H, $Si(CH_2CH_3)_3$), 0.53 (q, *J* = 7.9 Hz, 6H, $Si(CH_2CH_3)_3$).

^{13}C-NMR (101 MHz, $CDCl_3$): δ (ppm): 171.2 (*C*=O), 165.3 (*C*=O), 158.2 (C_{arom}), 148.4 ($C_{arom}HN_{arom}$), 136.5 ($C_{arom}H$), 129.5 (C_{arom}), 121.5 ($C_{arom}H$), 106.9 ($CH_2C{\equiv}C$), 82.4 ($CH_2C{\equiv}C$), 70.5 (CH_2), 70.5 (CH_2), 70.5 (CH_2), 70.5 (CH_2), 70.4 (CH_2), 70.4 (CH_2), 70.2 (CH_2), 70.2 (CH_2), 69.9 (CH_2), 69.8 (CH_2), 55.2 ($C_{arom}CH_2N_3$), 39.9 (OCH_2CH_2NHCO), 39.2 (OCH_2CH_2NHCO), 35.7 ($CH_2CH_2C{\equiv}C$), 16.3 ($CH_2CH_2C{\equiv}C$), 7.5 ($Si(CH_2CH_3)_3$), 4.4 ($Si(CH_2CH_3)_3$).

HR-MS (ESI): $C_{42}H_{75}O_{13}N_6Si$ $[M+H]^+$, calc.: 899.5156, found: 899.5135.

4.2.5 Synthesis of the picolyl azide/bis-TES protected alkyne linker (40)

2-(2-(2-(2-((*tert*-Butoxycarbonyl)amino)ethoxy)ethoxy)ethoxy)ethyl-(4'-methylbenzol-sulfonat) (38)

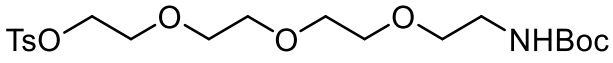

$C_{20}H_{33}NO_8S$
MW: 447.54 g/mol

11-Azido-3,6,9-trioxaundecanyl-(4'-methylbenzolsulfonat) **23** (7.42 g, 19.87 mmol, 1.0 eq.) was dissolved in dry methanol (15 mL) and 10% Pd/C (1.47 g, 3.97 mmol, 20 mol%) was added. The mixture was cooled to 0 °C and Boc_2O (11.71 g, 53.7 mmol, 2.7 eq.) was added. The reaction was stirred under H_2-atmosphere (1 bar) for 4 hours. The residue was filtered over celite, concentrated *in vacuo* and purified by flash column chromatography (Silica, *i*-Hex → *i*-Hex/EtOAc 1/1). The product **38** was obtained as a yellow oil (6.06 g, 13.5 mmol, 68 %).

^{1}H-NMR (400 MHz, $CDCl_3$): δ (ppm): 7.78 (d, *J* = 7.9 Hz, 2H, 2×CH_{arom}), 7.33 (d, *J* = 7.9 Hz, 2H, 2×CH_{arom}), 4.99 (s, 1H, N*H*), 4.20 – 4.11 (m, 2H, CH_2), 3.70 – 3.65 (m, 2H, CH_2), 3.61 – 3.57 (m, 8H, 4×CH_2), 3.51 (t, *J* = 5.2 Hz, 2H, CH_2), 3.33 – 3.24 (m, 2H, CH_2), 2.44 (s, 3H, CH_3), 1.43 (d, *J* = 3.0 Hz, 9H, 3×CH_3).

^{13}C-NMR (101 MHz, $CDCl_3$): δ (ppm): 156.0 (*C*=O), 144.8 (C_{arom}), 133.0 (C_{arom}), 129.8 (*C*H$_{arom}$), 128.0 (*C*H$_{arom}$), 79.2 (C_{tert}), 70.8 (*C*H$_2$), 70.6 (*C*H$_2$), 70.5 (*C*H$_2$), 70.2 (*C*H$_2$), 70.2 (*C*H$_2$), 69.2 (*C*H$_2$), 68.7 (*C*H$_2$), 40.3 (OCH$_2$*C*H$_2$NHCO), 28.4 (C(*C*H$_3$)$_3$), 21.7 (*C*H$_3$).

HR-MS (ESI): $C_{20}H_{34}O_8NS$ $[M+H]^+$, calc.: 448.2000, found: 448.2012.

Methyl-3,5-bis((2,2-dimethyl-4-oxo-3,8,11,14-tetraoxa-5-azahexadecan-16-yl)oxy)benzoate

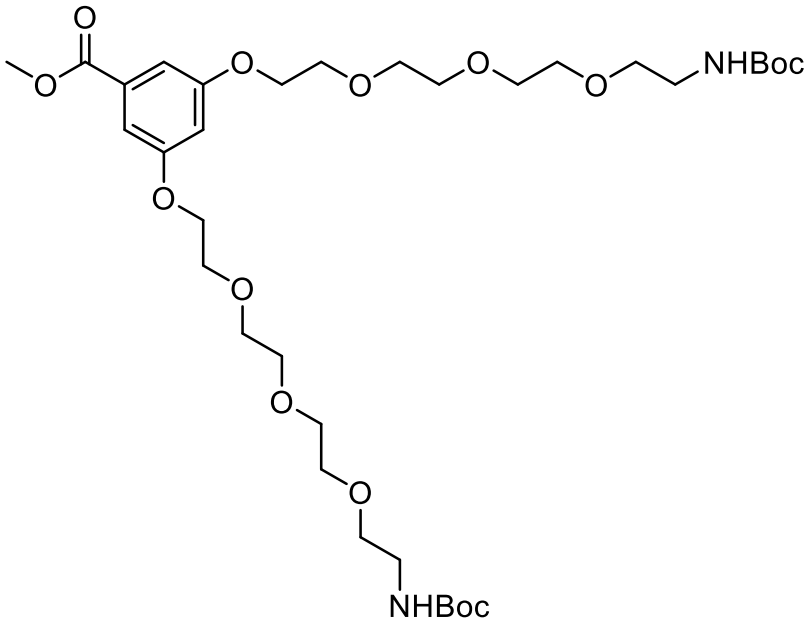

$C_{34}H_{58}N_2O_{14}$
MW: 718.84 g/mol

Methyl-3,5-dihydroxybenzoate **20** (32 mg, 190µmol) and 2-(2-(2-(2-((tertButoxycarbonyl)amino)ethoxy)ethoxy)ethoxy)ethyl-(4'-methylbenzol-sulfonat) **38** (187 mg, 419µmol, 2.2 eq.) were dissolved in acetone (2 mL). K_2CO_3 (184 mg, 1.33 mmol, 7.0 eq.) was added and the reaction was stirred at 60 °C for 20 hours. The solvent was removed *in vacuo* and the residue was taken up in DCM (10 mL) and water (10 mL). It was subsequently extracted with DCM (3×20 mL) and the combined organic layers were dried over $MgSO_4$ and filtered. The solvent was removed *in vacuo* and the crude product was purified by flash column chromatography (Silica, *i*-Hex → EtOAc). The product was obtained as a colourless oil (95 mg, 132 mmol, 70 %).

^{1}H-NMR (400 MHz, $CDCl_3$): δ (ppm): 7.18 (d, *J* = 2.3 Hz, 2H, 2×CH_{arom}), 6.68 (t, *J* = 2.4 Hz, 1H, CH_{arom}), 5.04 (s, 2H, 2×N*H*), 4.13 (t, *J* = 4.8 Hz, 4H, 2×CH_2), 3.88 (s, 3H, COOCH_3), 3.87 – 3.83 (m, 4H, 2×CH_2), 3.77 – 3.58 (m, 16H, 8×CH_2), 3.52 (t, *J* = 5.2 Hz, 4H, 2×CH_2), 3.30 (q, *J* = 5.4, 4.9 Hz, 4H, 2×CH_2), 1.42 (s, 18H, 6×CH_3).

^{13}C-NMR (101 MHz, $CDCl_3$): δ (ppm): 166.8 (*C*=O), 159.7 (2×NH*C*=O), 156.0 (2×C_{arom}), 131.9 (C_{arom}), 108.0 (2×*C*H$_{arom}$), 106.9 (*C*H$_{arom}$), 79.2 (2×C_{tert}), 70.9 (*C*H$_2$), 70.6 (*C*H$_2$), 70.6

(CH_2), 70.2 (CH_2), 70.2 (CH_2), 69.6 (CH_2), 67.7 (CH_2), 52.3 (CH_3), 40.4 (OCH_2CH_2NHCO), 28.4 ($2\times C(CH_3)_3$).

HR-MS (ESI): $C_{34}H_{62}O_{14}N_3$ $[M+NH_4]^+$, calc.: 736.4226, found: 736.4228.

3,5-bis((2,2-Dimethyl-4-oxo-3,8,11,14-tetraoxa-5-azahexadecan-16-yl)oxy)benzoic acid (39)

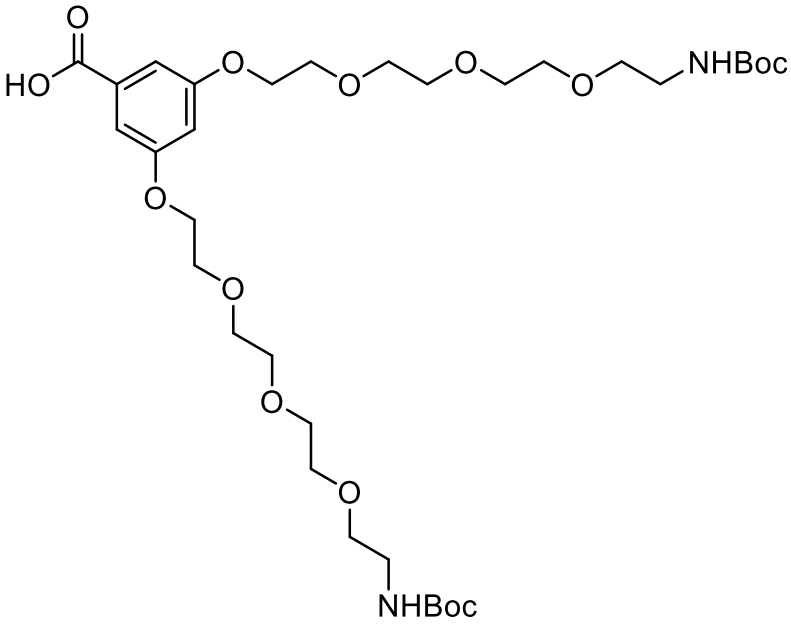

$C_{33}H_{56}N_2O_{14}$
MW: 704.81 g/mol

Methyl-3,5-bis((2,2-dimethyl-4-oxo-3,8,11,14-tetraoxa-5-azahexadecan-16-yl)oxy)benzoate (142 mg, 198µmol, 1.0 eq.) was dissolved in methanol (1 mL) and LiOH solution was added (2.0 M in water, 494 µL, 5.0 eq.). The reaction was stirred 12 hours at 50 °C and quenched with HCl solution (2.0 M in water, 0.5 mL). The residue was concentrated *in vacuo*, taken up in water (10 mL) and extracted with DCM (2×10 mL) and EtOAc (2×10 mL). The combined organic layers were dried over $MgSO_4$, filtered and the solvent was removed *in vacuo* to provide the product **39** as a transparent oil (139 mg, 198 µmol, quant.).

^{1}H-NMR (400 MHz, $CDCl_3$): δ (ppm): 7.24 – 7.20 (m, 2H, $2\times CH_{arom}$), 6.69 (d, J = 2.4 Hz, 1H, CH_{arom}), 5.09 (s, 2H, $2\times NH$), 4.19 – 4.07 (m, 4H, $2\times CH_2$), 3.84 (d, J = 5.0 Hz, 4H, $2\times CH_2$), 3.78 – 3.58 (m, 16H, $8\times CH_2$), 3.53 (t, J = 5.2 Hz, 4H, $2\times CH_2$), 3.30 (q, J = 5.4 Hz, 4H, $2\times CH_2$), 1.42 (s, 18H, $6\times CH_3$).

^{13}C-NMR (101 MHz, $CDCl_3$): δ (ppm): 170.0 (*C*=O), 159.8 (2×NH*C*=O), 156.1 (2×C_{arom}), 131.5 (C_{arom}), 108.5 (2×CH_{arom}), 107.4 (CH_{arom}), 79.3 (2×C_{tert}), 70.9 (CH_2), 70.6 (CH_2), 70.6 (CH_2), 70.2 (CH_2), 69.6 (CH_2), 67.7 (CH_2), 40.3 (OCH_2CH_2NHCO), 28.4 (2×$C(CH_3)_3$).
HR-MS (ESI): $C_{33}H_{60}O_{14}N_3$ $[M+NH_4]^+$, calc.: 722.4070, found: 722.4069.

Di-tert-butyl((((((((((5-((2-(2-(2-(6-(azidomethyl)nicotinamido)ethoxy)ethoxy)ethyl)carbamoyl)-1,3-phenylene)bis(oxy))bis(ethane-2,1-diyl))bis(oxy))bis(ethane-2,1-diyl))bis(oxy))bis(ethane-2,1-diyl))bis(oxy))bis(ethane-2,1-diyl))dicarbamate

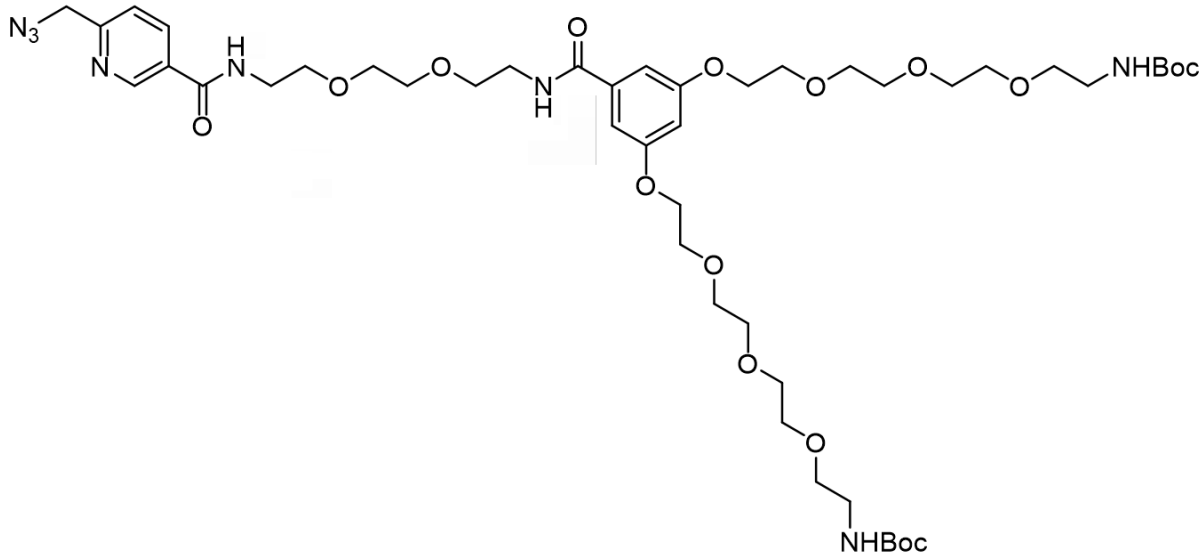

$C_{46}H_{74}N_8O_{16}$
MW: 995.14 g/mol

39 (90 mg, 128 µmol, 1.0 eq.) was dissolved in dry DMF (1 mL) and DIPEA (44.5 µL, 33 mg, 255 µmol, 2.0 eq.) and HATU (58 mg, 153 µmol, 1.2 eq.) were added. The reaction mixture was stirred 30 minutes at room temperature and **21** (43 mg, 140 µmol, 1.1 eq.) was added. The reaction was stirred overnight and the solvent was removed *in vacuo*. The residue was taken up in DCM (10 mL) and washed with brine (10 mL). The organic layer was dried over $MgSO_4$, filtered, concentrated *in vacuo* and purified by flash column chromatography (Silica, EtOAc → EtOAc/MeOH 98/2). The product was obtained as an orange oil (86 mg, 86 µmol, 68 %).
^{1}H-NMR (400 MHz, $CDCl_3$): δ (ppm): 9.01 (d, *J* = 2.2 Hz, 1H, C*H*$_{arom}$), 8.17 (dd, *J* = 8.1, 2.2 Hz, 1H C*H*$_{arom}$), 7.40 (d, *J* = 8.1 Hz, 1H, C*H*$_{arom}$), 6.93 (d, *J* = 2.2 Hz, 2H, 2×C*H*$_{arom}$), 6.55 (t, *J* = 2.3 Hz, 1H, C*H*$_{arom}$), 5.11 (s, 2H, 2×N*H*), 4.53 (s, 2H, $C_{arom}CH_2N_3$), 4.10 (t, *J* = 4.7 Hz, 4H,

2×CH_2), 3.83 (t, J = 4.7 Hz, 4H, 2×CH_2), 3.75 – 3.58 (m, 30H, 15×CH_2), 3.52 (t, J = 5.2 Hz, 4H, 2×CH_2), 3.28 (q, J = 5.4 Hz, 4H, 2×CH_2), 1.42 (s, 18H, 6×CH_3).

^{13}C-NMR (101 MHz, $CDCl_3$): δ (ppm): 167.3 (*C*=O), 165.2 (*C*=O), 159.8 (2×C_{arom}), 156.1 ($C_{arom}HN_{arom}$), 147.9 (2×NH*C*=O), 136.7 ($C_{arom}H$), 130.5 (C_{arom}), 129.5 (C_{arom}), 121.7 ($C_{arom}H$), 105.9 (2×$C_{arom}H$), 104.3 ($C_{arom}H$), 79.2 (2×C_{tert}), 70.8 (CH_2), 70.6 (CH_2), 70.6 (CH_2), 70.3 (CH_2), 70.2 (CH_2), 69.7 (CH_2), 69.6 (CH_2), 69.6 (CH_2), 67.6 (CH_2), 55.1 ($C_{arom}CH_2N_3$), 40.4 (OCH_2CH_2NHCO), 39.8 (OCH_2CH_2NHCO), 28.4 (2×C(CH_3)$_3$).

HR-MS (ESI): $C_{46}H_{75}O_{16}N_8$ $[M+H]^+$, calc.: 995.5296, found: 995.5299.

6-(Azidomethyl)-N-(2-(2-(2-(3,5-bis(2-(2-(2-(2-aminoethoxy)ethoxy)ethoxy)ethoxy)benzamido)ethoxy)ethoxy)ethyl)nicotinamide hydrochloride (41)

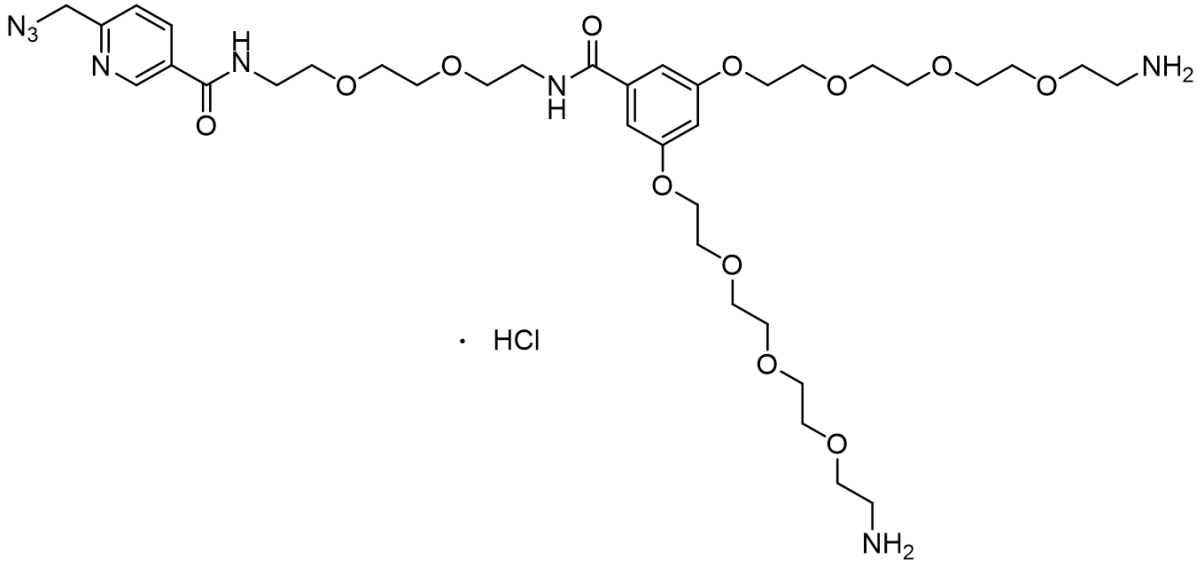

$C_{36}H_{59}ClN_8O_{12}$
MW: 831.36 g/mol

Di-tert-butyl((((((((((5-((2-(2-(2-(6(azidomethyl)nicotinamido)ethoxy)ethoxy)ethyl)-carbamoyl)-1,3-phenylene)bis(oxy))bis(ethane-2,1-diyl))bis(oxy))bis(ethane-2,1-diyl))bis(oxy))bis(ethane-2,1-diyl))bis(oxy))bis(ethane-2,1-diyl))dicarbamate (86 mg, 86 µmol, 1.0 eq.) was dissolved in HCl solution (4.0 M in dioxane, 864 µL, 3.46 mmol, 40.0 eq.) and stirred at 0 °C for 4 hours. The solvent was removed *in vacuo* and **41** was obtained as a colourless oil (72 mg, 86 µmol, quant).

^{1}H-NMR (400 MHz, MeOD): δ (ppm): 9.10 – 9.07 (m, 1H, CH_{arom}), 8.70 (dd, *J*=8.3, 2.1 Hz, 1H, CH_{arom}), 7.97 – 7.89 (m, 1H, CH_{arom}), 7.02 – 6.92 (m, 2H, 2×CH_{arom}), 6.63 (t, *J*=2.3 Hz, 1H CH_{arom}), 4.91 (s, 2H, $C_{arom}CH_2N_3$), 4.14 (t, *J* = 4.7 Hz, 4H, 2×CH_2), 3.85 (t, *J* = 4.7 Hz, 4H, 2×CH_2), 3.77 – 3.40 (m, 34H, 17×CH_2), 3.28 (q, *J* = 5.4 Hz, 4H, 2×CH_2), 3.10 (t, *J* = 5.0 Hz, 4H, 2×CH_2).

^{13}C-NMR (101 MHz, MeOD): δ (ppm): 168.3 (*C*=O), 163.4 (*C*=O), 160.0 (2×C_{arom}), 155.0 ($C_{arom}HN_{arom}$), 143.2 ($C_{arom}HN_{arom}$), 142.3 (C_{arom}), 136.3 ($C_{arom}H$), 131.7 (C_{arom}), 124.6 ($C_{arom}H$), 105.7 (2×$C_{arom}H$), 104.3 ($C_{arom}H$), 75.4 (CH_2), 75.3 (CH_2), 75.1 (CH_2), 73.0 (CH_2), 72.7 (CH_2), 70.2 (CH_2), 70.1 (CH_2), 70.0 (CH_2), 69.9 (CH_2), 69.8 (CH_2), 69.8 (CH_2), 69.3 (CH_2), 69.0 (CH_2), 68.8 (CH_2), 67.6 (CH_2), 67.5 (CH_2), 66.7 (CH_2), 66.5 (CH_2), 66.4 (CH_2), 56.9 ($C_{arom}CH_2N_3$), 39.8 (OCH_2CH_2NHCO), 39.3($OCH_2CH_2NH_2$).

HR-MS (ESI): $C_{36}H_{59}O_{12}N_8$ $[M+H]^+$, calc.: 795.4248, found: 795.4245.

N,N'-((((((((((5-((2-(2-(2-(6-(Azidomethyl)nicotinamido)ethoxy)ethoxy)ethyl)carbamoyl)-1,3-phenylene)bis(oxy))bis(ethane-2,1-diyl))bis(oxy))bis(ethane-2,1-diyl))bis(oxy))bis(ethane-2,1-diyl))bis(oxy))bis(ethane-2,1-diyl))bis(5-(triethylsilyl)pent-4-ynamide) (40)

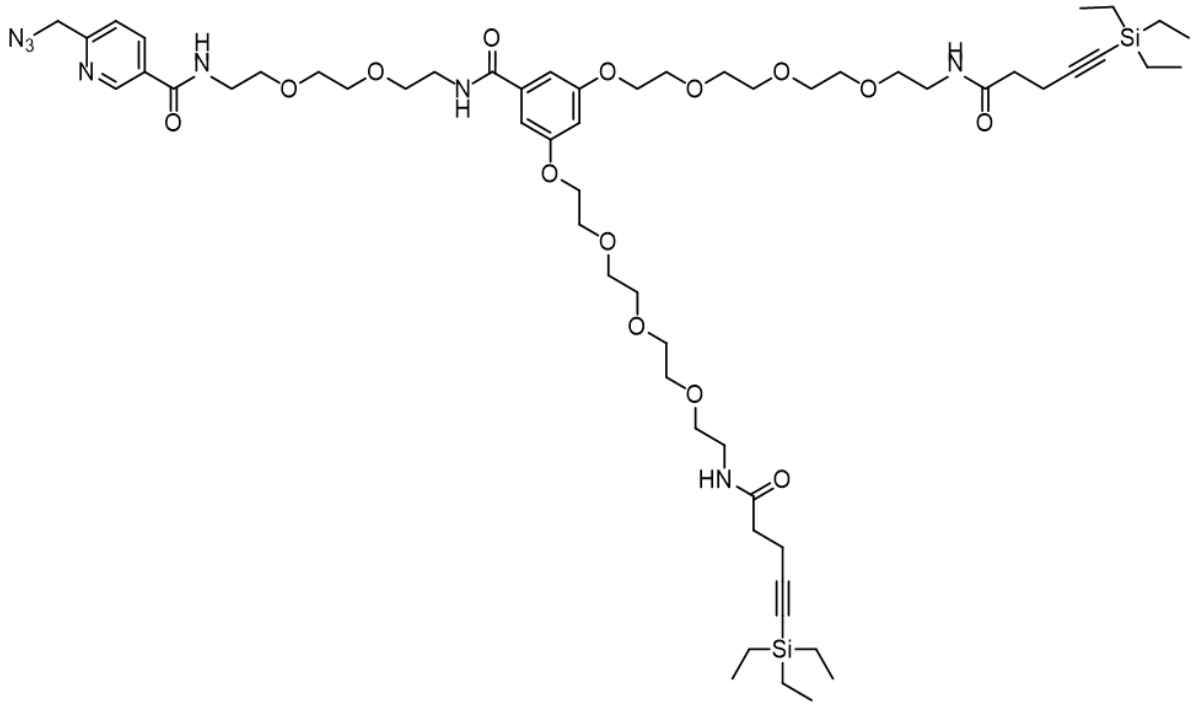

$C_{58}H_{94}N_8O_{14}Si_2$
MW: 1183.60 g/mol

5-(triethylsilyl)pent-4-ynoic acid **36** (12 mg, 57µmol, 3.0 eq.) was dissolved in dry DMF (200 µL). DIPEA (13 µL, 9.8 mg, 76 µmol, 4.0 eq.) and HATU (17.22 mg, 45.29 µmol, 2.4 eq.) were added and the reaction mixture was stirred 30 minutes at room temperature. A solution of **41** (15 mg, 19 µmol, 1.0 eq.) in DMF (200 µL) was added and the reaction was stirred overnight at room temperature. The solvent was removed *in vacuo* and the residue was taken up in DCM (10 mL) and washed with brine (10 mL). The organic layer was dried over $MgSO_4$, filtered, concentrated *in vacuo* and purified by flash column chromatography (Silica, DCM → DCM/MeOH 90:10). The product **40** was obtained as a clear yellow oil (22 mg, 19 µmol, 99 %).

^{1}H-NMR (599 MHz, $CDCl_3$): δ (ppm): 9.10 – 9.07 (m, 1H, CH_{arom}), 8.31 (dd, *J*=8.3, 2.1 Hz, 1H, CH_{arom}), 8.03 – 7.95 (m, 1H, CH_{arom}), 7.54 (d, *J* = 8.1 Hz, 1H, CH_{arom}), 6.96 – 6.84 (m, 2H,

2×C*H*$_{arom}$), 6.51 (t, *J*=2.3 Hz, 1H C*H*$_{arom}$), 4.63 (s, 2H, C$_{arom}$C*H*$_2$N$_3$), 4.10 (t, *J* = 4.7 Hz, 4H, 2×C*H*$_2$), 3.83 (t, *J* = 4.7 Hz, 4H, 2×C*H*$_2$), 3.76 – 3.58 (m), 3.52 (t, *J*=5.1, 2H), 3.39 (q, *J*=5.3, 2H), 3.17 (qd, *J*=7.4, 4.3, 2H) 2.66 – 2.48 (m, 8H, 4×C*H*$_2$), 0.96 (t, *J*=7.9, 18H, 2×Si(CH$_2$C*H*$_3$)$_3$), 0.56 (q, *J* = 7.9 Hz, 12H, 2×Si(C*H*$_2$CH$_3$)$_3$).

^{13}C-NMR (151 MHz, CDCl$_3$): δ (ppm): 175.9 (*C*=O), 162.9 (2×*C*$_{arom}$), 106.0 (CH$_2$*C*≡C), 105.7 (2×*C*$_{arom}$H), 104.0 (*C*$_{arom}$H), 82.9 (CH$_2$C≡*C*), 70.6 (*C*H$_2$), 70.6 (*C*H$_2$), 70.5 (*C*H$_2$), 70.3 (*C*H$_2$), 70.1 (*C*H$_2$), 69.8 (*C*H$_2$), 69.6 (*C*H$_2$), 69.5 (*C*H$_2$), 69.2 (*C*H$_2$), 67.5 (*C*H$_2$), 55.4 (C$_{arom}$*C*H$_2$N$_3$), 39.9 (OCH$_2$*C*H$_2$NHCO), 39.3 (OCH$_2$*C*H$_2$NHCO), 35.0 (2×*C*H$_2$CH$_2$C≡C), 33.3 (2×*C*H$_2$CO), 15.6 (2×CH$_2$*C*H$_2$C≡C), 7.5 (2×Si(CH$_2$*C*H$_3$)$_3$), 4.4 (2×Si(*C*H$_2$CH$_3$)$_3$).

HR-MS (ESI): C$_{58}$H$_{95}$O$_{14}$N$_8$Si$_2$ [M+H]$^+$, calc.: 1183.6501, found: 1183.6466.

4.2.6 Synthesis of C8-alkyne-dU

5-(Octa-1,7-diynyl)-2'-deoxyuridine

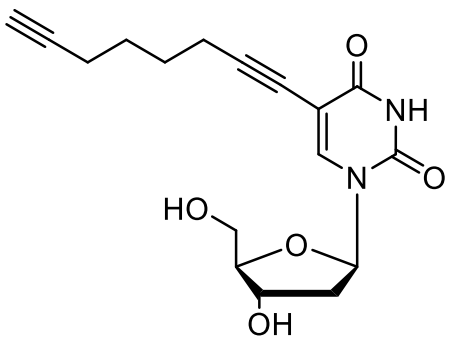

C$_{17}$H$_{20}$N$_2$O$_5$
MW: 332.36 g/mol

5-Iodo-2′-deoxyuridine (5.0 g, 14.12 mmol, 1.0 eq.) was dissolved in dry DMF (80 mL). DIPEA (12.3 mL, 9.13 g, 70.60 mmol, 5.0 eq.), 1,7-octadiyne (2.81 mL, 2.25 g, 21.18 mmol, 1.5 eq.) and bis(triphenylphosphine)palladium(II) dichloride (991 mg, 1.41 mmol, 10 mol%) were added. The solvent was degassed by four freeze pump thaw cycles and copper (I) iodide (538 mg, 2.82 mmol, 20 mol%) was added. The reaction was stirred over night at room temperature and the solvent was removed *in vacuo*. The residue was taken up in EtOAc (50 mL), washed with brine (3×50 mL) and the organic layer was dried over MgSO$_4$ and filtered.

After concentration *in vacuo*, the crude product was purified by flash column chromatography (Silica, *i*-Hex/EtOAc 1/0 → 0/1) to provide X as colourless solid (950 mg, 2.86 mmol, 21 %).
^{1}H-NMR (400 MHz, DMSO-d_6): δ (ppm): 11.10 (bs, 1H, N*H*), 8.07 (s, 1H, C6*H*), 6.10 (t, 1H, *J* = 6.5 Hz, C1'*H*), 5.22 (bd, 1H, *J* = 4.0 Hz, O*H*), 5.06 (t, 1H, *J* = 4.8 Hz, O*H*), 4.23 (m, 1H, C3'*H*), 3.78 (dd, 1H, *J*= 6.6, 3.5 Hz, C4'*H*), 3.55-3.65 (m, 2H, C5'*H*), 2.75 (m, 1H, C≡C*H*), 2.38 (m, 2H, C≡CCH_2), 2.19 (m, 2H, HC≡CCH_2), 2.11 (m, 2H, C2'*H*), 1.57 (m, 4H, 2×CH_2).
^{13}C-NMR (101 MHz, DMSO-d_6): δ (ppm): 161.5 (*C*4), 149.4 (*C*2), 142.6 (*C*6), 98.9 (*C*≡CCH2), 92.8 (C≡*C*CH2), 87.4 (*C*4'), 84.5 (*C*1'), 84.2 (HC≡*C*), 72.9 (*C*5), 71.3 (C≡*C*H), 70.1 (*C*3'), 60.9 (*C*5'), 39.9 (*C*2'), 27.1 (C≡CCH2CH2), 27.0 (C≡CCH_2*C*H_2), 18.2 (C≡C*C*H_2), 17.1 (HC≡C*C*H_2).
HR-MS (ESI): $C_{17}H_{21}O_5N_2$ $[M+H]^+$, calc.: 333.1445, found: 333.1447.

5-(Octa-1,7-diynyl)-5'-O-(4,4'-dimethoxytrityl-)-2'-deoxyuridine

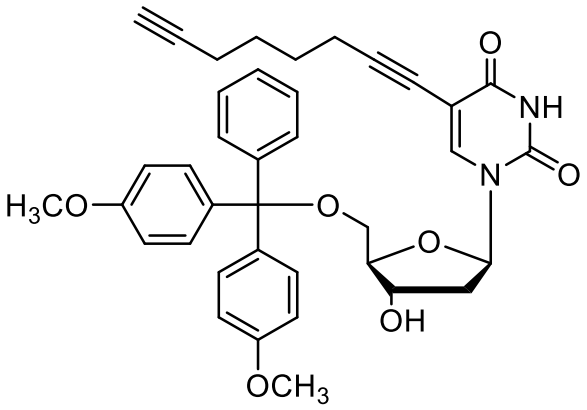

$C_{38}H_{38}N_2O_7$
MW: 634.73 g/mol

5-(Octa-1,7-diynyl)-2'-deoxyuridine (951 mg, 2.86 mmol, 1.0 eq.) was dissolved in dry pyridine (10 mL) under N_2 atmosphere. DMAP (35 mg, 286 µmol, 10 mol%) was added and the reaction was cooled to 0 °C. 4,4′-Dimethoxytrityl chloride (1.45 g, 4.29 mmol, 1.5 eq.) was added portion-wise over 45 minutes and the reaction was further stirred at room temperature for 5 hours. The reaction was quenched by addition of methanol (15 mL) and concentrated *in vacuo*. The residue was purified by flash column chromatography (Silica, DCM/MeOH with

0.1 % pyridine, 99/1 → 98/2) to provide 5-(Octa-1,7-diynyl)-5'-O-(4,4'-dimethoxytrityl-)-2'-deoxyuridine as a yellow oil (1.40 g, 2.21 mmol, 78 %).

^{1}H-NMR (400 MHz, CD_2Cl_2): δ (ppm): 7.97 (s, 1H, C$_6$*H*), 7.45 (dd, 2H, *J* = 8.6 Hz, 1.5, C*H*$_{arom}$), 7.36 (dd, 4H, *J* = 8.5, 1.9 Hz, C*H*$_{arom}$), 7.31 (m, 2H, C*H*$_{arom}$), 7.24 (m, 1H, C*H*$_{arom}$), 6.87 (d, 4H, *J* = 8.5 Hz, CH$_{arom}$), 6.29 (dd, 1H, *J* = 7.7, 5.8 Hz, C1'*H*), 4.55 (m, 1H, C3'*H*), 4.08 (dd, 1H, *J* = 6.2, 3.3 Hz, C4'*H*), 3.79 (s, 6H, 2×OC*H*$_3$), 3.34 (d, 2H, *J* = 3.3 Hz, C5'*H*), 2.46 (m, 1H, C2'*H*), 2.28 (m, 1H, C2'*H*), 2.15 (td, 2H, *J* = 7.1, 1.6 Hz, C*H*$_2$C≡C), 2.07 (td, 2H, *J* = 6.8, 2.5 Hz, C*H*$_2$C≡CH), 1.96 (t, 1H, *J* = 2.5 Hz, C≡C*H*), 1.42 (m, 4H, 2×CH$_2$).

^{13}C-NMR (101 MHz, CD_2Cl_2): δ (ppm): 163.3, 163.0, 153.9, 153.8, 149.1, 146.2, 146.0, 140.4, 140.0, 139.9, 134.4, 134.3, 132.4, 132.2, 131.3, 128.2, 128.0, 117.6, 105.0, 98.6, 91.3, 90.9, 89.6, 88.4, 76.5, 75.6, 72.6, 67.9, 59.6, 45.7, 30.0, 29.7, 21.2, 20.1.

HR-MS (ESI): $C_{38}H_{39}O_7N_2$ $[M+H]^+$, calc.: 635.2752, found: 635.2765.

5-(Octa-1,7-diynyl)-5'-O-(4,4'-dimethoxytrityl-)-3'-O-((2-cyanoethoxy)(diisopropylamino)phosphino)-2'-deoxyuridine

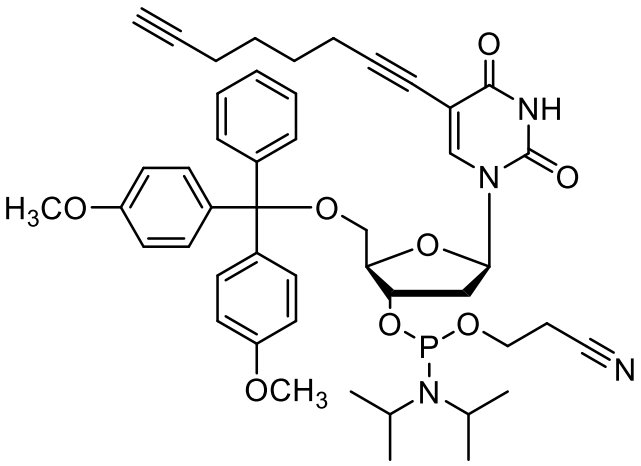

$C_{47}H_{55}N_4O_8P$
MW: 834.95 g/mol

5-(Octa-1,7-diynyl)-5'-O-(4,4'-dimethoxytrityl-)-2'-deoxyuridine (200 mg, 315,1 µmol, 1.0 eq.) was poured in a Schlenk tube previously baked over night at 150 °C and filled with argon. Dry DCM (1.2 mL) was added and the solvent was degassed by three freeze pump thaw cycles. Triisopropyl tetrazolide (27 mg, 157.6 µmol, 0.5 eq.) and 2-cyanoethyltetraisopropyl phosphoramidite (120 µL, 114 mg, 378.1 µmol, 1.2 eq.) were added. The reaction was stirred

at room temperature for 24 hours and the solvent was removed *in vacuo*. The crude mixture was purified by flash column chromatography with degassed eluent (Silica, *i*-Hex/EtOAc 1/3 with 1 % pyridine) under argon atmosphere to provide X as white solid (143 mg, 171.27 µmol, 54 %).

^{13}P NMR (80.9 MHz, CD_2Cl_2): δ (ppm): 149.9, 149.6.

HR-MS (ESI): $C_{47}H_{56}O_8N_4P$ $[M+H]^+$, calc.: 838.3831, found: 835.3824.

4.2.7 Synthesis of the caC phosphoramidite building block (42)

5-Iodo-3´,5´-*O*-(di-*tert*-butylsilanediyl)-2´-*O*-*tert*-butyldimethylsilyl-cytidine (44)

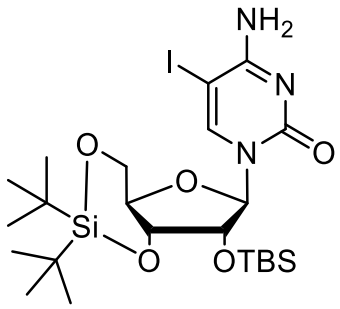

$C_{23}H_{42}IN_3O_5Si_2$
MW: 623.68 g/mol

3´,5´-*O*-(di-*tert*-butylsilanediyl)-2´-*O*-*tert*-butyldimethylsilyl-cytidine **43** (5.0 g, 10.04 mmol, 1.0 eq.) was dissolved in dry acetonitrile (100 mL). To the solution were added iodine (5.10 g, 20.09 mmol, 2.0 eq.) and Ammonium Cerium(IV) Nitrate (11.01 g, 20.09 mmol, 2.0 eq.) at room temperature. After being stirred for 2.5 hours at 50 °C, the reaction mixture was cooled down to room temperature. To the solution was added ethyl acetate (200 mL) and it was subsequently washed with $Na_2S_2O_3$ saturated aqueous solution/$NaHCO_3$ saturated aqueous solution (200 mL, 1/1). The organic phase was dried over Na_2SO_4, filtered and concentrated *in vacuo*. The residue was purified by flash column chromatography (Silica, *i*-Hex/EtOAc 1/0 → 7/3) to provide 5-iodo-3´,5´-*O*-(di-*tert*-butylsilanediyl)-2´-*O*-*tert*-butyldimethylsilyl-cytidine **44** (3.07 g, 4.92 mmol, 49 %).

^{1}H-NMR (400 MHz, $CDCl_3$): δ (ppm): 7.88 (s, 1H), 5.65 (s, 1H), 4.50 (dd, *J* = 8.4, 4.2 Hz, 1H), 4.42 (d, *J* = 4.7 Hz, 1H), 4.17 – 4.01 (m, 3H), 1.09 (s, 9H), 1.06 (s, 9H), 0.96 (s, 9H), 0.22 (s, 3H), 0.17 (s, 3H).

^{13}C-NMR (101 MHz, $CDCl_3$): δ (ppm): 165.6, 155.3, 148.8, 96.4, 77.1, 76.3, 75.9, 68.7, 57.6, 28.0, 27.7, 26.5, 23.6, 21.3, 19.2, -4.0, -4.6.

IR: νmax (cm^{-1}): 2933, 2858, 1646, 1616, 1472, 1058, 828, 776 cm^{-1}.

HR-MS (ESI): $C_{23}H_{43}IN_3O_5Si_2^+$ $[M+H]^+$, calc.: 624.1780, found: 624.1784.

5-(2-(*para*-Nitrophenyl)ethoxycarbonyl)-3´,5´-*O* -(di-*tert*-butylsilanediyl)-2´-*O*-*tert*-butyl dimethylsilyl-cytidine (45)

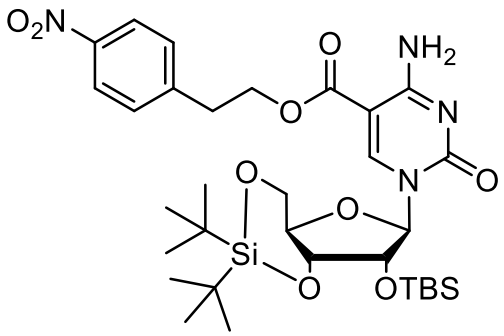

$C_{32}H_{50}N_4O_9Si_2$
MW: 690.94 g/mol

5-iodo-3´,5´-*O*-(di-*tert*-butylsilanediyl)-2´-*O*-*tert*-butyldimethylsilyl-cytidine **44** (1.50 g, 2.41 mmol, 1.0 eq.), *p*-nitrophenethyl alcohol (2.01 mg, 12.03 mmol, 5.0 eq.), $Pd_2(CH_3CN)_2Cl_2$ (63 mg, 0.24 mmol, 10 mol%) and diisopropylethylamine (840 µL, 4.82 mmol, 2.0 eq.) were added in a high pressure glass autoclave. The autoclave was flushed with CO three times to remove residual air and subsequently the reaction was stirred at a CO pressure of 3.5 bar at 80 °C for 16 hours. The CO was expelled and the residue was purified by flash column chromatography (Silica, DCM/MeOH, 100/0 → 98/2) to afford compound 5-(2-(*para*-nitrophenyl)ethoxycarbonyl)-3´,5´-*O* -(di-*tert*-butylsilanediyl)-2´-*O*-*tert*-butyldimethylsilyl-cytidine **45** (876 mg, 1.26 mmol, 52 %).

^{1}H-NMR (599 MHz, $CDCl_3$): δ (ppm): 8.28 (s, 1H), 8.24 – 8.19 (m, 2H), 7.88 – 7.80 (s, br, 1H), 7.41 (d, *J* = 8.5 Hz, 2H), 6.61 – 6.41 (s, br, 1H), 5.69 (s, 1H), 4.58 – 4.48 (m, 2H), 4.32 (d, *J* = 4.0 Hz, 1H), 4.31 – 4.24 (m, 1H), 3.81 (dd, *J* = 9.3 Hz, 1H), 3.74 (dd, *J* = 9.7, 4.1 Hz,

1H), 3.14 (t, *J* = 6.9 Hz, 2H), 1.04 (s, 1H), 1.02 (s, 9H), 1.01 (s, 9H), 0.95 (s, 9H), 0.24 (s, 3H), 0.16 (s, 3H).

^{13}C-NMR (151 MHz, $CDCl_3$): δ (ppm): 164.5, 163.5, 153.6, 147.3, 147.2, 144.8, 129.6, 124.2, 95.3, 94.4, 75.6, 75.3, 74.8, 68.0, 64.4, 35.1, 27.6, 27.4, 27.1, 26.0, 22.9, 20.5, 18.3, -4.2, -4.7.

IR: νmax (cm^{-1}): 3403, 3187, 2934, 2860, 1714, 1677, 1643, 1516, 1472, 1343, 1311, 1250, 1156, 1130, 1118, 1081, 1059, 830, 780 cm^{-1}.

HR-MS (ESI): $C_{32}H_{51}N_4O_9Si_2^+$ $[M+H]^+$, calc.: 691.3189, found: 691.3190.

***N*^{4}-*para*-Methoxybenzoyl-5-(2-(*para*-nitrophenyl)ethoxycarbonyl)-3´,5´-*O* -(di-*tert*-butylsilanediyl)-2´-*O*-*tert*-butyldimethylsilyl-cytidine (46)**

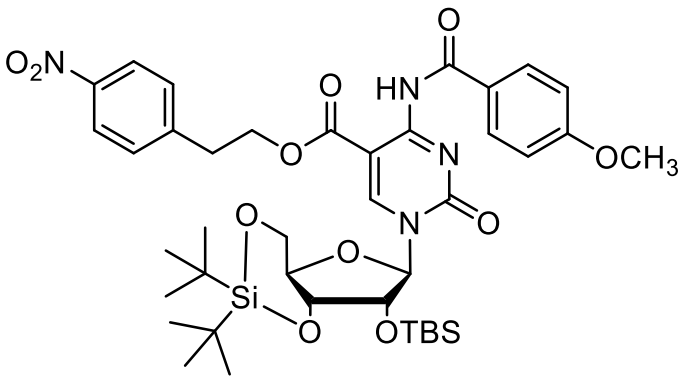

$C_{40}H_{56}N_4O_{11}Si_2$
MW: 825.08 g/mol

5-(2-(*para*-nitrophenyl)ethoxycarbonyl)-3´,5´-*O*-(di-*tert*-butylsilanediyl)-2´-*O*-*tert*-butyldimethylsilyl-cytidine **45** (350 mg, 505.1 µmol, 1.0 eq.) was dissolved in dry pyridine (10.5 mL). To the solution was added *p*-methoxybenzoyl chloride (140 µL, 1.03 mmol, 2.0 eq.) at room temperature. The reaction mixture was put on a pre-heated oil bath at 90 °C and stirred for 4 hours. The reaction mixture was cooled down to room temperature and EtOAc (70 mL) was added. The residue was washed with brine (3×15 mL) and the organic phase was dried over Na_2SO_4, filtered and concentrated *in vacuo*. The crude product was purified by flash column chromatography (Silica, iHex/DCM, 50/50 → 0/100 and then DCM/MeOH, 100/0 → 90/10). All the fractions were collected and concentrated *in vacuo*. The residue was dissolved again in DCM (5 mL) and washed with $NaHCO_3$ saturated aqueous solution (3×5 mL). The aqueous phase was retro-extracted with DCM (1×5 mL). The combined organic layers were

dried over Na_2SO_4, filtered and concentrated *in vacuo*. The residue was again purified by flash column chromatography (Silica, iHex/DCM, 50/50 → 0/100) to provide *N*^{4}*-para*-methoxybenzoyl-5-(2-(*para*-nitrophenyl)ethoxycarbonyl)-3´,5´-*O*-(di-*tert*-butylsilanediyl)-2´-*O*-*tert*-butyldimethylsilyl-cytidine **46** (340 mg, 412.1 µmol, 81%);

^{1}H-NMR (599 MHz, $CDCl_3$): δ (ppm): 8.48 (s, 1H), 8.22 (d, *J* = 8.6 Hz, 2H), 7.95 (d, *J* = 8.4 Hz, 2H), 7.44 – 7.41 (m, 2H), 7.00 – 6.96 (m, 2H), 5.71 (s, 1H), 4.65 – 4.58 (m, 2H), 4.52 (dd, *J* = 9.2, 5.3 Hz, 1H), 4.36 (d, *J* = 4.1 Hz, 1H), 4.33 (td, *J* = 10.1, 5.2 Hz, 1H), 3.89 – 3.87 (m, 3H), 3.78 (dd, *J* = 10.0 Hz, 1H), 3.68 (dd, *J* = 9.8, 4.1 Hz, 1H), 3.19 (t, *J* = 6.9 Hz, 2H), 1.03 (s, 9H), 1.01 (s, 9H), 0.95 (s, 9H), 0.26 (s, 3H), 0.17 (s, 3H).

^{13}C-NMR (151 MHz, $CDCl_3$): δ (ppm):165.3, 163.6, 163.0, 160.1, 152.9, 147.9, 147.3, 144.5, 130.1, 129.6, 126.0, 124.2, 114.3, 96.6, 94.5, 77.4, 77.2, 76.9, 75.6, 75.0, 68.0, 65.1, 55.7, 34.9, 29.8, 27.6, 27.0, 26.0, 22.9, 20.5, 18.3, -4.2, -4.7.

IR: νmax (cm^{-1}): 3283, 2933, 2859, 1682, 1605, 1562, 1515, 1470, 1345, 1309, 1253, 1171, 1113, 1080, 1058, 999, 835, 794, 780, 751, 734, 687, 653 cm^{-1}.

HR-MS (ESI): $C_{40}H_{57}N_4O_{11}Si_2^+$ $[M+H]^+$, calc.: 825.3557, found: 825.3567.

N^4-*para*-Methoxybenzoyl-5-(2-(*para*-nitrophenyl)ethoxycarbonyl)- 2´-*O*-*tert*-butyldimethylsilyl-cytidine (47)

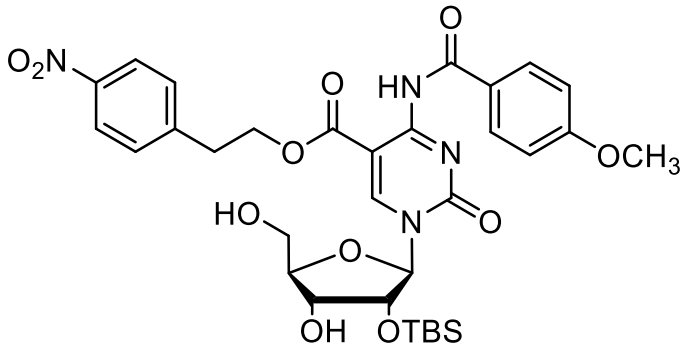

$C_{32}H_{40}N_4O_{11}Si$
MW: 684.77 g/mol

In a 50 mL polypropylene tube, N^4-*para*-methoxybenzoyl-5-(2-(*para*-nitrophenyl)ethoxycarbonyl)-3´,5´-*O*-(di-*tert*-butylsilanediyl)-2´-*O*-*tert*-butyldimethylsilyl-cytidine **46** (269 mg, 326.0 µmol, 1.0 eq.) was dissolved in dry DCM (8.06 mL) and dry pyridine (3.25 mL). To the solution were added pyridine hydrofluoride (~70% hydrogen fluoride, 118 µL, 4.92 mmol, 15.0 eq.) at 4 °C. After being stirred for 30 minutes at 4 °C, methoxytrimethylsilane (3.2 mL) was added. After being further stirred for 1 hour at room temperature, the reaction mixture was concentrated *in vacuo*. The residue was purified by flash column chromatography (Silica, DCM/MeOH, 100/0 → 98/2) to obtain N^4-*para*-methoxybenzoyl-5-(2-(*para*-nitrophenyl)ethoxycarbonyl)- 2´-*O*-*tert*-butyldimethylsilyl-cytidine **47** (198 mg, 289.1 µmol, 89%).

^{1}H-NMR (800 MHz, DMSO-d_6): δ (ppm): 11.47 (s, 1H), 9.38 (s, 1H), 8.14 (d, *J* = 8.7 Hz, 2H), 7.87 (d, *J* = 8.8 Hz, 2H), 7.58 (d, *J* = 8.7 Hz, 2H), 7.09 (d, *J* = 8.8 Hz, 2H), 5.70 (d, *J* = 1.4 Hz, 1H), 5.36 (t, *J* = 4.3 Hz, 1H), 5.06 (d, *J* = 5.6 Hz, 1H), 4.47 (dt, *J* = 10.8, 6.7 Hz, 2H), 4.16 (dd, *J* = 4.0, 1.4 Hz, 1H), 4.05 – 3.99 (m, 2H), 3.91 – 3.88 (m, 1H), 3.85 (s, 3H), 3.71 – 3.66 (m, 1H), 3.13 – 3.09 (m, 2H), 0.90 (s, 9H), 0.14 (s, 3H), 0.10 (s, 3H).

^{13}C-NMR (201 MHz, DMSO-d_6): δ (ppm): 164.9, 163.5, 163.0, 159.8, 153.2, 149.5, 146.4, 146.2, 130.2, 129.8, 125.5, 123.4, 114.2, 98.6, 91.2, 83.3, 76.5, 67.1, 64.9, 58.5, 55.6, 33.8, 25.8, 18.0, -4.7, -4.8.

IR: νmax (cm^{-1}): 3500, 3259, 2954, 2931, 2858, 2252, 1669, 1639, 1605, 1518, 1429, 1346, 1323, 1253, 1174, 1109, 1087, 1030, 911, 882, 841, 782, 732, 698 cm^{-1}.

HR-MS (ESI): $C_{32}H_{41}N_4O_{11}Si^+$ $[M+H]^+$, calc.: 685.2536, found: 685.2545.

***N*^{4}-*para*-Methoxybenzoyl-5-(2-(*para*-nitrophenyl)ethoxycarbonyl)- 5´-O-(4,4´-dimethoxy trityl)-2´-*O*-*tert*-butyldimethylsilyl-cytidine (48)**

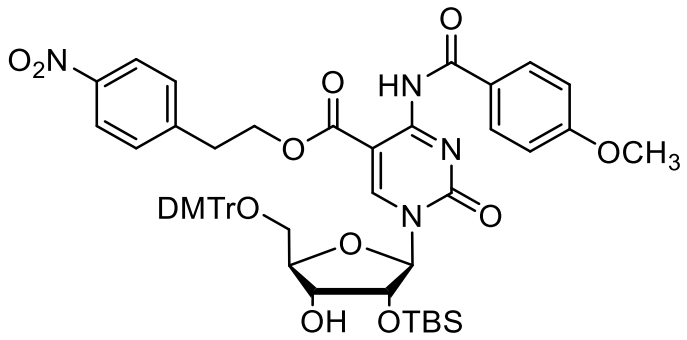

$C_{53}H_{58}N_4O_{13}Si$
MW: 987.15 g/mol

4,4´-dimethoxytritylchloride (2.03 g, 6.00 mmol, 1.0 eq.) was dissolved in dry DCM (20 mL). To the solution was added silver triflate (1.54 g, 6.00 mmol, 1.0 eq.) at room temperature to prepare 4,4´-dimethoxytrityl triflate salt. After being stirred for 1.5 hours, the 4,4´-dimethoxytrityl triflate salt solution (1.20 mL, 0.36 mmol, 1.5 eq.) was added to a solution of *N*^{4}-*para*-methoxybenzoyl-5-(2-(*para*-nitrophenyl)ethoxycarbonyl)- 2´-*O*-*tert*-butyldimethylsilyl-cytidine **47** (165 mg, 241.0 µmol) in dry DCM/dry pyridine (4.8 mL, 1/1) at room temperature. After being stirred for 1.5 hours, additional solution of 4,4´-dimethoxytrityl triflate salt (0.4 mL, 0.12 mmol, 0.5 eq.) was added to the reaction mixture and further stirred for 19.5 hours. DCM (20 mL) was added to the solution and washed with $NaHCO_3$ saturated aqueous solution (3×20 mL). The aqueous phase was extracted again with DCM (1×20 mL). The combined organic layers were dried over Na_2SO_4, filtered and concentrated *in vacuo*. The residue was purified by flash column chromatography (Silica, *i*-Hex/EtOAc 1/0 → 1/1) to afford compound *N*^{4}-*para*-methoxybenzoyl-5-(2-(*para*-nitrophenyl)ethoxycarbonyl)- 5´-O-(4,4´-dimethoxytrityl)-2´-*O*-*tert*-butyldimethylsilyl-cytidine **48** (226 mg, 228.9 µmol, 95%).

^{1}H-NMR (800 MHz, DMSO-d_6): δ (ppm): 11.44 (s, 1H), 8.70 (s, 1H), 8.07 (d, *J* = 8.7 Hz, 2H), 7.88 (d, *J* = 8.9 Hz, 2H), 7.43 (d, *J* = 7.6 Hz, 2H), 7.31 – 7.26 (m, 6H), 7.23 – 7.20 (m, 3H), 7.09 (d, *J* = 8.9 Hz, 2H), 6.88 – 6.84 (m, 4H), 5.77 (d, *J* = 1.9 Hz, 1H), 5.11 (d, *J* = 6.4 Hz,

1H), 4.27 (dd, *J* = 4.6, 2.0 Hz, 1H), 4.17 – 4.12 (m, 1H), 4.01 – 3.97 (m, 1H), 3.86 (s, 3H), 3.84 – 3.81 (m, 1H), 3.71 (s, 3H), 3.70 (s, 3H), 3.62 – 3.57 (m, 1H), 3.39 – 3.37 (m, 1H), 3.22 (dd, *J* = 10.9, 4.8 Hz, 1H), 2.53 – 2.52 (m, 1H), 2.48 – 2.46 (m, 1H), 0.90 (s, 9H), 0.14 (s, 3H), 0.09 (s, 3H).

^{13}C-NMR (201 MHz, DMSO-d_6): δ (ppm): 164.2, 163.8, 163.0, 159.9, 158.1, 158.1, 153.2, 146.2, 145.7, 144.7, 135.3, 135.3, 130.0, 129.9, 129.8, 129.7, 127.9, 127.8, 127.7, 127.6, 125.3, 123.4, 123.4, 114.3, 114.2, 113.2, 99.6, 91.9, 85.5, 82.1, 76.1, 68.6, 64.2, 62.4, 55.6, 55.0, 40.0, 39.9, 39.9, 39.8, 39.8, 39.7, 39.7, 39.6, 39.6, 39.5, 39.5, 39.4, 39.3, 39.2, 33.5, 25.8, 18.0, -4.7, -4.9.

IR: νmax (cm^{-1}): 3290, 3078, 2954, 2930, 2856, 2280, 1716, 1679, 1606, 1558, 1511, 1465, 1346, 1309, 1249, 1174, 1116, 1085, 1034, 836, 795 cm^{-1}.

HR-MS (ESI): $C_{53}H_{59}N_4O_{13}Si^+$ $[M+H]^+$, calc.: 987.3842, found: 987.3864.

N^4-*para*-Methoxybenzoyl-5-(2-(*para*-nitrophenyl)ethoxycarbonyl)-5´-O-(4,4´-dimethoxytrityl)-2´-*O*-*tert*-butyldimethylsilyl-cytidine 3´-(2-cyanoethyl)-*N*,*N*-diisopropylphosphoramidite (42)

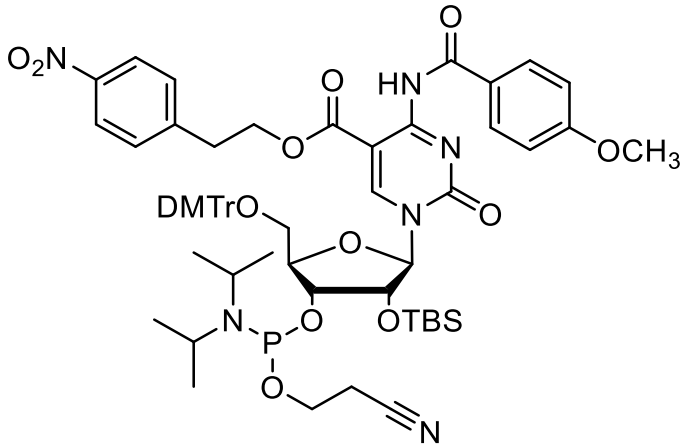

$C_{62}H_{75}N_6O_{14}PSi$
MW: 1187.37 g/mol

N^4-*para*-methoxybenzoyl-5-(2-(*para*-nitrophenyl)ethoxycarbonyl)- 5´-O-(4,4´-dimethoxytrityl)-2´-*O*-*tert*-butyldimethylsilyl-cytidine **48** (152 mg, 154 µmol, 1.0 eq.) was dissolved in degassed dry DCM (1.5 mL). To the solution were added diisopropylethylamine (107 µL, 61.6 µmol, 4.0 eq.) and 2-cyanoethyl *N*,*N*-diisopropylchlorophosphoramidite (138 µL, 61.6 µmol, 4.0 eq.) at room temperature. After being stirred for 2 hours, DCM (10 mL) was added and the residue was washed with $NaHCO_3$ saturated aqueous solution (2×10 mL) and brine (1×20 mL). The organic phase was dried over Na_2SO_4, filtered and concentrated *in vacuo*. The residue was purified by flash column chromatography with degassed eluent (Silica, *i*-Hex/EtOAc 1/1) under argon atmosphere to afford caC amidite **42** (137 mg, 115.4 µmol, 75%) as a diastereo mixture.

^{1}H-NMR (400 MHz, C_6D_6): δ (ppm): 12.00 (d, *J* = 55.4 Hz, 1H), 9.25 (s, 1H), 8.13 (d, *J* = 8.5 Hz, 2H), 7.84 – 7.78 (m, 2H), 7.70 – 7.63 (m, 2H), 7.50 (dt, *J* = 8.7, 6.4 Hz, 4H), 7.23 (t, *J* = 7.7 Hz, 2H), 7.10 – 7.03 (m, 1H), 6.90 – 6.79 (m, 4H), 6.62 – 6.49 (m, 4H), 6.01 (s, 1H), 5.02 – 4.88 (m, 1H), 4.72 – 4.50 (m, 2H), 3.98 (dd, *J* = 22.0, 10.8 Hz, 1H), 3.85 – 3.60 (m, 2H), 3.45 (dt, *J* = 10.3, 6.8 Hz, 1H), 3.37 (t, *J* = 3.6 Hz, 7H), 3.35 – 3.23 (m, 2H), 3.13 (d, *J* = 3.0 Hz, 4H), 3.00 – 2.68 (m, 2H), 2.21 (d, *J* = 31.5 Hz, 2H), 1.15 (d, *J* = 11.1 Hz, 9H), 1.04 – 0.91 (m, 12H), 0.88 (d, *J* = 6.8 Hz, 3H), 0.61 (s, 3H).

^{13}C-NMR (101 MHz, C_6D_6): δ (ppm): 159.3, 159.3, 159.3, 147.1, 145.3, 144.9, 136.3, 135.9, 131.0, 130.9, 130.9, 130.3, 129.9, 129.8, 129.7, 129.1, 127.3, 123.7, 123.6, 123.6, 114.2, 113.7, 113.7, 113.6, 113.5, 76.0, 64.4, 55.0, 55.0, 54.9, 54.9, 54.8, 54.8, 43.2, 43.1, 34.4, 26.5, 26.4, 24.8, 24.8, 24.7, 24.7, 24.7, 18.6, 18.5, 1.4, -3.3, -4.8.

^{31}P-NMR (162 MHz, C_6D_6): δ (ppm): 153.0, 149.3.

IR: νmax (cm^{-1}): 2964, 2961, 1681, 1606, 1560, 1511, 1469, 1346, 1306, 1252, 1176, 1118, 4082, 1034, 836, 794.

HR-MS (ESI): $C_{62}H_{76}N_6O_{24}PSi^+$ $[M+H]^+$, calc.: 1187.4921, found: 1187.494

4.3 Oligonucleotide synthesis

4.3.1 General information

The oligodeoxynucleotide strands containing only the canonical bases (d)A, (d)C, (d)G, d(T) and U were purchased from *Sigma Aldrich* and were used without further purification. The synthesis of both DNA and RNA strands containing special bases was performed on an *Applied Biosystems* Incorporated 394 automated synthesizer by the phosphoramidite method. All the strands were synthesized on a 1 μmol scale using CPG resin. The synthesis and the coupling efficiency were assessed by monitoring the trityl cation absorbance (498 nm) during the deblocking step. Dry acetonitrile (<10 ppm H_2O, *Roth*) was used as solvent for all the phosphoramidites. The identification of the synthesized strands was achieved by MALDI-TOF mass spectrometry and the purity was assessed by analytical RP-HPLC.

4.3.2 Synthesis and deprotection of oligodeoxynucleotides containing C8-alkyne-dU

The ODN syntheses were performed on pre-loaded CPG resin (N^6-Bz-dA or N^2-dmf-dG or N^4-Bz-C or dT) from *Link Technologies*. Phosphoramidites (N^6-Bz-dA, N^2-dmf-dG, N^4-Bz-C and dT) were obtained from *Sigma Aldrich* and the coupling time was 5 minutes. The C8-alkyne-dU phosphoramidite was coupled for 10 minutes.

The synthesizer was equipped with the following solutions and reagents:

Phosphoramidites: 0.10 M in acetonitrile;

Activator: 0.25 M 5-[3, 5-bis(trifluoromethyl)phenyl]-1*H*-tetrazole in acetonitrile (solution from *Sigma-Aldrich)*;

Deblock: 3% (v/v) dichloroacetic acid in DCM;

Oxidation: 25 mM iodine in 65:30:5 (v/v) acetonitrile: H_2O:lutidine;

Capping A: 20:50:30 (v/v) acetic anhydride:acetonitrile:lutidine;

Capping B: 20% (v/v) *N*-methylimidazol in acetonitrile.

After the synthesis, the solid support was dried under high vacuum for 10 minutes and transferred in a 1.5 mL Eppendorf tube. The cleavage of the strands off the solid support and the removal of all the protecting groups was achieved by incubation in 500 µL of a freshly prepared 1:1 mixture of 40% aqueous ammonia and 28% aqueous methylamine (AMA) at 65 °C for 10 minutes. After cooling to room temperature, the resulting solution was centrifuged for 15 minutes at the speed of 13000 rpm. The supernatant was removed and the pellet was washed with ddH_2O, centrifuged again for 15 minutes at the speed of 13000 rpm and its supernatant was also transferred. This operation was repeated one more time and the combined supernatant were concentrated by centrifugal evaporation. The resulting pellet was dissolved in ddH_2O and was proceeded to HPLC analysis, purification, or stored at -20 °C freezer.

4.3.3 Synthesis and deprotection of oligonucleotides containing caC

The ON synthesis were performed on pre-loaded CPG resin (N^4-Ac-C or N^2-dmf-G) from *Link Technologies*. Phosphoramidites (N^6-Bz-A, N^2-dmf-G, N^4-Ac-C and U) were obtained from *Glen Research* or *Link Technologies* and the coupling time was 10 min. The caC phosphoramidite **42** was coupled for 20 minutes. The synthesizer was equipped with the following solutions and reagents:

- Phosphoramidites: 0.15 M in acetonitrile;
- Activator: 0.25 M 5-[3,5-bis(trifluoromethyl)phenyl]-1*H*-tetrazole in acetonitrile (solution from *Sigma-Aldrich*);
- Deblock:15% (v/v) dichloroacetic acid in DCM;
- Oxidation: 25 mM iodine in 65:30:5 (v/v) acetonitrile:H_2O:lutidine;
- Capping A: 20:50:30 (v/v) acetic anhydride:acetonitrile:pyrdine;
- Capping B: 20% (v/v) *N*-methylimidazol in acetonitrile.

After the synthesis, the solid support was dried in high vacuum for at least 30 min. Then the pre-dried solution of DBU-ACN (1 mL, 1:9, v/v) was flew through the solid support over 1-3 minutes using a disposable syringe followed by washing with d acetonirile and dry in high vacuum. Then the solid support was transferred into a 1.5 mL Eppendorf tube. To the tube, pre-dried DBU-THF (1 mL, 1:9, v/v) solution was added and reacted for 2 hours on a preheated thermomixer (45 °C) followed by washing with dry THF. The supernatant was removed and

the solid support was dried at room temperature. To the tube, absolute ethanol (200 µL) and 28% NH_4OH aqueous solution (600 µL) were added at room temperature. The tube was then placed on a preheated thermomixer (55 °C) and mixed for 18 hours. The reaction was then cooled down to room temperature and the supernatant was transferred to a 2.0 mL Eppendorf tube followed by the washing of the CPG resins with ddH_2O-EtOH (3:1, v/v) solution (3×200-300 µL). The resulting solution was dried down using a centrifugal evaporator and lyophilisation. Into the tube, 100 µL of DMSO and 125 µL of triethylamine trihydrofluoride solution were added. The tube was then placed on a preheated thermomixer (65 °C) and mixed for 1.5 hours. The tube was placed on ice and 25 µL of 3 M NaOAc aqueous solution was added followed by the addition of *n*-butanol (1 mL). The resulting solution was then stored in -80 °C over night. The resulting solution was centrifuged for 1 hour at 4 °C at the speed of 21130 rpm. The supernatant was removed and the residue was washed once with EtOH-ddH_2O (4:1, v/v) and centrifuged again for 30 minutes with the same conditions. The supernatant was removed and the residue was dried at room temperature for at least 30 minutes. The residue was dissolved in 0.5 M triethylammonium acetate buffer (pH 7.0) and was proceeded to HPLC analysis, purification, or stored at -20 °C freezer.

4.4 Click protocols

4.4.1 Oligodeoxyribonucleotide functionalization, characterisation and purification

Click reaction on ODN

The desired amount (in nmol) of oligodeoxynucleotide in solution was aliquoted in a 1.5 mL Eppendorf tube and concentrated until dryness with a Speedvac. The ODN was subsequently resuspended in ddH_2O with a volume corresponding to a concentration of 10 mM. The linker (in solution in tBuOH/DMSO 3:1) to be conjugated with the ODN and all the reagents were added and the mixture was degassed using argon. The tube was placed in a thermomixer (25 °C) and shaken for 4 hours at 950 rpm. The reaction was stopped by diluting the mixture in ddH_2O, frozen in liquid nitrogen and immediately lyophilized. The residue was resuspended in ddH_2O in order to be analysed (MALDI-ToF and RP-HPLC) and purified (preparative RP-HPLC). The percentage of completion of the reaction was determined by integration of the HPLC trace of the crude product at 260 nm.

TES alkyne protected group removal

The ODN conjugated as described in the previous section to a linker bearing an alkyne protected by a triethylsilyl protecting group were resuspended in a NaF solution (400 mM in water) in a 1.5 mL Eppendorf tube and incubated in a thermomixer for 48 hours, at 950 rpm and 40 °C. After cooling down, the mixture was filtered and washed with ddH_2O (3×500 µL) on an *Amicon Ultra-0.5 mL* centrifugal membrane filter with a molecular weight cut-off of 3 kDa. The residue was resuspended in ddH_2O, analysed (MALDI-ToF and RP-HPLC), lyophilized and stored at -20 °C.

4.4.2 Template-assisted double conjugation

The functionalized oligodeoxynucleotide probes which comprised one ODN bearing two azides and two ODNs bearing one alkyne (1 nmol each) and the template strand (1 nmol) were combined in a 1.5 mL Eppendorf tube and concentrated until dryness in a Speedvac. The ODNs were resuspended in NaCl solution (0.2 M in water, 100 µL) and annealed in a thermomixer at 95 °C for 15 minutes without shaking. The temperature was then gradually decreased by 10 °C every 15 minutes until 25 °C was reached. A click catalyst Master Mix solution was prepared as following:

Master Mix preparation: final volume = 50 µL				
	[Stock] in 0.2 M aqueous NaCl	Volume from stock solution	[Final] in 0.2 M aqueous NaCl	Stoichiometry
$CuSO_4$	40 mM	5 µl	4 mM	1
BTTAA	50 mM	30 µl	30 mM	7.5
Na ascorbate	133 mM	15 µl	40 mM	10

10 µL of this Master Mix was added to the oligonucleotides at the following equivalents per click reaction:

- $CuSO_4$: 20 eq.
- Na ascorbate: 200 eq.
- BTTAA: 140 eq.

The reaction mixture was degassed with argon for 1 to 2 minutes and shaken in a thermomixer at room temperature and 300 rpm for 3 hours. The reaction was stopped by diluting the mixture in ddH_2O and was filtered and washed with ddH_2O (3×500 µL) on an *Amicon Ultra-0.5 mL* centrifugal membrane filter with a molecular weight cut-off of 3 kDa. The conjugated oligonucleotides were lyophilized and suspended again in ddH_2O prior analysis by PAGE.

4.5 Biochemical experiments

4.5.1 Melting Curve Experiments

Melting profiles were measured on a *Jasco* V-650 spectrometer using quartz glass cuvettes with 10.0 mm path length. Final samples contained the two oligonucleotide of which the dissociation-characteristics are to be assessed each at 2 µM concentration, 0.2 M NaCl aqueous solution, 10 mM aqueous sodium phosphate buffer in a final volume of 400 µL. Measurements were repeated at least three times per sample. Before the measurement, the oligonucleotides were hybridized at 95 °C for 5 minutes followed by cooling down to 4 °C over a period of 40 minutes. For the UV-measurements the solutions were covered with silicon oil and tightly plugged. Absorbance was recorded in the forward and reverse direction at temperatures from 15 °C to 85 °C at 0.1 °C/3 seconds. At least three denaturing and renaturing ramps were performed and averaged for evaluation of the melting temperature. T_m values were calculated as the zero-crossing of 2_{nd} derivate of the 349 nm background-corrected change in hyperchromicity at 260 nm.

4.5.2 DNA PAGE

ODN strands and products from the click conjugations were analysed by 20% denaturing polyacrylamide gel electrophoresis on 20 x 20 cm gels of 1 mm thickness. The samples to analyse were prepared in order to contain approximately 300 ng of ODN for the 11 mer strands and 150 ng for the 15 mer strands in 5 µL of ddH_2O. To each sample was added 5 µL of loading buffer prepared as described in the recipe table. The gels were run in TBE buffer (see below recipe table) at 40 °C applying a constant current of 40 mA per gel (maximum 1000 V) for about 5-6 hours. The gels were stained with SYBR® green II for 30 minutes (in ddH_2O, 100 mL) and then visualized using a LAS-3000 imaging system (*Raytest*).

Recipes	
Loading buffer	- 875 µL 8 M Urea - 25 µL ddH_2O - 100 µL 10× TBE buffer - 120 mg Ficoll 400 - ≈ 1 mg bromophenol blue
Polyacrylamide gel	- 32 mL Rotiphorese® sequencing gel concentrate - 4 mL 8 M urea - 4 mL 10 x TBE buffer - 200 µL APS - 20 µL TEMED
TBE 10× buffer	- 108 g Tris - 55 g boric acid - 9.3 g EDTA - 1 L final volume with ddH_2O - pH 8.0 at 25 °C

4.5.3 Enzymatic digestion of ON

1 nmol of ONs were dissolved in ddH_2O (35 µL). Subsequently it was added an aqueous solution (7.5 µL) of 480 µM $ZnSO_4$, containing 42 units Nuclease S1, 5 units Antarctic phosphatase and the digestion mixture was incubated at 37 °C for 3 hours in a thermomixer. After addition of a 520 µM $[Na]_2$-EDTA solution (7.5 µL) containing 0.2 units snake venom phosphodiesterase I, the sample was further incubated for 3 hours at 37 °C. The total volume was 50 µL and the digested product was filtered on paper using an AcroPrep™ Advance 96 filter plate 0.2 µm Supor® from *Pall Life Sciences* by centrifugation at 4 °C at 14000 rpm for 30 minutes. The samples were stored at -20 °C until analysis LC-MS/MS as described in the next section.

4.6- UHPLC-MS analysis

The analysis of the digested RNAs were performed by LC-ESI-MS on a *Thermo Finnigan* LTQ Orbitrap XL and were chromatographed by a *Dionex* Ultimate 3000 HPLC system with a flow of 0.15 mL/min over an *Interchim* Uptisphere120A-3µm-HDO C18 column. The column temperature was maintained at 30 °C. Eluting buffers were buffer A (2 mM $HCOONH_4$ in ddH_2O (pH 5.5)) and buffer B (2 mM $HCOONH_4$ in ddH_2O/MeCN 20/80 (pH 5.5)). The gradient for all samples was from 100% to 94% buffer A over 55 min. The elution was monitored at 260 nm (*Dionex* Ultimate 3000 Diode Array Detector). The chromatographic eluent was directly injected into the ion source without prior splitting. Ions were scanned by use of a positive polarity mode over a full-scan range of m/z 120-1000 with a resolution of 30000.

5. ABBRIEVATIONS

(d)A	(deoxy)Adenine/Adenosine (depending on context)
(d)C	(deoxy)Cytosine/Cytidine (depending on context)
(d)G	(deoxy)Guanine/Guanosine (depending on context)
(d)T	(deoxy)Thymine/Thymidine (depending on context)
(d)U	(deoxy)Uracil/Uridine (depending on context)
°C	Degree Celsius (temperature)
Ac	Acetyl
ACN	Acetonitrile
AMA	1:1 mixture of 40% aqueous ammonia/28% aqueous methylamine
APS	Ammonium persulfate
Boc_2O	Di-*tert*-butyl dicarbonate
bp	Base pair
br	Broad
BTTAA	2-(4-((bis((1-(*tert*-butyl)-1H-1,2,3-triazol-4-yl)methyl)amino)methyl)-1H-1,2,3-triazol-1-yl)acetic acid
Bz	Benzoyl
caC	5-carboxy cytosine
CAN	Ceric ammonium nitrate
COSY	Correlation spectroscopy (2D NMR)
CPG	Controlled pore glass
CuAAC	Cu(I)-catalyzed alkyne azide cycloadditions
d	Doublet
DBU	1,8-Diazabicyclo[5.4.0]undec-7-ene
DCM	Dichloromethane
ddH_2O	Double-distilled water

DIPEA	N,N-Diisopropylethylamine
DMAP	4-Dimethylaminopyridine
DMF	Dimethylformamide
DMSO	Dimethoxysulfoxide
DMTr	4,4´-Dimethoxytrityl
DNA	Deoxyribonucleic acid
e.g.	Latin “exempli gratia”, meaning: for example
EDTA	Ethylenediaminetetraacetate
eq.	Equivalent(s)
ESI	Electrospray ionization
et al.	*Et alii* (latin = and others)
EtOAc	Ethylacetate
EtOH	Ethanol
FISH	Fluorescence *in situ* hybridization
FTICR	Fourier-transform ion cyclotron resonance
g	Gram, 10–3 kg
HATU	(1-[Bis(dimethylamino)methylene]-1H-1,2,3-triazolo[4,5-b]pyridinium 3-oxid hexafluorophosphate
HMBC	Heteronuclear multiple-bond correlation spectroscopy
HPA	Hydroxypicolinic acid
HPLC	High-pressure liquid chromatography/High-performance liquid chromatography
HR	High-resolution
HRMS	High-resolution mass spectrometry
HSQC	Heteronuclear single quantum coherence/correlation
Hz	Herz
*i*Hex	Isohexane
in vacuo	In a vacuum

IR	Infrared
J	Coupling constant
kDa	Kilodalton
L	Liter(s)
LC	Liquid chromatography
m	Meter(s)
M	Molar concentration
m	Multiplet
m/z	Mass to charge ratio
MALDI-TOF	Matrix assisted laser desorption/ionization time-of-flight
MeCN	Acetonitrile
MeOH	Methanol
mol	Mole(s)
mRNA	Messenger RNA
MS	Mass spectrometry
NaOAc	Sodium acetate
NMR	Nuclear magnetic resonance
O(D)N	Oligo(deoxyribo)nucleotide
PAGE	Polyacrylamide gel electrophoresis
PCR	Polymerase chain reaction
PDC	Pyridinium dichromate
pH	The negative decimal logarithm of the hydrogen ion activity
PLA	Proximity ligation assay
ppm	Parts per million
q	Quartet
R_f	Retention factor (thin-layer chromatography)

RCA	Rolling circular amplification
RNA	Ribonucleic acid
ROS	Reactive oxygen species
RP	Reversed-phase
RT-PCR	Real time-PCR
s	Singlet
t	Triplet
TBE	Tris/Borate/EDTA
TBS	*tert*-Butyldimethylsilyl
TBTA	Tris[(1-benzyl-1*H*-1,2,3-triazol-4-yl)methyl]amine
tBuOH	*tert*-butanol
TEMED	Tetramethylethylenediamine
TES	Triethylsilyl
THF	Tetrahydrofuran
THPTA	Tris[(1-hydroxypropyl-1*H*-1,2,3-triazol-4-yl)methyl]amine
Tm	Melting temperature
Tris	Tris(hydroxymethyl)aminomethane
UHPLC-MS	Micro HPLC-MS
UV	Ultraviolet
v/v	Volume per volume
δ	Chemical shift

6. REFERENCES

[1] S. Fredriksson, M. Gullberg, J. Jarvius, C. Olsson, K. Pietras, S. M. Gustafsdottir, A. Ostman, U. Landegren, *Nat. Biotechnol.* **2002**, *20*, 473-477. *Protein detection using proximity-dependent DNA ligation assays.*

[2] O. Söderberg, M. Gullberg, M. Jarvius, K. Ridderstråle, K.-J. Leuchowius, J. Jarvius, K. Wester, P. Hydbring, F. Bahram, L.-G. Larsson, U. Landegren, *Nat. Methods* **2006**, *3*, 995. *Direct observation of individual endogenous protein complexes in situ by proximity ligation.*

[3] P. M. E. Gramlich, C. T. Wirges, A. Manetto, T. Carell, *Angew. Chem. Int. Ed.* **2008**, *47*, 8350-8358. *Postsynthetic DNA Modification through the Copper-Catalyzed Azide–Alkyne Cycloaddition Reaction.*

[4] W. S. Brotherton, H. A. Michaels, J. T. Simmons, R. J. Clark, N. S. Dalal, L. Zhu, *Org. Lett.* **2009**, *11*, 4954-4957. *Apparent copper(II)-accelerated azide-alkyne cycloaddition.*

[5] Z. Yuan, G.-C. Kuang, R. J. Clark, L. Zhu, *Org. Lett.* **2012**, *14*, 2590-2593. *Chemoselective Sequential "Click" Ligation Using Unsymmetrical Bisazides.*

[6] C. Deans, K. A. Maggert, *Genetics* **2015**, *199*, 887-896. *What Do You Mean, "Epigenetic"?*

[7] R. Jaenisch, A. Bird, *Nat. Genet.* **2003**, *33*, 245. *Epigenetic regulation of gene expression: how the genome integrates intrinsic and environmental signals.*

[8] C. Thomas, K. M. Q., M. Markus, R. Martin, S. Fabio, *Angew. Chem. Int. Ed.* **2018**, *57*, 4296-4312. *Non-canonical Bases in the Genome: The Regulatory Information Layer in DNA.*

[9] J. E. Squires, H. R. Patel, M. Nousch, T. Sibbritt, D. T. Humphreys, B. J. Parker, C. M. Suter, T. Preiss, *Nucleic Acids Res.* **2012**, *40*, 5023-5033. *Widespread occurrence of 5-methylcytosine in human coding and non-coding RNA.*

[10] S. M. Huber, P. van Delft, L. Mendil, M. Bachman, K. Smollett, F. Werner, E. A. Miska, S. Balasubramanian, *Chembiochem* **2015**, *16*, 752-755. *Formation and abundance of 5-hydroxymethylcytosine in RNA.*

[11] L. Fu, C. R. Guerrero, N. Zhong, N. J. Amato, Y. Liu, S. Liu, Q. Cai, D. Ji, S.-G. Jin, L. J. Niedernhofer, *J. Am. Chem. Soc* **2014**, *136*, 11582-11585. *Tet-mediated formation of 5-hydroxymethylcytosine in RNA.*

[12] H.-Y. Zhang, J. Xiong, B.-L. Qi, Y.-Q. Feng, B.-F. Yuan, *Chem. Commun.* **2016**, *52*, 737-740. *The existence of 5-hydroxymethylcytosine and 5-formylcytosine in both DNA and RNA in mammals.*

[13] W. Huang, M.-D. Lan, C.-B. Qi, S.-J. Zheng, S.-Z. Wei, B.-F. Yuan, Y.-Q. Feng, *Chemical Science* **2016**, *7*, 5495-5502. *Formation and determination of the oxidation products of 5-methylcytosine in RNA.*

[14] J. M. Berg, J. L. Tymoczko, L. Stryer, *Biochemistry*, W.H. Freeman, Basingstoke, **2012**.

[15] R. Dahm, *Hum. Genet.* **2008**, *122*, 565-581. *Discovering DNA: Friedrich Miescher and the early years of nucleic acid research.*

[16] P. A. Levene, *J. Biol. Chem.* **1919**, *40*, 415-424. *The Stucture of Yeast Nucleic Acid: IV. Ammonnia Hydrolysis.*

[17] O. T. Avery, C. M. MacLeod, M. McCarty, *J. Exp. Med.* **1944**, *79*, 137-158. *Studies on the chemical nature of the substance inducing transformation of pneumonocal types : induction of transformation by a desoxyribonucleic acid fraction isolated from pneumonococcus type III.*

[18] J. D. Watson, F. H. C. Crick, *Nature* **1953**, *171*, 737. *Molecular Structure of Nucleic Acids: A Structure for Deoxyribose Nucleic Acid.*

[19] M. H. F. Wilkins, A. R. Stokes, H. R. Wilson, *Nature* **1953**, *171*, 738. *Molecular Structure of Nucleic Acids: Molecular Structure of Deoxypentose Nucleic Acids.*

[20] J. D. Watson, F. H. C. Crick, *Nature* **1953**, *171*, 964. *Genetical Implications of the Structure of Deoxyribonucleic Acid.*

[21] R. Wing, H. Drew, T. Takano, C. Broka, S. Tanaka, K. Itakura, R. E. Dickerson, *Nature* **1980**, *287*, 755. *Crystal structure analysis of a complete turn of B-DNA.*

[22] M. Meselson, F. W. Stahl, *Proc. Natl. Acad. Sci. USA* **1958**, *44*, 671-682. *The Replication of DNA in Escherichia Coli.*

[23] M. W. Nirenberg, J. H. Matthaei, *Proc. Natl. Acad. Sci. USA* **1961**, *47*, 1588-1602. *The dependence of cell-free protein synthesis in E. coli upon naturally occurring or synthetic polyribonucleotides.*

[24] M. Nirenberg, P. Leder, *Science* **1964**, *145*, 1399-1407. *RNA Codewords and Protein Synthesis. The Effect of Trinucleotides upon the Biding of sRNA to Ribosomes.*

[25] A. Michael, *J. Prakt. Chem.* **1893**, *48*, 94-95. *Ueber die Einwirkung von Diazobenzolimid auf Acetylendicarbonsäuremethylester.*

[26] R. Huigsen, *Proc. Chem. Soc.* **1961**, 357-396. *1,3-Dipolar Cycloadditions.*

[27] R. Huisgen, *Angew. Chem. Int. Ed.* **1963**, *2*, 565-598. *1,3-Dipolar Cycloadditions. Past and Future.*

[28] C. W. Tornøe, M. Meldal, in *Peptides: The Wave of the Future: Proceedings of the Second International and the Seventeenth American Peptide Symposium, June 9–14, 2001, San Diego, California, U.S.A.* (Eds.: M. Lebl, R. A. Houghten), Springer Netherlands, Dordrecht, **2001**, pp. 263-264.

[29] C. W. Tornoe, C. Christensen, M. Meldal, *J. Org. Chem.* **2002**, *67*, 3057-3064. *Peptidotriazoles on solid phase: [1,2,3]-triazoles by regiospecific copper(i)-catalyzed 1,3-dipolar cycloadditions of terminal alkynes to azides.*

[30] V. V. Rostovtsev, L. G. Green, V. V. Fokin, K. B. Sharpless, *Angew. Chem. Int. Ed.* **2002**, *41*, 2596-2599. *A stepwise huisgen cycloaddition process: copper(I)-catalyzed regioselective "ligation" of azides and terminal alkynes.*

[31] F. Himo, T. Lovell, R. Hilgraf, V. V. Rostovtsev, L. Noodleman, K. B. Sharpless, V. V. Fokin, *J. Am. Chem. Soc.* **2005**, *127*, 210-216. *Copper(I)-Catalyzed Synthesis of Azoles. DFT Study Predicts Unprecedented Reactivity and Intermediates.*

[32] R. Berg, B. F. Straub, *Beil. J. Org. Chem.* **2013**, *9*, 2715-2750. *Advancements in the mechanistic understanding of the copper-catalyzed azide–alkyne cycloaddition.*

[33] B. T. Worrell, J. A. Malik, V. V. Fokin, *Science* **2013**, *340*, 457. *Direct Evidence of a Dinuclear Copper Intermediate in Cu(I)-Catalyzed Azide-Alkyne Cycloadditions.*

[34] L. Jin, D. R. Tolentino, M. Melaimi, G. Bertrand, *Sci. Adv.* **2015**, *1*. *Isolation of bis(copper) key intermediates in Cu-catalyzed azide-alkyne "click reaction".*

[35] Z. Lei, B. C. J., Z. Xiaoguang, G. P. M., C. R. J., *Chem. Rec.* **2016**, *16*, 1501-1517. *On the Mechanism of Copper(I)-Catalyzed Azide–Alkyne Cycloaddition.*

[36] H. C. Kolb, M. G. Finn, K. B. Sharpless, *Angew. Chem. Int. Ed.* **2001**, *40*, 2004-2021. *Click Chemistry: Diverse Chemical Function from a Few Good Reactions.*

[37] X. Wang, B. Huang, X. Liu, P. Zhan, *Drug Discovery Today* **2016**, *21*, 118-132. *Discovery of bioactive molecules from CuAAC click-chemistry-based combinatorial libraries.*

[38] X. Liang, L. Yongjun, L. Yuliang, *Asian J. Org. Chem.* **2014**, *3*, 582-602. *Application of "Click" Chemistry to the Construction of Supramolecular Functional Systems.*

[39] L. Li, Z. Zhang, *Molecules* **2016**, *21*, 1393. *Development and Applications of the Copper-Catalyzed Azide-Alkyne Cycloaddition (CuAAC) as a Bioorthogonal Reaction.*

[40] V. Hong, N. F. Steinmetz, M. Manchester, M. G. Finn, *Bioconjugate Chem.* **2010**, *21*, 1912-1916. *Labeling Live Cells by Copper-Catalyzed Alkyne−Azide Click Chemistry.*

[41] D. C. Kennedy, C. S. McKay, M. C. B. Legault, D. C. Danielson, J. A. Blake, A. F. Pegoraro, A. Stolow, Z. Mester, J. P. Pezacki, *J. Am. Chem. Soc.* **2011**, *133*, 17993-18001. *Cellular Consequences of Copper Complexes Used To Catalyze Bioorthogonal Click Reactions.*

[42] G. J. Brewer, *Chem. Res. Toxicol.* **2010**, *23*, 319-326. *Risks of Copper and Iron Toxicity during Aging in Humans.*

[43] T. R. Chan, R. Hilgraf, K. B. Sharpless, V. V. Fokin, *Org. Lett.* **2004**, *6*, 2853-2855. *Polytriazoles as Copper(I)-Stabilizing Ligands in Catalysis.*

[44] V. Hong, S. I. Presolski, C. Ma, M. G. Finn, *Angew. Chem. Int. Ed.* **2009**, *48*, 9879-9883. *Analysis and optimization of copper-catalyzed azide-alkyne cycloaddition for bioconjugation.*

[45] C. Besanceney-Webler, H. Jiang, T. Zheng, L. Feng, D. Soriano del Amo, W. Wang, L. M. Klivansky, F. L. Marlow, Y. Liu, P. Wu, *Angew. Chem. Int. Ed.* **2011**, *50*, 8051-8056. *Raising the Efficacy of Bioorthogonal Click Reactions for Bioconjugation: A Comparative Study.*

[46] G. C. Rudolf, S. A. Sieber, *ChemBioChem* **2013**, *14*, 2447-2455. *Copper-assisted click reactions for activity-based proteomics: fine-tuned ligands and refined conditions extend the scope of application.*

[47] C. Uttamapinant, A. Tangpeerachaikul, S. Grecian, S. Clarke, U. Singh, P. Slade, K. R. Gee, A. Y. Ting, *Angew. Chem. Int. Ed.* **2012**, *51*, 5852-5856. *Fast, Cell-Compatible Click Chemistry with Copper-Chelating Azides for Biomolecular Labeling.*

[48] P. M. Gramlich, S. Warncke, J. Gierlich, T. Carell, *Angew. Chem. Int. Ed.* **2008**, *47*, 3442-3444. *Click-click-click: single to triple modification of DNA.*

[49] E. Paredes, S. R. Das, *ChemBioChem* **2011**, *12*, 125-131. *Click Chemistry for Rapid Labeling and Ligation of RNA.*

[50] M.-L. Winz, A. Samanta, D. Benzinger, A. Jäschke, *Nucleic Acids Res.* **2012**, *40*, e78-e78. *Site-specific terminal and internal labeling of RNA by poly(A) polymerase tailing and copper-catalyzed or copper-free strain-promoted click chemistry.*

[51] R. Kumar, A. El-Sagheer, J. Tumpane, P. Lincoln, L. M. Wilhelmsson, T. Brown, *J. Am. Chem. Soc.* **2007**, *129*, 6859-6864. *Template-Directed Oligonucleotide Strand Ligation, Covalent Intramolecular DNA Circularization and Catenation Using Click Chemistry.*

[52] I. Manuguerra, S. Croce, A. H. El-Sagheer, A. Krissanaprasit, T. Brown, K. V. Gothelf, A. Manetto, *Chem. Commun.* **2018**, *54*, 4529-4532. *Gene assembly via one-pot chemical ligation of DNA promoted by DNA nanostructures.*

[53] S. Y. Lim, W. Y. Chung, H. K. Lee, M. S. Park, H. G. Park, *Biochem. Biophys. Res. Commun.* **2008**, *376*, 633-636. *Direct and nondestructive verification of PNA immobilization using click chemistry.*

[54] K. Fauster, M. Hartl, T. Santner, M. Aigner, C. Kreutz, K. Bister, E. Ennifar, R. Micura, *ACS Chem. Biol.* **2012**, *7*, 581-589. *2'-Azido RNA, a Versatile Tool for Chemical Biology: Synthesis, X-ray Structure, siRNA Applications, Click Labeling.*

[55] J. Lietard, A. Meyer, J.-J. Vasseur, F. Morvan, *J. Org. Chem.* **2008**, *73*, 191-200. *New Strategies for Cyclization and Bicyclization of Oligonucleotides by Click Chemistry Assisted by Microwaves.*

[56] J. Gierlich, G. A. Burley, P. M. Gramlich, D. M. Hammond, T. Carell, *Org. Lett.* **2006**, *8*, 3639-3642. *Click chemistry as a reliable method for the high-density postsynthetic functionalization of alkyne-modified DNA.*

[57] J. Gierlich, K. Gutsmiedl, P. M. Gramlich, A. Schmidt, G. A. Burley, T. Carell, *Chemistry* **2007**, *13*, 9486-9494. *Synthesis of highly modified DNA by a combination of PCR with alkyne-bearing triphosphates and click chemistry.*

[58] K. B. Mullis, *Sci. Am.* **1990**, *262*, 56-65. *The Unusual Origin of the Polymerase Chain Reaction.*

[59] K. B. Mullis, F. A. Faloona, *Methods Enzymol.* **1987**, *155*, 335-350. *Specific synthesis of DNA in vitro via a polymerase-catalyzed chain reaction.*

[60] G. T. Walker, M. S. Fraiser, J. L. Schram, M. C. Little, J. G. Nadeau, D. P. Malinowski, *Nucleic Acids Res.* **1992**, *20*, 1691-1696. *Strand displacement amplification—an isothermal, in vitro DNA amplification technique.*

[61] J. C. Guatelli, K. M. Whitfield, D. Y. Kwoh, K. J. Barringer, D. D. Richman, T. R. Gingeras, *Proc. Natl. Acad. Sci. USA* **1990**, *87*, 1874-1878. *Isothermal, in vitro amplification of nucleic acids by a multienzyme reaction modeled after retroviral replication.*

[62] H. U. Weier, J. W. Gray, *DNA (Mary Ann Liebert, Inc.)* **1988**, *7*, 441-447. *A programmable system to perform the polymerase chain reaction.*

[63] R. K. Saiki, S. Scharf, F. Faloona, K. B. Mullis, G. T. Horn, H. A. Erlich, N. Arnheim, *Science* **1985**, *230*, 1350-1354. *Enzymatic amplification of beta-globin genomic sequences and restriction site analysis for diagnosis of sickle cell anemia.*

[64] J. S. Chamberlain, R. A. Gibbs, J. E. Rainer, P. N. Nguyen, C. Thomas, *Nucleic Acids Res.* **1988**, *16*, 11141-11156. *Deletion screening of the Duchenne muscular dystrophy locus via multiplex DNA amplification.*

[65] T. D. Brock, H. Freeze, *J. Bacteriol.* **1969**, *98*, 289-297. *Thermus aquaticus gen. n. and sp. n., a nonsporulating extreme thermophile.*

[66] R. Higuchi, G. Dollinger, P. S. Walsh, R. Griffith, *Bio/technology* **1992**, *10*, 413-417. *Simultaneous amplification and detection of specific DNA sequences.*

[67] R. Higuchi, C. Fockler, G. Dollinger, R. Watson, *Bio/technology* **1993**, *11*, 1026-1030. *Kinetic PCR analysis: real-time monitoring of DNA amplification reactions.*

[68] B. J. Bassam, T. Allen, S. Flood, J. Stevens, P. Wyatt, K. J. Livak, *Nucleic acid sequence detection systems: Revolutionary automation for monitoring and reporting PCR products, Vol. 6*, **1996**.

[69] H. D. VanGuilder, K. E. Vrana, W. M. Freeman, *Biotechniques* **2008**, *44*, 619-626. *Twenty-five years of quantitative PCR for gene expression analysis.*

[70] K. M. Ririe, R. P. Rasmussen, C. T. Wittwer, *Anal. Biochem.* **1997**, *245*, 154-160. *Product differentiation by analysis of DNA melting curves during the polymerase chain reaction.*

[71] W. Wang, K. Chen, C. Xu, *Anal. Biochem.* **2006**, *356*, 303-305. *DNA quantification using EvaGreen and a real-time PCR instrument.*

[72] D. Whitcombe, J. Theaker, S. P. Guy, T. Brown, S. Little, *Nat. Biotechnol.* **1999**, *17*, 804-807. *Detection of PCR products using self-probing amplicons and fluorescence.*

[73] S. Tyagi, F. R. Kramer, *Nat. Biotechnol.* **1996**, *14*, 303-308. *Molecular beacons: probes that fluoresce upon hybridization.*

[74] P. M. Holland, R. D. Abramson, R. Watson, D. H. Gelfand, *Proc. Natl. Acad. Sci. USA* **1991**, *88*, 7276-7280. *Detection of specific polymerase chain reaction product by utilizing the 5'----3' exonuclease activity of Thermus aquaticus DNA polymerase.*

[75] P. E. Nielsen, M. Egholm, R. H. Berg, O. Buchardt, *Science* **1991**, *254*, 1497-1500. *Sequence-selective recognition of DNA by strand displacement with a thymine-substituted polyamide.*

[76] H. Kaur, A. Arora, J. Wengel, S. Maiti, *Biochemistry* **2006**, *45*, 7347-7355. *Thermodynamic, Counterion, and Hydration Effects for the Incorporation of Locked Nucleic Acid Nucleotides into DNA Duplexes.*

[77] G. H. Reed, C. T. Wittwer, *Clin. Chem.* **2004**, *50*, 1748-1754. *Sensitivity and specificity of single-nucleotide polymorphism scanning by high-resolution melting analysis.*

[78] M. Louie, L. Louie, A. E. Simor, *Can. Med. Assoc. J.* **2000**, *163*, 301-309. *The role of DNA amplification technology in the diagnosis of infectious diseases.*

[79] P. S. Bernard, C. T. Wittwer, *Clin. Chem.* **2002**, *48*, 1178-1185. *Real-time PCR technology for cancer diagnostics.*

[80] C. Greenwood, D. Ruff, S. Kirvell, G. Johnson, H. S. Dhillon, S. A. Bustin, *Biomol. Detect. Quantif.* **2015**, *4*, 10-16. *Proximity assays for sensitive quantification of proteins.*

[81] O. Soderberg, M. Gullberg, M. Jarvius, K. Ridderstrale, K. J. Leuchowius, J. Jarvius, K. Wester, P. Hydbring, F. Bahram, L. G. Larsson, U. Landegren, *Nat. Methods* **2006**, *3*, 995-1000. *Direct observation of individual endogenous protein complexes in situ by proximity ligation.*

[82] M. Gullberg, S. M. Gústafsdóttir, E. Schallmeiner, J. Jarvius, M. Bjarnegård, C. Betsholtz, U. Landegren, S. Fredriksson, *Proc. Natl. Acad. Sci. USA* **2004**, *101*, 8420. *Cytokine detection by antibody-based proximity ligation.*

[83] M. M. Ali, F. Li, Z. Zhang, K. Zhang, D. K. Kang, J. A. Ankrum, X. C. Le, W. Zhao, *Chem. Soc. Rev.* **2014**, *43*, 3324-3341. *Rolling circle amplification: a versatile tool for chemical biology, materials science and medicine.*

[84] I. Weibrecht, K.-J. Leuchowius, C.-M. Clausson, T. Conze, M. Jarvius, W. M. Howell, M. Kamali-Moghaddam, O. Söderberg, *Expert Rev. Proteomics* **2010**, *7*, 401-409. *Proximity ligation assays: a recent addition to the proteomics toolbox.*

[85] C. Coppola, L. Simeone, L. De Napoli, D. Montesarchio, *Eur. J. Org. Chem.* **2011**, *2011*, 1155-1165. *On the Compatibility of Azides in Phosphoramidite-Based Couplings: Synthesis of a Novel, Convertible Azido-Functionalized CyPLOS Analogue.*

[86] M. A. Fomich, M. V. Kvach, M. J. Navakouski, C. Weise, A. V. Baranovsky, V. A. Korshun, V. V. Shmanai, *Org. Lett.* **2014**, *16*, 4590-4593. *Azide phosphoramidite in direct synthesis of azide-modified oligonucleotides.*

[87] T. Wada, A. Mochizuki, S. Higashiya, H. Tsuruoka, S.-i. Kawahara, M. Ishikawa, M. Sekine, *Tetrahedron Lett.* **2001**, *42*, 9215-9219. *Synthesis and properties of 2-azidodeoxyadenosine and its incorporation into oligodeoxynucleotides.*

[88] G. Pourceau, A. Meyer, J.-J. Vasseur, F. Morvan, *J. Org. Chem.* **2009**, *74*, 6837-6842. *Azide Solid Support for 3'-Conjugation of Oligonucleotides and Their Circularization by Click Chemistry.*

[89] L. M. Smith, S. Fung, M. W. Hunkapiller, T. J. Hunkapiller, L. E. Hood, *Nucleic Acids Res.* **1985**, *13*, 2399-2412. *The synthesis of oligonucleotides containing an aliphatic amino group at the 5' terminus: synthesis of fluorescent DNA primers for use in DNA sequence analysis.*

[90] P. Kočalka, A. H. El-Sagheer, T. Brown, *ChemBioChem* **2008**, *9*, 1280-1285. *Rapid and Efficient DNA Strand Cross-Linking by Click Chemistry.*

[91] J. Gierlich, G. A. Burley, P. M. Gramlich, D. M. Hammond, T. Carell, *Org. Lett.* **2006**, *8*, 3639-3642. *Click chemistry as a reliable method for the high-density postsynthetic functionalization of alkyne-modified DNA.*

[92] K. Onizuka, T. Chikuni, T. Amemiya, T. Miyashita, K. Onizuka, H. Abe, F. Nagatsugi, *Nucleic Acids Res.* **2017**, *45*, 5036-5047. *Pseudorotaxane formation via the slippage process with chemically cyclized oligonucleotides.*

[93] S. S. Pujari, H. Xiong, F. Seela, *J. Org. Chem.* **2010**, *75*, 8693-8696. *Cross-linked DNA generated by "bis-click" reactions with bis-functional azides: site independent ligation of oligonucleotides via nucleobase alkynyl chains.*

[94] S. S. Pujari, F. Seela, *J. Org. Chem.* **2013**, *78*, 8545-8561. *Parallel stranded DNA stabilized with internal sugar cross-links: synthesis and click ligation of oligonucleotides containing 2'-propargylated isoguanosine.*

[95] G.-C. Kuang, H. A. Michaels, J. T. Simmons, R. J. Clark, L. Zhu, *J. Org. Chem.* **2010**, *75*, 6540-6548. *Chelation-Assisted, Copper(II) Acetate-Accelerated Azide-Alkyne Cycloaddition.*

[96] S. A. Ingale, F. Seela, *J. Org. Chem.* **2013**, *78*, 3394-3399. *Stepwise click functionalization of DNA through a bifunctional azide with a chelating and a nonchelating azido group.*

[97] C. Ö. Dinç, G. Kibarer, A. Güner, *J. Appl. Polym. Sci.* **2010**, *117*, 1100-1119. *Solubility profiles of poly(ethylene glycol)/solvent systems. II. comparison of thermodynamic parameters from viscosity measurements.*

[98] L. A. Carpino, *J. Am. Chem. Soc.* **1993**, *115*, 4397-4398. *1-Hydroxy-7-azabenzotriazole. An efficient peptide coupling additive.*

[99] M. S. Wendland, S. C. Zimmerman, *J. Am. Chem. Soc.* **1999**, *121*, 1389-1390. *Synthesis of Cored Dendrimers.*

[100] V. Aucagne, D. A. Leigh, *Org. Lett.* **2006**, *8*, 4505-4507. *Chemoselective formation of successive triazole linkages in one pot: "click-click" chemistry.*

[101] T. W. Greene, P. G. M. Wuts, in *Protective Groups in Organic Synthesis*, John Wiley & Sons, Inc., **2002**, pp. 654-659.

[102] P. A. Ledin, F. Friscourt, J. Guo, G. J. Boons, *Chemistry* **2011**, *17*, 839-846. *Convergent assembly and surface modification of multifunctional dendrimers by three consecutive click reactions.*

[103] G. Hayashi, N. Kamo, A. Okamoto, *Chem. Commun.* **2017**, *53*, 5918-5921. *Chemical synthesis of dual labeled proteins via differently protected alkynes enables intramolecular FRET analysis.*

[104] S. Thyagarajan, N. N. Murthy, A. A. Narducci Sarjeant, K. D. Karlin, S. E. Rokita, *J. Am. Chem. Soc.* **2006**, *128*, 7003-7008. *Selective DNA Strand Scission with Binuclear Copper Complexes: Implications for an Active Cu(2)-O(2) Species.*

[105] G. H. Keller, M. M. Manak, *DNA probes*, Macmillan Publishers Ltd, Basingstoke, **1989**.

[106] Y. Liu, A. Kuzuya, R. Sha, J. Guillaume, R. Wang, J. W. Canary, N. C. Seeman, *J. Am. Chem. Soc.* **2008**, *130*, 10882-10883. *Coupling across a DNA Helical Turn Yields a Hybrid DNA/Organic Catenane Doubly Tailed with Functional Termini.*

[107] K. Onizuka, F. Nagatsugi, Y. Ito, H. Abe, *J. Am. Chem. Soc.* **2014**, *136*, 7201-7204. *Automatic pseudorotaxane formation targeting on nucleic acids using a pair of reactive oligodeoxynucleotides.*

[108] S. Kriaucionis, N. Heintz, *Science* **2009**, *324*, 929-930. *The nuclear DNA base 5-hydroxymethylcytosine is present in Purkinje neurons and the brain.*

[109] M. Tahiliani, K. P. Koh, Y. Shen, W. A. Pastor, H. Bandukwala, Y. Brudno, S. Agarwal, L. M. Iyer, D. R. Liu, L. Aravind, A. Rao, *Science* **2009**, *324*, 930-935. *Conversion of 5-methylcytosine to 5-hydroxymethylcytosine in mammalian DNA by MLL partner TET1.*

[110] T. Pfaffeneder, B. Hackner, M. Truß, M. Münzel, M. Müller, C. A. Deiml, C. Hagemeier, T. Carell, *Angew. Chem. Int. Ed.* **2011**, *50*, 7008-7012. *The Discovery of 5-Formylcytosine in Embryonic Stem Cell DNA.*

[111] S. Ito, L. Shen, Q. Dai, S. C. Wu, L. B. Collins, J. A. Swenberg, C. He, Y. Zhang, *Science* **2011**, *333*, 1300. *Tet Proteins Can Convert 5-Methylcytosine to 5-Formylcytosine and 5-Carboxylcytosine.*

[112] S. Kriaucionis, N. Heintz, *Science* **2009**, *324*, 929-930. *The nuclear DNA base 5-hydroxymethylcytosine is present in Purkinje neurons and the brain.*

[113] M. Tahiliani, K. P. Koh, Y. Shen, W. A. Pastor, H. Bandukwala, Y. Brudno, S. Agarwal, L. M. Iyer, D. R. Liu, L. Aravind, *Science* **2009**, *324*, 930-935. *Conversion of 5-methylcytosine to 5-hydroxymethylcytosine in mammalian DNA by MLL partner TET1.*

[114] Y.-F. He, B.-Z. Li, Z. Li, P. Liu, Y. Wang, Q. Tang, J. Ding, Y. Jia, Z. Chen, L. Li, *Science* **2011**, *333*, 1303-1307. *Tet-mediated formation of 5-carboxylcytosine and its excision by TDG in mammalian DNA.*

[115] R. M. Kohli, Y. Zhang, *Nature* **2013**, *502*, 472-479. *TET enzymes, TDG and the dynamics of DNA demethylation.*

[116] C. G. Spruijt, F. Gnerlich, A. H. Smits, T. Pfaffeneder, P. W. Jansen, C. Bauer, M. Münzel, M. Wagner, M. Müller, F. Khan, *Cell* **2013**, *152*, 1146-1159. *Dynamic readers for 5-(hydroxy) methylcytosine and its oxidized derivatives.*

[117] T. Pfaffeneder, B. Hackner, M. Truss, M. Munzel, M. Muller, C. A. Deiml, C. Hagemeier, T. Carell, *Angew. Chem. Int. Ed.* **2011**, *50*, 7008-7012. *The discovery of 5-formylcytosine in embryonic stem cell DNA.*

[118] M. Basanta-Sanchez, R. Wang, Z. Liu, X. Ye, M. Li, X. Shi, P. F. Agris, Y. Zhou, Y. Huang, J. Sheng, *ChemBioChem* **2017**, *18*, 72-76. *TET1-Mediated Oxidation of 5-Formylcytosine (5fC) to 5-Carboxycytosine (5caC) in RNA.*

[119] C. He, *Nature chemical biology* **2010**, *6*, 863-865. *Grand challenge commentary: RNA epigenetics?*

[120] C. Willyard, *Nature* **2017**, *542*, 406-408. *An epigenetics gold rush: new controls for gene expression.*

[121] C. Riml, R. Micura, *Synthesis* **2016**, *48*, 1108-1116. *Synthesis of 5-Hydroxymethylcytidine- and 5-Hydroxymethyl-uridine-Modified RNA.*

[122] C. Riml, A. Lusser, E. Ennifar, R. Micura, *J. Org. Chem.* **2017**, *82*, 7939-7945. *Synthesis, Thermodynamic Properties, and Crystal Structure of RNA Oligonucleotides Containing 5-Hydroxymethylcytosine.*

[123] H. Lusic, E. M. Gustilo, F. A. Vendeix, R. Kaiser, M. O. Delaney, W. D. Graham, V. A. Moye, W. A. Cantara, P. F. Agris, A. Deiters, *Nucleic Acids Res.* **2008**, *36*, 6548-6557. *Synthesis and investigation of the 5-formylcytidine modified, anticodon stem and loop of the human mitochondrial tRNAMet.*

[124] E. Westmanu, R. Stromberg, *Nucleic Acids Res.* **1994**, *22*, 2430-2431. *Removal of f-butyldimethylsilyl protection in RNA-synthesis. Triethylamine trihydrofluoride (TEA, 3HF) is a more reliable alternative to tetrabutylammonium fluoride (TBAF).*

[125] M. Sumino, A. Ohkubo, H. Taguchi, K. Seio, M. Sekine, *Biorg. Med. Chem. Lett.* **2008**, *18*, 274-277. *Synthesis and properties of oligodeoxynucleotides containing 5-carboxy-2'-deoxycytidines.*

[126] M. Münzel, U. Lischke, D. Stathis, T. Pfaffeneder, A. Gnerlich Felix, A. Deiml Christian, C. Koch Sandra, K. Karaghiosoff, T. Carell, *Chem. Eur. J.* **2011**, *17*, 13782-13788. *Improved Synthesis and Mutagenicity of Oligonucleotides Containing 5-Hydroxymethylcytosine, 5-Formylcytosine and 5-Carboxylcytosine.*

[127] R. W. Chambers, *Biochemistry* **1965**, *4*, 219-226. *The chemistry of pseudouridine. IV. Cyanoethylation.*

[128] K. K. Ogilvie, S. L. Beaucage, *Nucleic Acids Res.* **1979**, *7*, 805-823. *Fluoride ion promoted deprotection and transesterification in nucleotide triesters.*

[129] J. Solomon, I. Cote, M. Wortman, K. Decker, A. Segal, *Chem. Biol. Interact.* **1984**, *51*, 167-190. *In vitro alkylation of calf thymus DNA by acrylonitrile. Isolation of cyanoethyl-adducts of guanine and thymine and carboxyethyl-adducts of adenine and cytosine.*

[130] B. Prokopczyk, P. Bertinato, D. Hoffmann, *Carcinogenesis* **1988**, *9*, 2125-2128. *Synthesis and kinetics of decomposition of 7-(2-cyanoethyl) guanine and O 6-(2-*

cyanoethy) guanine, markers for reaction of acrylonitrile and 3-(methylnitrosamino) propionitrile with DNA.

[131] M. Mag, J. W. Engels, *Nucleic Acids Res.* **1988**, *16*, 3525-3543. *Synthesis and structure assignments of amide protected nucleosides and their use as phosphoramidites in deoxyoligonucleotide synthesis.*

[132] D. C. Capaldi, H. Gaus, A. H. Krotz, J. Arnold, R. L. Carty, M. N. Moore, A. N. Scozzari, K. Lowery, D. L. Cole, V. T. Ravikumar, *Org. Process Res. Dev.* **2003**, *7*, 832-838. *Synthesis of High-Quality Antisense Drugs. Addition of Acrylonitrile to Phosphorothioate Oligonucleotides: Adduct Characterization and Avoidance.*

[133] Y. Nomura, N. Haginoya, Y. Ueno, A. Matsuda, *Biorg. Med. Chem. Lett.* **1996**, *6*, 2811-2816. *Nucleosides and nucleotides. 161. Incorporation of 5-(N-aminoalkyl)carbamoyl-2'-deoxycytidines into oligodeoxyribonucleotides by a convenient post-synthetic modification method.*

[134] B. Willi, T. Arnold, *Helv. Chim. Acta* **1987**, *70*, 175-186. *A Simple and Effective Chemical Phosphorylation Procedure for Biomolecules.*

[135] M. H. Caruthers, *Acc. Chem. Res.* **1991**, *24*, 278-284. *Chemical synthesis of DNA and DNA analogs.*

[136] Cornelia G. Spruijt, F. Gnerlich, Arne H. Smits, T. Pfaffeneder, Pascal W. T. C. Jansen, C. Bauer, M. Münzel, M. Wagner, M. Müller, F. Khan, H. C. Eberl, A. Mensinga, Arie B. Brinkman, K. Lephikov, U. Müller, J. Walter, R. Boelens, H. van Ingen, H. Leonhardt, T. Carell, M. Vermeulen, *Cell* **2013**, *152*, 1146-1159. *Dynamic Readers for 5-(Hydroxy)Methylcytosine and Its Oxidized Derivatives.*

[137] H. E. Gottlieb, V. Kotlyar, A. Nudelman, *J. Org. Chem.* **1997**, *62*, 7512-7515. *NMR Chemical Shifts of Common Laboratory Solvents as Trace Impurities.*